# ASSEMENT OF ABOVE GROUND BIOMASS WITH TERRESTRIAL LiDAR USING 3D QUANTITATIVE STRUCTURE MODELLING IN TROPICAL RAIN FOREST OF AYER HITAM FOREST RESERVE, MALAYSIA

MADHIBHA TASIYIWA PRISCILLA
FEBRUARY, 2016

SUPERVISORS:
Dr. Y.A. Hussin
Ir.L.M. van Leeuwen
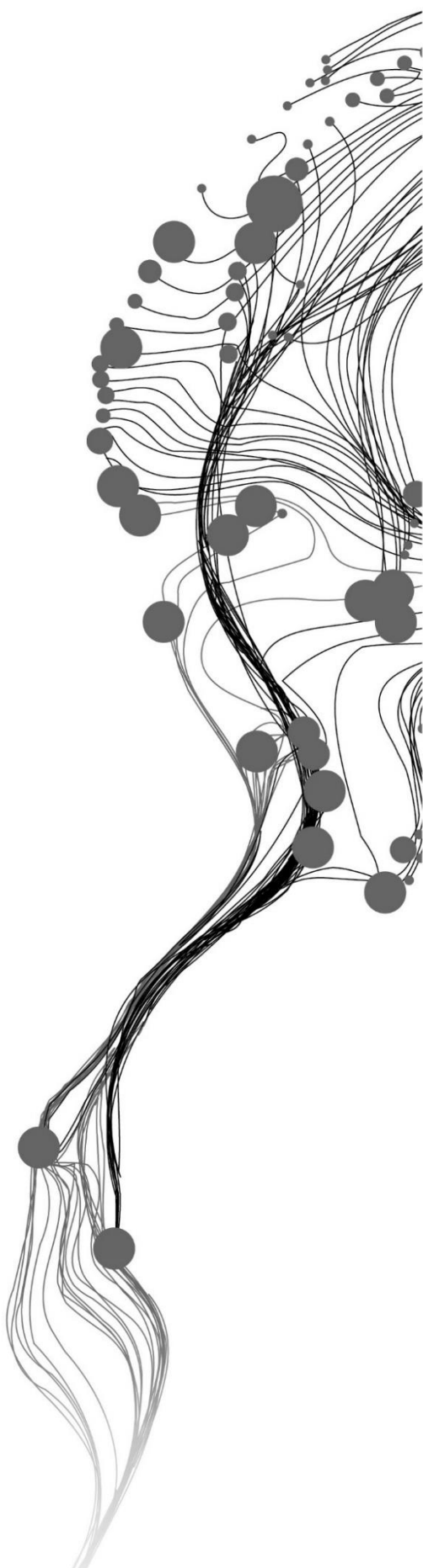
ASSESSMENT OF ABOVE GROUND BIOMASS WITH TERRESTRIAL LiDAR USING 3D QUANTITATIVE STRUCTURE MODELLING IN TROPICAL RAIN FOREST OF AYER HITAM FOREST RESERVE,MALAYSIA

MADHIBHA TASIYIWA PRISCILLA
Enschede, The Netherlands, February, 2016

ABSTRACT

20% of global carbon dioxide is from deforestation and forest degradation. REDD+ is an international framework for reducing emissions from deforestation and degradation and rewards those who reduce emissions. There is a need for an accurate Measuring Reporting and Verification (MRV) system, which is proposed by REDD+, that is still a challenge. Using TLS and Quantitative Structure Modelling (QSM) is an option of estimating Above Ground Biomass (AGB) and has the potential to be used as one of the techniques of MRV system.

This study explored the feasibility of using Terrestrial Laser Scanner (TLS) and QSM to assess AGB in a tropical rain forest of Ayer Hitam Forest Reserve, Malaysia. Point clouds were acquired from 26 circular plots of $500m^2$ using a RIEGL VZ 400 Terrestrial Laser Scanner. Registration, extraction of individual trees and measurement of DBH and height were conducted in RISCAN PRO v 2.1. Hundred (100) trees were selected for the QSM reconstruction based on extraction quality and DBH distribution. TLS derived DBH and height with wood density was used to calculate AGB from allometric equations. AGB was calculated from the QSM derived volume and wood density. The DBH and height derived from the TLS was compared to the DBH and height measured from the field. The AGB biomass derived from allometric equations was compared with the AGB derived from QSM and the distribution of AGB along the different parts of the trees was assessed. Sensitivity analysis was carried out on parameters that affect the volume reconstruction. These parameters are the number of runs, cover set diameters and nmin values. Above Ground Carbon (AGC) per tree was calculated by using a conversion factor of 0.47 to convert the AGB/tree into AGC/tree.

Field measured DBH with TLS derived DBH showed a high correlation with an R^2 of 0.993 and an RMSE of 1.1cm whilst field height and TLS height showed a low correlation with an R^2 of 0.589 and an RMSE of 3.4 metres. Of the 100 trees, 29 observations had trunk biomass greater than canopy and 71 observations had canopy biomass greater than trunk biomass. Of the 29 observations, there was a strong relationship between AGB from allometric equations and from QSM. An R^2 of 0.968 with an RMSE of 120Kg/tree was observed when using the FAO default wood density value for Asia ($0.57g/cm^3$) and an R^2 of 0.934 and an RMSE of 131.61Kg/tree was obtained using species specific wood density. The 71 observations showed a slightly lower relationship with an R^2 of 0.817 and an RMSE of 163Kg/tree using $0.57g/cm^3$ wood density and an R^2 of 0.797 with an RMSE of 198Kg/tree using species specific wood density. Compared to the allometry reference AGB was overestimated by 47% for the 100 trees. No statistical significant difference was observed in either using the FAO default wood density value and species specific wood density in calculating AGB. The average AGC per tree was 294Kg/tree using species specific wood density values and 281Kg/tree using the FAO default wood density value.

This study shows the potential of TLS and QSM in estimating AGB but further work is needed for accurate reconstruction of trees in a heterogeneous forest. Reconstruction of the trees was not very successful as many factors play a role in producing a robust reconstruction. There is a need to develop algorithms that properly extract individual trees from point clouds, accurately separate the branches and leafs before reconstruction and also automate the process of finding optimum modelling parameters to suit the variety of species.

Keywords: Terrestrial LiDAR, Quantitative Structure Modelling, Above Ground Biomass, REDD+, Point cloud data, Allometric equation, Above Ground carbon

ACKNOWLEDGEMENTS

Dedicated to my husband, Mr Blessed Muumbe, for the encouragement, support and love.

TABLE OF CONTENTS

LIST OF FIGURES

LIST OF TABLES

LIST OF APPENDIXES

LIST OF ACRONYMS

AGC	Above Ground Carbon
AGB	Above Ground Biomass
ANOVA	Analysis of Variance
AHFR	Ayer Hitam Forest Reserve
DBH	Diameter at Breast Height
FAO	Food and Agricultural Organization of the United Nations
GHG	Green House Gases
GLCS	Geographic Coordinate System
IPCC	Intergovernmental Panel on Climate Change
LiDAR	Light Detection And Ranging
MRV	Measuring Reporting and Verification
MSA	Multi Station Adjustment
PRCS	Project Coordinate System
QSM	Quantitative Structure Modelling
REDD+	Reduced Emissions from Deforestation and Forest Degradation
RGB	Red, Green, Blue
RMSE	Residual Mean Squared Error
SOCS	Scanner's Own Coordinate System
TLS	Terrestrial Laser Scanner
UNDP	United Nations Development Programme
UNEP	United Nations Environment Programme
UNFCCC	United Nations Framework Convention on Climate Change
UPM	University Putra Malaysia
3D	Three Dimensional

1 INTRODUCTION

1.1 Background

Forests cover approximately 30% of the global land area and of this only 2% is covered by tropical rain forests. The carbon dynamics of a forest are dominated by photosynthesis, respiration and decomposition (Malhi & Grace, 2000). Forests sequester and store carbon more than any other terrestrial ecosystem and, therefore, are central in climate change mitigation (Gibbs et al., 2007).

In light of global climate change, measures are being taken to reduce Green House Gases (GHGs) (Englhart et al., 2013). Reduced Emissions from Deforestation and Forest Degradation (REDD+) is an example of a climate change mitigation programme which aims at conservation, forest management and carbon stock enhancement (Campbell, 2009). Tropical forests are the focus of REDD+ projects because there are a reservoir of 40% of terrestrial carbon (FAO, 2009).

Forest ecosystems add to climate change mitigation by acting as carbon sinks of excess carbon in the atmosphere and thus, the Kyoto Protocol recognises the value of estimating forest biomass and carbon stocks (Castedo-Dorado et al., 2012). Above Ground Biomass (AGB) is the total amount of biological material present above the soil and is expressed as oven-dry biomass per unit area in tonnes/hectare (Drake et al., 2003; Heng & Tsai, 1999). Forest carbon stocks are derived from AGB by assuming a carbon content of 50% (Goetz & Dubayah, 2011). AGB is important because it changes through time, it is used to estimate terrestrial carbon pools and it gives an indication of the net primary productivity (Goetz & Dubayah, 2011). Terrestrial carbon monitoring and accounting is important for REDD+ which requires developing countries to have robust and transparent national forest monitoring systems (Næsset et al., 2013).

The most direct way to quantify the carbon stored in AGB is to harvest all trees in a known area, oven dry them and weigh the biomass and convert to carbon by taking half of the biomass (Gibbs et al., 2007). This method is time consuming, destructive and impractical (Gibbs et al., 2007). Stephenson et al. (2014) also highlighted that large trees are not taken into account when developing allometric equations because there are usually not measured or harvested. Using allometry can also result in errors in some cases over 30% (Calders et al., 2015). Accurate and effective methods of assessing biomass and carbon stocks are necessary to satisfy the requirements of Kyoto protocol (Castedo-Dorado et al., 2012). Use of remote sensing in combination with ground based inventories is recommended for Measuring, Reporting and Verification (MRV) system under the REDD+ United Nations Framework Convention on Climate Change (UNFCCC) (Hirata et al., 2012).

Terrestrial Laser Scanner (TLS) is an active remote sensing technique which transmits laser pulses and measure distance by analysis of the returned energy as a function of time (Calders et al., 2015). Biomass has a positive correlation with the number of hits in the TLS point cloud and thus tree biomass and its changes can be measured (Holopainen et al., 2012). TLS is essential in estimating AGB because of its capability to provide accurate three-dimensional (3D) tree data (Kaasalainen et al., 2014). TLS ensures high accuracies because AGB can be inferred from estimates of tree volume. Structures of the trees can be studied in depth based on TLS measurements using 3D Quantitative Structure Modelling (QSM) (Raumonen et al., 2013).

QSM characterize trees as ranked collections of cylinders, from the cylinders volume is derived that is essential to estimate biomass (Raumonen et al., 2015). The input of the model is point clouds from multiple positions of a single tree to ensure a comprehensive cover of the branching structure (Raumonen et al., 2013). The input can also be point clouds of trees at plot level registered into a common coordinate system (Raumonen et al., 2015). Using TLS and QSM, it is possible to accurately estimate the volume, branching structure and distribution and also detect growth changes without destructive sampling (Kaasalainen et al., 2014). It is also possible to determine the volume and AGB and its distribution along the tree.

Studies using TLS and QSM have been conducted and it was demonstrated that TLS measurements can be modelled to a reasonable accuracy with QSM. For example Calders et al. (2015), conducted a study to estimate AGB using TLS in a native Eucalyptus open forest in Victoria, Australia and concluded that AGB is not evenly spread within the tree. For a Eucalypt open forest, 80% of the AGB at plot level is located in the lower 60% of the trees. Kaasalainen et al. (2014) conducted change detection of tree biomass with TLS and QSM on a Maple tree and concluded that changes in the tree branching structure can be duplicated with about ±10% accuracy. Also Raumonen et al. (2015), conducted massive tree modelling from TLS data on a 30 metre diameter English Oak plot and an 80 m diameter Eucalyptus plot. He concluded that the Oak plot biomass was overestimated by 17% and the Eucalyptus by 8.5% but concluded that the method provides precise and fast tree modelling capabilities for biomass estimation.

Calders et al. (2015) highlighted that this method can be applied in many forest types and can assist in the standardization of broad scale biomass maps. The method has the potential to monitor natural gradual changes in biomass but also unexpected changes caused by fires or storm damage. Although this method seems promising there are areas that still need investigation. Raumonen et al. (2015) highlighted that leaf on conditions, dense understory and higher stem density is likely to reduce visibility. Plots that have a lot of dissimilar tree species might require different modelling parameters to suit each species.

The different scenarios presented by different forest types need investigation and to add on, most of the studies carried out have focused on conifers, broad-leafed and plantation forests with little focus on tropical forests. It is within this background that a study to assess AGB with TLS using 3D QSM was carried out in the Tropical Rain Forest of Ayer Hitam Forest Reserve, Malaysia. The results tested the feasibility of this method in a diverse heterogeneous forest characterised by high stem density, dense understory and high species diversity. The REDD+ MRV element requires an accurate method to estimate carbon stocks and the use of TLS and 3D QSM is a potential method to bridge this gap. The results of the study can be used to estimate tropical forest biomass in line with REDD+ programs in different parts of the world.

1.2 Problem Statement and Justification

Climate change is caused mainly by an increase in Green House Gases (GHG) emission and the most significant one is the atmospheric carbon dioxide (Hirata et al., 2012). Deforestation and forest degradation account for 20% of the global carbon dioxide emissions after fossil fuel combustion (Hirata et al., 2012). REDD+ is an international framework for reducing emissions from deforestation and degradation and rewards those who reduce emissions from deforestation and degradation (Angelsen & Wertz-Kanounnikoff, 2008). Support to reduce emissions has been expressed at the highest political levels that is the UN General Assembly and this resulted in its inclusion in the Bali Action of the UNFCCC in December 2007 (FAO, UNDP, & UNEP, 2008). The challenges for carbon incentives is the need for a sound and transparent MRV system that can estimate the change in carbon accurately (Bhattarai et al., 2015). Change is inherent and forms the basis for any financial compensation and thus, measurement over time requires monitoring

(Herold & Skutsch, 2011). This implies that the national MRV should be based on sound scientific evidence (Hirata et al., 2012).

The measuring component of MRV consists of documenting the extent and changes in forest area and the carbon stock associated with the changes (Goetz & Dubayah, 2011). Accurate and timely monitoring are the core of a functional monitoring system for carbon emission trading (Houghton, 2005), but uncertainty in prescribing initial forest carbon stocks is a major source of error in estimating surface carbon (Houghton & Goetz, 2008). Spatially explicit estimates of biomass and other forest structures are required to understand how forests will respond to climate change (Clark et al., 2004). Estimating AGB is therefore a critical step in quantifying and monitoring the change of carbon in tropical forests (Gibbs et al., 2007).

Given that MRV must be highly accurate before credits can be issued, a monitoring system that combines remote sensing with ground based inventories is recommended (Hirata et al., 2012). Patenaude et al. (2005) highlighted the capability of remote sensing to monitor terrestrial ecosystems at various temporal and spatial scales and its use in land cover mapping and forestry applications. A variety of remote sensing techniques are employed for estimation of forest resources. These techniques are considered important for REDD+ monitoring and to improve the precision of the estimates significantly (Næsset et al., 2013). Effective monitoring is based on satellite or airborne observations due to the inaccessibility of some forests (Gibbs et al., 2007).

Modern Remote Sensing techniques such as LiDAR that is both Airborne and Terrestrial can accurately estimate carbon in tropical forests because of their ability to see through spaces in the forest canopies and detect three-dimensional forest structure (Asner et al., 2012). Airborne LiDAR has advantages of covering a large area but the precision and reliability depends on the validity of the assumptions made in the models applied to derive inventory parameters from point clouds (Maas et al., 2008). Terrestrial LiDAR on the other hand combined with automatic data provides a tool to bridge the gap between field inventories and airborne LiDAR (Maas et al., 2008). TLS offers an alternative for rapid and accurate information containing 3D structure (Burt et al ., 2013).

TLS measurements in combination with 3D QSM can characterize in detail the structure of trees (Kaasalainen et al., 2014). The QSM reconstruction algorithm retrieves branch size distributions from TLS points clouds (Raumonen et al., 2013). Other statistical models are limited in precision to give accurate quantitative and geometric information of trees but QSM gives detailed information on branch size distribution and thus, AGB can be calculated accurately from trees (Krooks et al., 2014). One option for assembling whole-tree AGB measurements without harvesting the tree is to use Terrestrial LiDAR to estimate the volume of individual branches and stems (Hildebrandt & Iost, 2012). With additional wood specific density measurements, it is possible to estimate tree AGB to a good accuracy without felling the tree and this approach accelerates the acquisition of tree biometrics data (Hildebrandt & Iost, 2012). The REDD+ MRV element requires an accurate method to estimate carbon stocks and the use of TLS and 3D QSM is a potential method to bridge this gap. It is within this background that this research explored the feasibility of using TLS and 3D QSM to assess AGB in a Tropical Rain Forest of Ayer Hitam Forest Reserve in Malaysia.

1.3 Research Objectives

The main aim of this study was to assess Above Ground Biomass using Terrestrial LiDAR and 3D Quantitative Structure Modelling (QSM) in a Tropical Rain Forest.

1.3.1   Specific Objectives

1. To assess TLS derived tree parameters, Diameter at Breast Height (DBH) and height with ground measurements.
2. To estimate above ground biomass through Terrestrial LiDAR using Quantitative Structure Modelling derived volume estimates.
3. To compare Terrestrial LiDAR and Quantitative Structure Modelling derived above ground biomass with above ground biomass derived from allometric equations.
4. To determine the distribution of above ground biomass along the different parts of the tree.
5. To compare the difference in using default or species specific wood density values in estimating above ground biomass.
6. To accurately assess above ground biomass and carbon stock of individual trees.

1.4   Research Questions

1. How accurate is Terrestrial LiDAR derived tree Diameter at Breast Height and height?
2. How accurate is Terrestrial LiDAR and Quantitative Structure Modelling derived Above Ground Biomass?
3. What is the difference in Terrestrial LiDAR and Quantitative Structure Modelling derived Above Ground Biomass and Above Ground Biomass derived from allometric equations?
4. How is Above Ground Biomass distributed along the different parts of the tree?
5. What is the difference in using default or species specific wood density in estimating above ground biomass?
6. What is the Above Ground Biomass and carbon stock of individual trees?

1.5   Research Hypothesis

H_0: There is no significant difference between Diameter at Breast Height derived from Terrestrial LiDAR and Diameter at Breast Height derived from ground measurements.
H_a: There is a significant difference between Diameter at Breast Height derived from Terrestrial LiDAR and Diameter Breast Height derived from ground measurements.

H_o: There is no significant difference between height derived from Terrestrial LiDAR and height from ground measurements.
H_a: There is a significant difference between height derived from Terrestrial LiDAR and height derived from ground measurements.

H_o: There is no significant difference between Terrestrial LiDAR and Quantitative Structure Modelling derived above ground biomass and allometry derived above ground biomass.
H_a: There is a significant difference between Terrestrial LiDAR and Quantitative Structure Modelling derived above ground biomass and allometry derived above ground biomass.

H_o: There is no significant difference in the distribution of above ground biomass along the different parts of the tree.
H_a: There is a significant difference in the distribution of above ground biomass along the different parts of the tree.

Ho: There is no significant difference in using either default or species specific wood density in estimating above ground biomass.
Ha: There is a significant difference in using either default or species specific wood density in estimating above ground biomass.

2 LITERATURE REVIEW

2.1 Terrestrial Laser Scanning

Light Detection and Ranging (LiDAR) is an active remote sensing technology that defines ranges by taking the speed of light and the time required for an emitted laser to travel to the target object (Lim et al., 2003). TLS has grown in interest because of its ability to produce reliable and accurate 3D point cloud data. Airborne LiDAR has been used for traditional forest inventories but it provides limited information at the tree scale or under the canopy, but TLS can obtain information at tree or plot scales (Dassot et al., 2011). Airborne LiDAR is also limited to stand wise average parameters rather than individual tree parameters (Maas et al., 2008). Figure 1 shows the principles of the TLS.
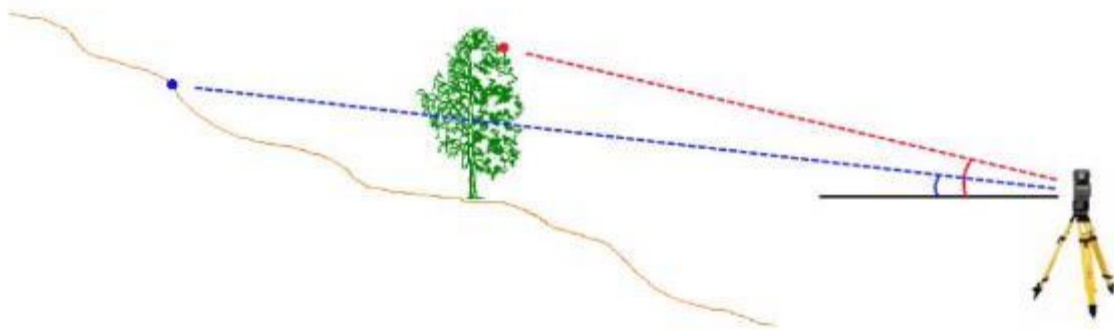
Figure 1: Scanning Principle of Terrestrial Laser Scanner (Panholzer & Prokop, 2013)

The TLS can produce either a single scan or multiple scans. In a single scan, the TLS is placed at a single location usually, the centre of the plot and only one scan is made whilst in a multiple scan several scans usually 3 or 4 are made around the objects (Dassot et al., 2011). Multiple scan set ups provide the best plot coverage and ensure a complete 3D descriptions of objects although panoramic single scans are sometimes preferred for economic reasons (Maas et al., 2008; Dassot et al., 2011). In this study, a multi-scan was performed.

Terrestrial LiDAR is classified into two classes according to the range measurement principle that is phase shift or pulsed time of flight (Dassot et al., 2011). These are the TLS systems commonly used for outdoor applications (Lemmens, 2011). The phase shift technology emits beams which are modulated as sine waves (Lemmens, 2011). Then the phase of the reflected part is measured and compared to the phase of the outgoing one then the distance is calculated from the difference in phase (phase shift) (Lemmens, 2011). The time of flight technology makes use of a pulse that is emitted in the direction of the object, the time taken by the part of the pulse reflected back to reach the instrument is measured (Lemmens, 2011). The distance is calculated by multiplying the travel time by the speed of light and dividing the result by two (Lemmens, 2011).

The TLS used in this study is a RIEGL VZ – 400 (Figure 2) and its specifications are highlighted in Table 1. This TLS model is suitable for forestry inventories because it meets the standards specified by Maas et al. (2008). A laser scanner to be used in forest inventory should have a maximum range of at least 50m to allow for scanning typical forest inventory plots with a radius of 12-15m with trees of height up to 40m, the data rate should be at least 10 000 points per second and for flexibility in data acquisition, a scanner should offer a panoramic or hemispheric field of view. The range measurement precision should be better than 10mm to allow for an adequate precision in stem diameter determination (Maas et al., 2008).

Table 1: RIEGL VZ-400 Specifications (RIEGL, 2014)

Descriptions	Performance
Laser Class	1
Laser wavelength	Near infrared
Range finder	Time of flight
Field of view	100°- 360°
Measurement of range	1.5 to 600m
Accuracy	5mm
Precision	3mm
Points per second	122 000
Beam divergence	0.35mrad
Weight	9.6kg (approximate)
Data interface	LAN/WLAN

Figure 2: RIEGL VZ-400

2.2 Quantitative Structure Modelling

QSM is a reconstruction algorithm developed by Raumonen et al. (2013).The reconstruction of 3D models and quantitative analysis of trees is possible from TLS multi-scan point clouds (Raumonen et al., 2013). The quantitative models of trees are produced through a computational method from the point clouds (Krooks et al., 2014). Through a process of segmentation, the point cloud is segmented into stems and branches by covering the point cloud with small sets matching to connected surface patches in the tree surface (Krooks et al., 2014). The sets are the smallest elements used to segment the point cloud (Raumonen et al., 2013). The segmented branches and stem are modelled as collections of cylinders (Raumonen et al., 2013). The cylinders provide the volume and diameter which are needed to estimate the biomass (Raumonen et al., 2015). TLS in combination with QSM can estimate the volume, branching structure and branch size distribution and can also detect changes in trees accurately without destructive sampling (Kaasalainen et al., 2014). Figure 3 shows TLS point clouds and their corresponding completed cylinder models. The QSM is described in detail in the methods section of the document.
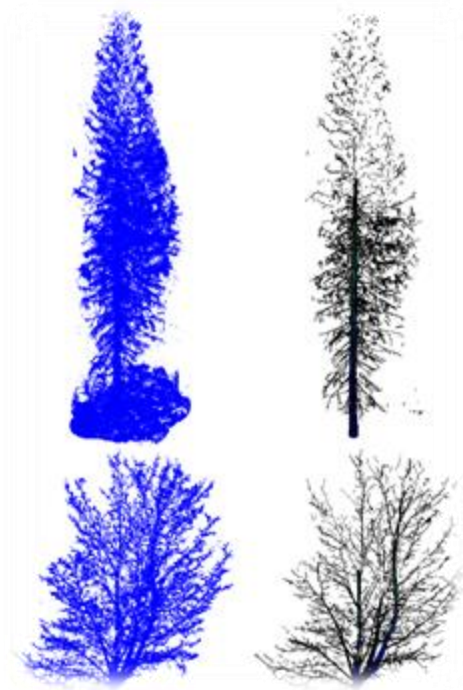
(Source: Raumonen et al., 2013)

Figure 3: Point Clouds (blue) and their final cylinder (black) models 7070 & 6820 cylinders respectively

2.3 Biomass and carbon

Above Ground Biomass is defined as the total amount of biological material (oven – dried) present above the soil surface in a specified area (Drake et al., 2003). The Intergovernmental Panel on Climate Change (IPCC) recognized five carbon pools that is; above ground biomass, below ground biomass, litter, woody debris and soil organic matter (Vashum & Jayakumar, 2012) (Figure 4). Carbon is derived from above ground biomass by assuming 50%, 45% or 47% of the dry biomass (Basuki et al., 2009; Vashum & Jayakumar, 2012; IPCC, 2006). Above ground biomass of the tree is mainly the largest carbon pool and is affected by degradation and deforestation and thus, it is important to estimate above ground biomass in quantifying carbon fluxes from tropical forests (Gibbs et al., 2007). Forest biomass can be estimated through field measurements, remote sensing and GIS and in this study remote sensing with 3D Quantitative Structure Modelling was used to assess above ground biomass.

Forest Carbon Pools

AGB: living vegetation above the soil including stems, branches, bark, foliage
BGB: live roots >2 mm
CWD: non-living biomass not contained in litter; either standing or fallen; includes wood lying on surface, dead roots, and stumps >10 cm diameter
Litter: non-living biomass of size greater than SOM limit (~2mm) and less than CWD limit (~10cm) lying dead above soil
SOC: organic carbon in mineral soils and in live or dead fine roots (<2mm)

Figure 4: Forest Carbon Pools (DiRocco et al., 2014).

2.4 Allometric equations

The use of allometric equations is the most widely used method for estimating biomass in forest ecosystems (Vashum & Jayakumar, 2012). The equations are a form of non-destructive method of estimating above ground biomass and are developed and applied to forest inventory data to assess the biomass and carbon stocks (Vashum & Jayakumar, 2012). They can either be developed for single species or for a mixture of species for specific sites or for large scale global areas (Vashum & Jayakumar, 2012). Allometric equations still need validation and this is done by cutting and weighing of tree components (Nelson et al., 1999). Ryan et al. (2011) stated that one needs to consider, the applicability of the equation for a particular area, forest type and tree species. Thus, the equations should not be used beyond their range of validity. In this study, the allometric equation developed by Chave et al. (2014), was used which is suitable for tropical forests.

$$AGB = [0.0673 * (p*D^2H)^{0.976}] \dots\dots\dots\dots\dots\dots \textbf{Equation 1}$$

Where ABG: Above Ground Biomass (Kg)
p: Wood specific gravity (gcm^{-3})
D: diameter at breast height (DBH cm); and
H: tree height (m)

2.5 Works related to the study

Calders et al. (2015) conducted a study to estimate total AGB with Terrestrial LiDAR and QSM in a *Eucalyptus* open forest plots in Australia. Through QSM volume estimates were made, the volume and wood density was used to derive AGB. The Terrestrial LiDAR derived AGB estimates were validated by comparing them with destructively sampled AGB and showed high correlations of 98%. The total AGB of the 65 sampled trees was overestimated by 9.86% whilst using allometric equations AGB was underestimated by 36.57- 29.85% and showed a correlation of 0.68-0.78 compared to the reference data. The research also showed that AGB is not evenly distributed within the tree, for *Eucalyptus* open forest, 80% of the AGB at plot level is located in the lower 60% of the trees. The results showed that TLS measurements can be efficiently modelled with QSM.

Raumonen et al. (2015) presented a method for automatic extraction of individual trees from point clouds in a forest plot. The method was tested on a 30 metre diameter English Oak plot and an 80 metre diameter Australian *Eucalyptus* plot. All the trees inside the oak plot were found and correctly extracted with errors on small branches and this was true also for the *Eucalypt* plot. Bigger errors were observed on multi-stem trees as a result of difficulties in separating the trees. Results showed that total biomass was overestimated by 17% when compared to allometry reference (N=15) whilst for the eucalypts it was overestimated by 8.5% when compared to the destructive reference (N=27).

QSM was applied to produce detailed information on branch size distribution and volume. The study also investigated the feasibility of predicting tree branch size distributions for trees in similar environments. The QSM enabled the comparison of structure between a large number of trees. Branch size distribution was found to be similar for trees of different heights in similar growing conditions. The results suggested that tree height can be used to estimate branch size distribution in similar environments (Krooks et al., 2014).

Kaasalainen et al. (2014) conducted a change detection of tree biomass with TLS and QSM. They examined the viability of the approach with two case studies on trees and assessed the accuracy with laboratory reference measurements to identify the main sources of error. Results showed that the changes in the tree branching structure can be replicated with an accuracy of ±10% and QSM provides a non-destructive method for monitoring forest characteristics.

QSM from TLS point clouds was applied on data acquired from *Eucalyptus racemosa* woodland using RIEGL VZ -400 instrument. 3D reconstruction was carried out on the simulated point clouds to account for errors of sampling and reconstruction. The results showed that total volume could be recreated with 10.8% underestimate (Burt et al., 2013).

The use of QSM produces accurate 3D cylinder models from TLS data. The studies carried out have focused on conifers, broad-leafed and plantation forests with little focus on tropical forests thus, there was a need to apply QSM on TLS point clouds from tropical forests. This method also presents an opportunity for REDD+MRV which requires an accurate method to estimate carbon stock.

3 MATERIALS AND METHODS

3.1 Study Area

3.1.1 Geographic Location and Overview

The study was carried out in Ayer Hitam Forest Reserve (AHFR) Latitude 2° 56'N-3° 16'N and Longitude of 101°30'E-101°46'E (Hasmadi et al., 2008). The forest is classified as a secondary disturbed Kelat-Kedondong - Mixed Dipterocarp type of lowland forest because it was selectively logged several times between 1936 and 1965 (Nurul-Shida et al., 2014; Ibrahim, 1999). Ayer Hitam is located in the state of Selangor in Peninsular Malaysia, approximately 20km south-west of Kuala Lumpur city centre (Figure 5). Originally the forest was covering an area of 3500 hectares but was reduced to 1248 hectares since the 1980s (Nurul-Shida et al., 2014). The decrease in size is a result of socio-economic development projects such as housing estates, oil palm plantations, new townships, factories and highways (Hani et al., 2005). The Selangor State Government leased the forest to University Putra Malaysia (UPM) in 1996 for 80 years (Lepun et al., 2007). The reserve has 6 compartments named 1, 2,12,13,14 and 15 entrusted to the Faculty of Forestry for teaching, research and extension activities (Abdullah et al., 1999). Ayer Hitam was home to the Orang Asli (indigenous people) of the Temuan tribe for 400 years and they named important landmarks like rivers and hills in the area (Bawon & Yaman, 2007).
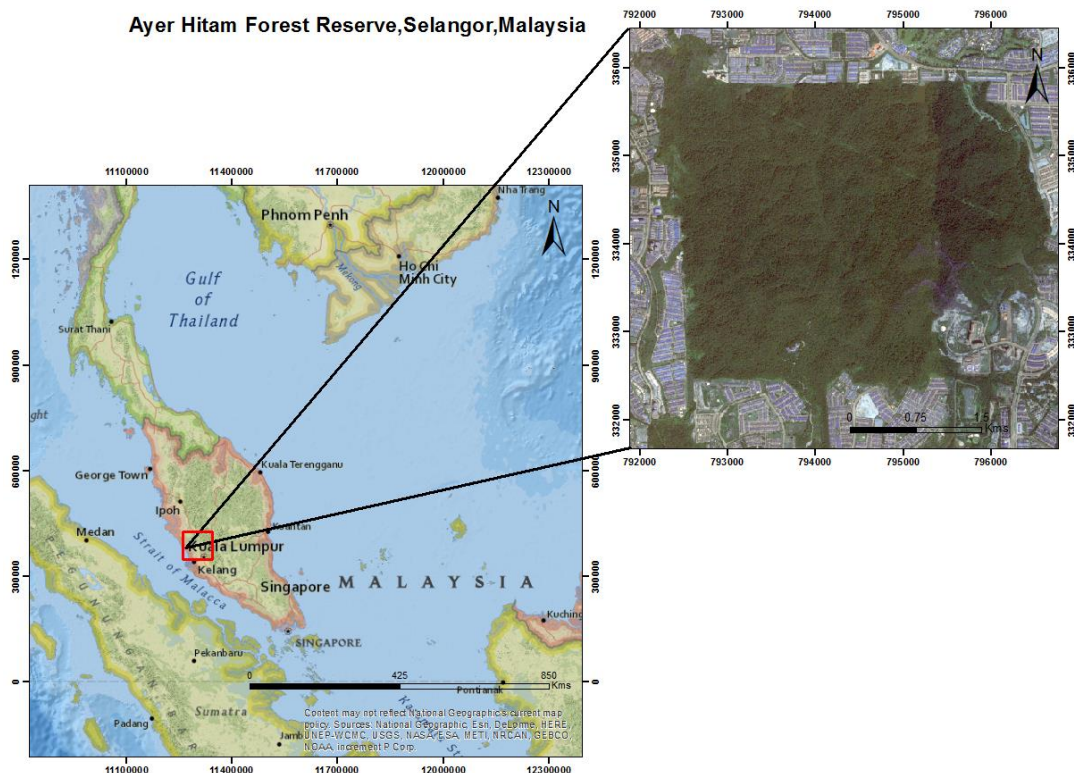
Figure 5: Study Area location

3.1.2 Topography and Climate

The altitude of the study area ranges between 15 and 233m with a slope up to 34° (Nurul-Shida et al., 2014; Yu Abit et al., 2012). The highest point located in compartment 15 (Hasmadi et al., 2008). The minimum and maximum temperatures are 22.7° and 32.1°C with an average temperature of 26.6°C (Bawon & Yaman, 2007). The relative humidity is 87.6% with a maximum of 97.8% and a minimum of 77.4% (Ibrahim, 1999).

The average rainfall is 2178mm (Ibrahim, 1999) and two main rivers flow in the forest that is the Sungai Rasau and Sungai Bohol (Nurul-Shida et al., 2014).

3.1.3   Geology and Soil

The lithology of the area is an igneous rock with granite as the main component (Hasmadi et al., 2008). The internal part of the soils are metamorphic with secondary minerals of ferromagnesium (Bawon & Yaman, 2007). The soil in the forest reserve can be described as alluvium – colluvium soil shaped from metamorphic rocks with a sandy clay loam soil texture (Ibrahim, 1999).

3.1.4   Biodiversity

The biodiversity of the area can be described in three ways that is ecosystem, species and genetic (Bawon & Yaman, 2007). In terms of flora, the forest is home to 127 species from 36 families with 3% of them being from the Dipterocarp species (Bawon & Yaman, 2007). Research conducted revealed also 98 species of medical herbs from 83 genus and 53 families (Bawon & Yaman, 2007). In terms of fauna, five species of mammals, thirty-eight (38) families of birds, three families of reptiles, four families of amphibians and five families of fish were found (Bawon & Yaman, 2007). The genetic diversity is described in the sense of polymorphism and heterozygosis (Bawon & Yaman, 2007).

3.2 Materials

Various equipment in terms of hardware and software was used in this study. The software and hardware used are described in the sections below.

3.2.1   Maps and Field equipment

To collect the data in the field various instruments designed to measure forest parameters were used. A topographic map scale 1: 25000 and a World View 3 image were used for sampling. Table 2 shows the instruments used and their respective functions.

Table 2: Field Equipment

Instrument	Function
Terrestrial Laser Scanner (RIEGL VZ 400)	Point cloud data acquisition
50 metre measuring tape	Plot delineation
Diameter tape (5m)	Measuring diameter at breast height
Suunto Compass	Measuring bearing
Suunto Clinometer	Measuring slope
Leica DISTO D510 Laser Ranger	Measuring height
Densitometer	Crown Cover
Field work data sheet	Recording data
Slope correction table	Adjusting radius of plot

3.2.2   Software

Various software was used for data processing and analysis. Table 3 shows the software used and its respective functions.

Table 3: Software used

Software	Function
Carry Map Observer	Navigation
RISCAN PRO v 2.1	Point cloud processing
	DBH measurement
	Height measurement
ArcGIS 10.3.1	Generation of maps
MATLAB R2015b	Quantitative Structure Modelling reconstruction
RStudio	Statistical analysis
SPSS	Statistical analysis
MS Office 2010	Data analysis and thesis writing

3.3 Research Method

The research was conducted in three major stages that is field data collection, data processing and analysis and above ground biomass estimation using volume derived from Quantitative Structure Modelling. Biometrics data such as tree height, DBH, tree species and the crown cover was collected from direct field observations. Point clouds were collected through multi-scanning with a Terrestrial Laser Scanner. It further included analysis of the remotely sensed data and deriving DBH and height from the Terrestrial Laser Scanner. Volume was derived from Quantitative Structure Modelling and together with density, above ground biomass and therefore the carbon was deduced. Figure 6 shows the flowchart of the methods used to achieve the objectives of the study.
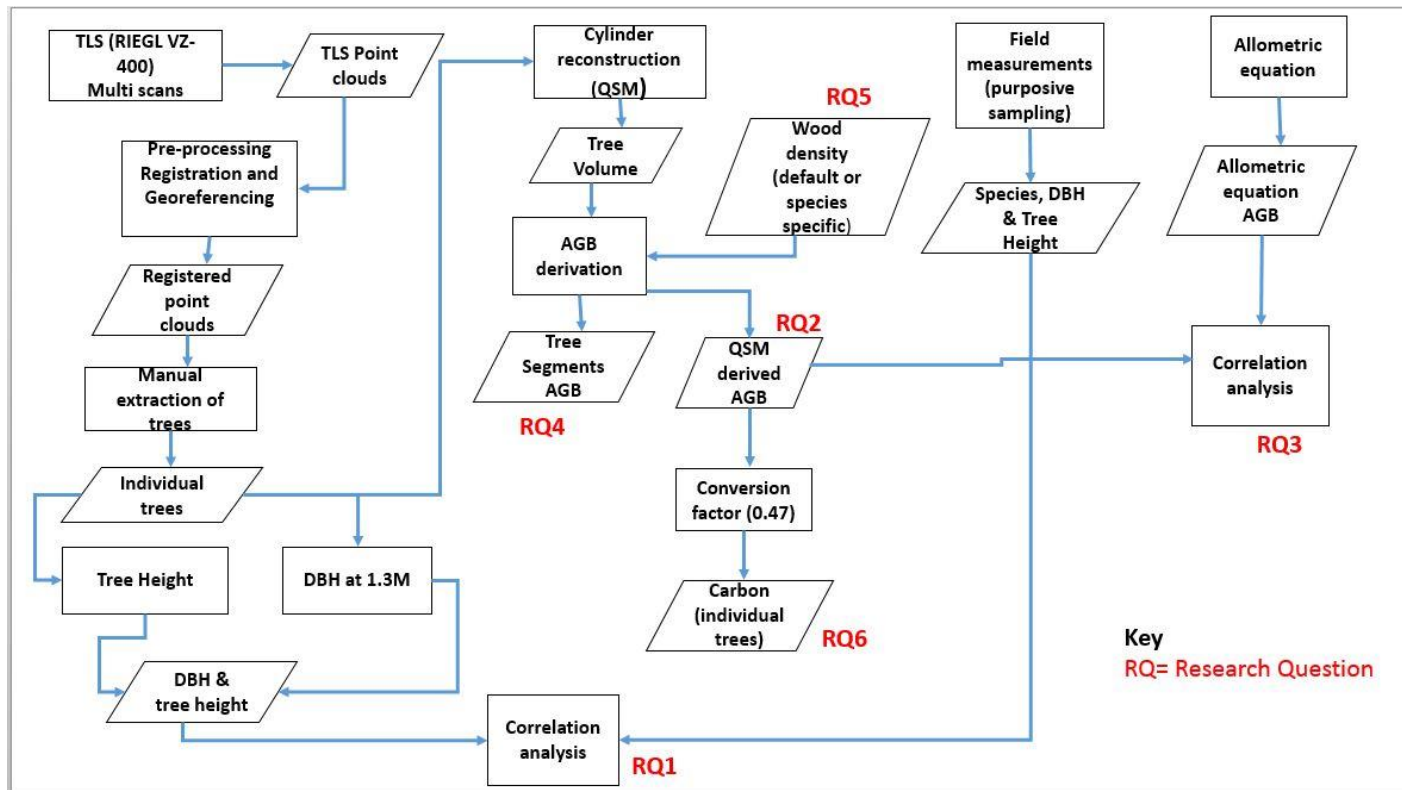
Figure 6: Flowchart of the methods used in this study.

3.4   Pre Field work

Preparation before going to the field involved:

➢ Preparation of field measurement forms.
➢ Acquisition of field equipment, ensuring its working and practising on how to operate it.
➢ Generating of equal grids and sampling units on the Pan-sharpened World View 3 in ArcGIS 10.3.1.
➢ Converting the World View image to CMF format and uploading it into a mobile device for navigation in the field.

3.5   Plot Size

Estimation of forest structure attributes is based on plot size and LiDAR point cloud density but plot size is of importance (Ruiz et al., 2014). Circular plots with an area of 500-600m² are recommended for volume and biomass estimates (Ruiz et al., 2014). Circular plots are relatively easy to establish and are less vulnerable to errors, especially when the radius is not very large (Boon, 1966). An assumption is made that the terrain is flat otherwise a slope correction will be implemented (Boon, 1966). Frazer et al. (2011) mentioned that plots need to be large because they maintain a high degree of spatial overlap in the presence of GPS positional errors, exhibit less between plot variance and are less affected by co-registration error that occurs between ground and LiDAR samples. In this study, a circular plot with a radius of 12.62 m and a resulting area of 500m² was used (Figure 7). This minimized the edge effect associated with LiDAR measurements that is, trees that are outside the boundary having a portion of their crowns falling within the plot and trees inside the plot having their crowns falling outside the plot (Frazer et al., 2011).
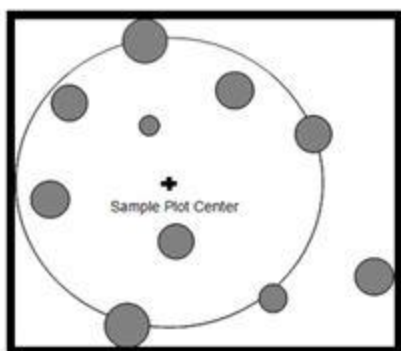
"With circular sample plots, all trees are taken as samples trees that are within a defined distance (radius) from the sample point, which constitutes the plot centre"
("Fixed area plots - AWF-Wiki," 2013)

Figure 7: Circular Sample Plot

3.6 Sampling Design

Purposive sampling was the strategy that was used to sample plots in Ayer Hitam forest Reserve. Purposive sampling also known as judgmental sampling is a non-probability technique where the sampling is done based on the judgement of the researcher (IPCC, 2003). This sampling strategy was employed because of the terrain of the forest and considering the weight of the Terrestrial Laser Scanner which is approximately 27kgs including the camera. Plots were selected based on accessibility and the amount of undergrowth as slashing needed to be conducted to avoid occlusion of the stems. A total of 26 plots each 500m² in size were sampled in the forest (Figure 8). Some plots were sampled in the same grid as long as the distance between them was greater than 50metres. Plot centres were chosen randomly usually in clear view of the TLS.
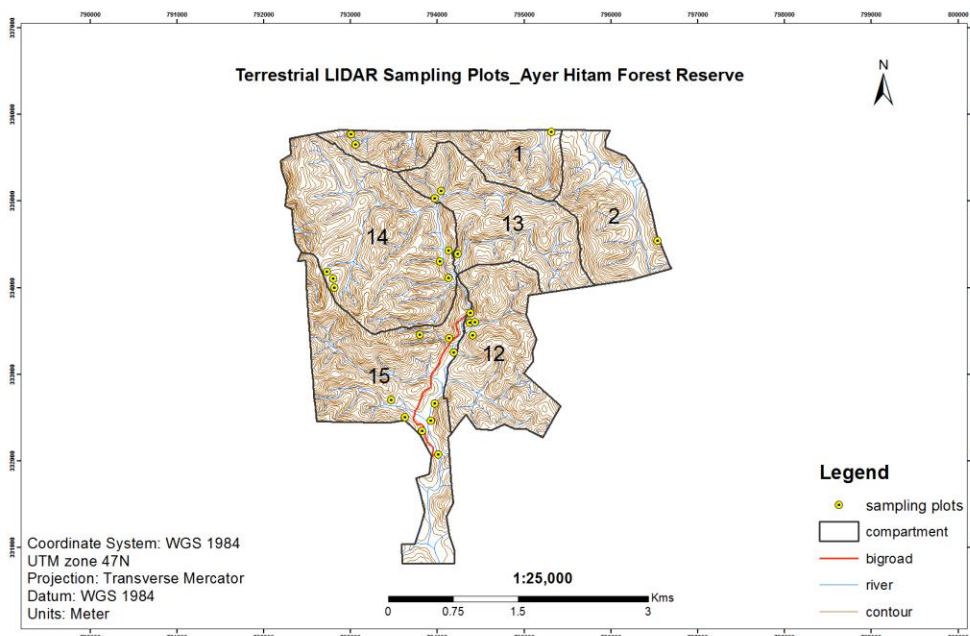
Figure 8: Samples Location in Ayer Hitam Forest Reserve

3.7 TLS plot setup

Setting a TLS plot required several steps to be conducted before actual scanning could be done. These steps included identification of the plot centre, tree labelling and clearing of undergrowth. The steps are described in detail in the following sections.

3.7.1 Centre of the Plot identification

The centre of each plot was determined in relation to the location of the three outside scans in terms of space, slope and undergrowth. The centre of the plot was adjusted accordingly to fit the position of the three outer scans after the slope was measured and the radius was corrected accordingly using a slope correction table. Challenges were encountered in levelling the TLS, especially on sloppy plots.

3.7.2 Tree Labelling

After a defined radius was set according to the slope of the plot, the boundary of the plot was marked by using a measuring tape. All the trees that were inside the defined plot and were equal or greater than 10cm in DBH were marked with a chalk and were labelled with tree numbers that were printed in bold black on an A4 laminated bond paper. The tree labels were placed on the stem of the tree facing the direction of the central scan position. Tree labelling is done to reduce errors in tree detection and identification. Figure 9 shows labelled trees in a plot.

Figure 9: Tree Labels.

3.7.3 Clearing of undergrowth

Ayer Hitam Forest Reserve is a secondary forest because it was once logged over and as a result, it is characterised by a lot of undergrowth. To prevent occlusion of the stem of the trees and for the reflectors to be clearly visible when scanning the plot had to be cleared. This was a time consuming task that lengthened the time needed to set up and scan a single plot.

3.8 Terrestrial Laser Scanner data acquisition

Using a RIEGL VZ 400 multi scans were collected, one in the centre and three outside scans. A multi scan rather than a single scan was preferred in order to get a 3-dimensional view of the trees. With a single scan, scanning is faster but also occlusion is unavoidable whilst in a multi scan the level of detail is higher (Dassot et al., 2011). The three outside scans were set approximately at 120° around the circular plot (Figure 10). The position of the three outer scans was determined by approximating with the legs of the tripod (e.g., 120 degrees). The scanner was placed at a distance of three metres outside the edge or the boarder of the circular plot. Figure 10 shows the difference between a single scan and a multi scan using TLS.
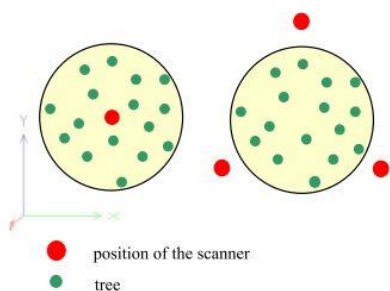
Figure 10: Single and multi-scan mode (Bienert et al., 2006)

3.8.1   Reference targets

When a multi scan is conducted as in the case of this research, the scans are merged into one point cloud by geometric transformation using reference targets placed in the scene and common to the scans (Bienert et al., 2006). The reference targets used are two types of retro reflectors three to four circular that were placed on trees and 12 cylindrical that were placed at the position of the three outer scan positions. The circular retro reflectors placed on the trees were placed in such a way that they were visible from the central scan position and, at least, one circular reflector was visible from each of the three outer scan positions. The cylindrical retro reflectors were also placed in such a way that there were all visible and not obscured from the central scan position and were evenly distributed but not in a linear pattern. The reflectors were securely placed so that they would not be displaced from their position once scanning had started. It was ensured that from the three outer scan positions a minimum of five reflectors were visible that is one circular reflector and four cylindrical reflectors used as tie points and were placed at a distance from the scanner that does not exceed the maximum range of the scanner. Figure 11 shows the two types that were used in scanning.

 (a)   (b)

Figure 11: (a) circular & (b) cylindrical retro reflectors

3.8.2   Scanning with TLS

The RIEGL VZ 400 that was used in this study comes with a camera a Nikon D610 that captures images that can be used to colour the point clouds Red, Green, Blue (RGB) and also takes photographs of the whole scene. The TLS was mounted on a tripod and the camera was mounted on top of the TLS. In order to minimize the roll and the pitch the TLS was levelled by adjusting the legs of the tripod. This was achieved by using the setting on the scanner entitled instrument position setup. Using a circular levelling tool, the instrument was set by manually adjusting the legs of the tripod until the scanner was within at least 1° or less of level. Figure 12 shows a levelled instrument.

Figure 12: Levelled Terrestrial Laser Scanner

After levelling the instrument, scanner settings were set. The settings that were used in all scans throughout the study are specified in Table 4.

Table 4: Scanner settings

Minimum range	1.5m
Reflector diameter	0.10
Reflectance threshold	0.10
Image acquisition	ON
Reflector Search	ON
Register Reflector auto	ON
Registration Mode	Reflector Local
Scan mode	Panorama 60

At each plot a new project that contains all four (4) scan positions was set before scanning started. To test the camera, a test image was taken to see the quality of the images that would be taken. The camera was set to take overlapping images of the plot. The instrument was set to panorama 60 because this allowed acquiring a 360-degree field of view of the plot. After the panorama scan was complete the TLS finds and fine scans and registers the reflectors. The scanned retro reflectors appear red on the screen of the TLS. Figure 13 shows the results of the scanned plots.

Figure 13: Scanned plot in 3D Linear Scaled showing reflectors in red

3.9 Biometrics data

Measurements of DBH, tree height, identification of tree species and crown cover was done in the field. Species information was important for wood density derivation that was used with the QSM derived volume to estimate AGB. Trees with a DBH greater than 10cm (DBH ≥ 10cm) were only measured as trees with a DBH less than 10cm are considered to be insignificant in contributing to the total AGB (Brown, 2002; Talbot et al., 2014). The slope was measured if the sampled plot was not on flat ground and the radius was adjusted accordingly. The biometrics data was collected so as to assess the relationship between the TLS derived parameters height and DBH with height and DBH measured in the field. The field measurement form used is found in Appendix 1 and the slope correction table is found in Appendix 2.

3.9.1 Diameter at Breast Height

DBH was taken at 1.3m height above the ground with a diameter tape. A standardized stick measuring 1.3m was used to mark the DBH position on all the trees since breast height differs per individuals. In the case

of buttress trees and trees with deformities, the 1.3 measurement was taken above the buttress or the trunk deformity (Chave et al., 2014). The team faced challenges in measuring DBH on trees with very large buttresses. Trees that had a fork below 1.3m were taken as two individual trees but if the fork was above 1.3m then it was taken as one tree.

3.9.2   Tree Height

Tree height was measured in metres using a Laser range finder (Leica DISTO D510). Challenges were faced in measuring tree height because of intermingling canopies, it was difficult to distinguish the actual crown of individual trees.

3.9.3   Crown Cover

Crown Cover of each plot was measured using a densitometer. The crown cover percentage was measured from five positions in the plot that is the centre of the plot and from four cardinal positions and then an average was made of the whole plot.

3.9.4   Tree Species

Tree species in all the plots were identified with the aid of a forest ranger. The local name was written in the field and back in the office using a Tree Guide book the scientific name was identified. More than hundred (100) different species were identified.

3.10   Pre-processing of Point Cloud Data

Dassot et al. (2011) described point clouds as unstructured data that needs to be reconstructed by dedicated programmes to provide information. In this study pre-processing of point clouds was done using RISCAN PRO v 2.1. The pre-processing stages that were taken are described in the following section.

3.10.1   Registration of Scan Positions

TLS projects scanned with RIEGL instruments and analysed using RISCAN PRO, have three coordinate systems that is Scanner's Own Coordinate System (SOCS), Project Coordinate System (PRCS) and Geographic Coordinate System (GLCS) (Riveiro et al., 2011). SOCS describes coordinates for each position with respect to the centre, PRCS is user defined and common to all scans of the scanned object and GLCS refers to the cartographic coordinates (Riveiro et al., 2011). The transformation process of the local systems into a common reference system is called registration and often the central viewpoint defines the common reference system (Bienert & Maas, 2009). To be able to analyse different laser scanner positions requires a common reference system and the transformation. In this study, a marker based registration was conducted by finding corresponding tie points/control points to match the different scan positions to the central scan position. Control points in RISCAN PRO are defined by tie points that match to the centre of the retro-reflectors (Riveiro et al., 2011). This method is described as a reliable and a precise method although it can be time consuming (Bienert & Maas, 2009). After registration using tie points, fine registration was conducted on the point clouds. The fine registration was done using Multi Station Adjustment (MSA) algorithm in RISCAN PRO (Appendix 3). MSA algorithm modifies the orientation and position to calculate the best overall fit (Calders et al., 2014; Riegl., 2005). The point clouds were converted into poly-data to run the MSA using the plane patch filter. Figure 14 shows a registered plot displayed in single scan colour. The scan positions displayed in green, red, yellow and blue. Table 5 shows the errors in metres after MSA.
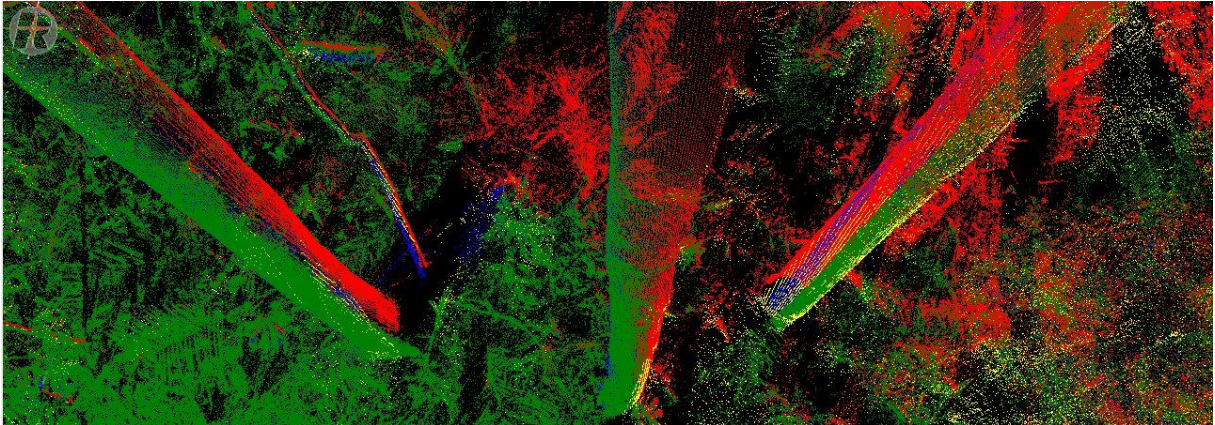
Figure 14: Registered Plot displayed in 3D -single colour

Table 5: Plot Registration errors

Plot	1	2	3	4	5	6
Error(m)	0.0185	0.0162	0.02	0.0153	0.016	0.0138
Plot	7	8	9	10	11	12
Error(m)	0.0149	0.014	0.0201	0.0149	0.0127	0.0146
Plot	13	14	15	16	17	18
Error(m)	0.0163	0.0157	0.0206	0.0177	0.0224	0.0155
Plot	19	20	21	22	23	24
Error(m)	0.0179	0.0195	0.0206	0.0158	0.0184	0.0148
Plot	25	26				
Error(m)	0.0169	0.0158				

3.10.2   Extraction of single trees

Extraction of trees was conducted manually in RISCAN PRO. The point clouds were displayed either in 3D linear scaled or true colour to enhance visualization of the tree tags. The point cloud was displayed in top view and all the point clouds associated with the point cloud of an individual tree were selected with a selection tool in RISCAN PRO. The point cloud selected had crowns from other trees because of the overlapping nature of the canopies of the trees in the study area. Point clouds from other trees and undergrowth were removed until a good representation of the tree was achieved. This is a time consuming task and it was challenging to separate the crowns of individual trees because of the large overlap among tree crowns and thus, Terrestrial LiDAR scanners still remain a technological challenge because of the structural complexity of forests (Dassot et al., 2011). Figure 15 shows an extracted tree. Two types of errors occur when extracting trees and these are type I and type II errors. Type I errors occur when trees are not detected mainly due to full or partial occlusion of the stems (Maas et al., 2008). Type II occurs in a false detection when a tree is given a wrong tag (Maas et al., 2008). Type II errors can be eliminated by checking the height and stem profile (Maas et al., 2008).
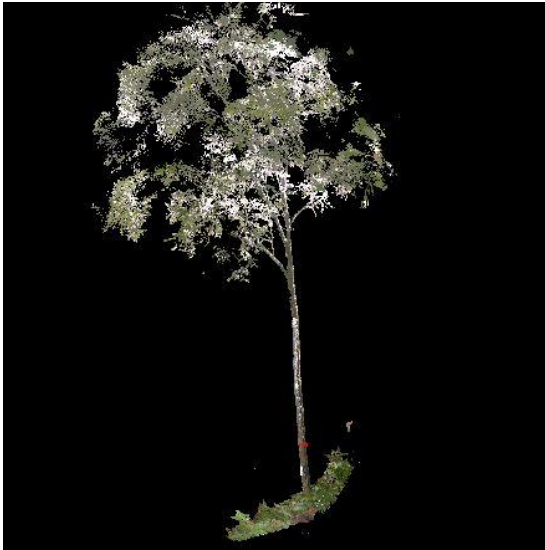
Figure 15: Extracted Tree displayed in true colour

3.11   Extraction of Tree Parameters

DBH and Height was measured from the point clouds in RISCAN PRO. The details of how the parameters were measured are described in the sections below.

3.11.1   DBH measurement

Using the distance tool in RISCAN PRO, DBH was measured as the horizontal distance at 1.3m above the base of the stem. For buttress trees, a representative point cloud above the buttress was selected as the starting point in measuring the 1.3 metres. This was done to ensure consistency in the method that was used in the field to measure DBH. Figure 16 shows the measurement of DBH on point cloud data.

(a)   (b)
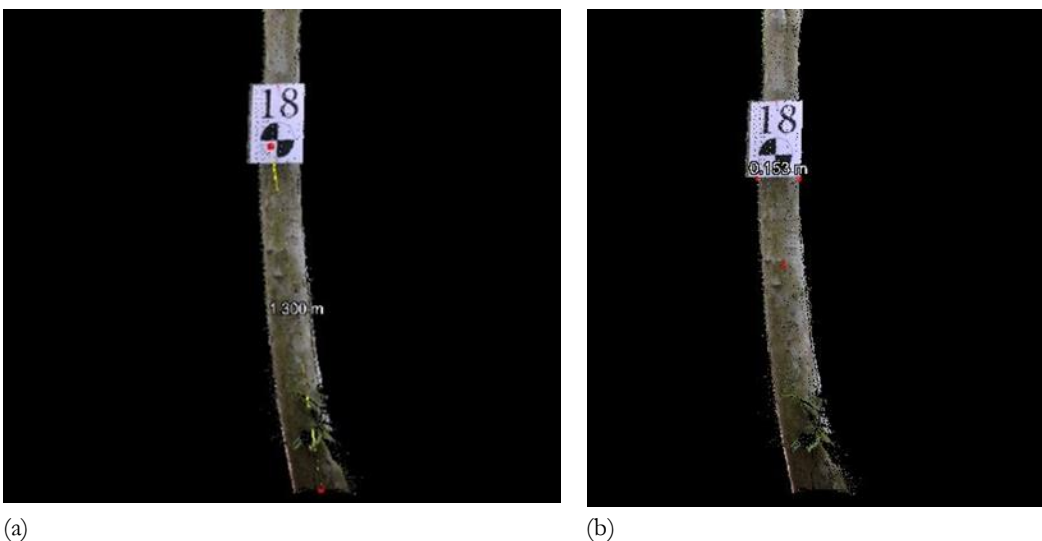
Figure 16: Measuring of DBH (a) vertical distance 1.3m above ground (b) horizontal distance at 1.3 m above the ground

3.11.2 Height Measurement

Tree height is derived by the difference between the highest point of the point cloud and the representative ground points (Maas et al., 2008; Bienert et al., 2006) (Figure 17). Using the distance tool in RISCAN PRO tree height was measured by identifying the lowest and highest point and measuring the distance between the two. Maas et al. (2008) stated that this procedure leads to an underestimation of the tree height as a result of the under sampling character of the TLS and occlusions of tree crowns.

Figure 17: Tree height measurement

3.12 Quantitative Structure Modelling

Running the QSM involved conversion of point clouds into an x, y, z format, in this case, an ASCII text file, filtering and selection of optimum modelling parameters. Each of the stages is explained in detail in the following sections.

3.12.1 Conversion of point cloud to ASCII file

To be able to run the QSM on the point clouds, the point clouds need to be in any x, y, z format. In the case of this study, the extracted trees were saved as poly-data in RISCAN PRO. Using the export function in RISCAN PRO the poly-data was converted into an ASCII text file that was readable in MATLAB for the reconstruction process.

3.12.2 Filtering of point clouds

There are two kinds of filtering that take place to a point cloud in the reconstruction. The first filtering takes place before the QSM reconstruction and the second one takes place during the construction of the QSM (Åkerblom, 2012). The first filtering is done to remove noise or isolated points from the point cloud (Raumonen et al., 2013). The initial filtering removes groups of isolated points which are usually noise or irrelevant measurements (Åkerblom, 2012). Points are considered to be isolated if the neighbour cover sets are empty and thus, there are discarded from the analysis (Åkerblom, 2012). This first filtering does not consider the structure of the tree (Åkerblom, 2012). The second filtering that takes place during the construction of the QSM identifies the ground and components that are part of another tree, undergrowth or some irrelevant objects and considers the geometry of the tree (Åkerblom, 2012). The approach of filtering is based on cover sets and it works by forming small sets using a random point as the centre and sets that are not part of the large component are removed (Åkerblom, 2012). To reject the isolated points in the cloud the point cloud is covered by cover sets, and the cover sets with fewer than the set number of points are rejected (Raumonen et al., 2013). The size of the cover sets and the number of points depend on

the density of the points in the data (Raumonen et al., 2013). The values of the filtering parameters and their results on the resulting tree model depend on the noise and its distribution in the data (Raumonen et al., 2013). The same parameter values work for similar trees and scanner parameters (Raumonen et al., 2013). The output of the filtering is a logical vector of points (Figure 18). The following filtering code describes the parameters used when conducting the filtering process on the point clouds.

Pass = filtering (P0, r1, n1, d2, r2, n2, Scaling, Comp);
P = P0 (Pass, :);

P0	Unfiltered point cloud.
r1	Radius of the balls used in the first filtering.
n1	Minimum number of points in the accepted balls of the first filtering.
d2	Minimum distance between the centres of the balls in the second filtering.
r2	Radius of the balls used in the second filtering.
n2	Minimum number of balls in the components passing the second filtering.
Optional inputs,	default value false
Scaling	If true, the first filtering threshold "n1" is scaled along the height with average point density.
Comp	If true does the first filtering process for every point.

Because the same scanner parameters were used for scanning all the trees, filtering was conducted on all the tree species using the same parameters keeping in mind the following rules of thumbs. The units of the parameters were converted to metres because the point cloud data used in the study was in metres.

r1 = the smallest size of the branches to be modelled (Åkerblom, 2012) (1.5cm = 0.015m used in this case).
d2 = in trees d the recommended value is approximately 1 to 3cm (0.01m to 0.03m) (Raumonen et al., 2013).
r2 = r2 > d2. This ensures that clusters to be removed are clearly from other points. It is recommended that r2 should be either greater by half a centimetre or a centimetre than d2 (Raumonen et al., 2013).
Scaling & Comp = 1 if true or 0 if false

(a) Extracted tree   (b) Classified image   (c) Filtered image
(151 492 points)   (14 965 points removed in red)   (136 527 points)
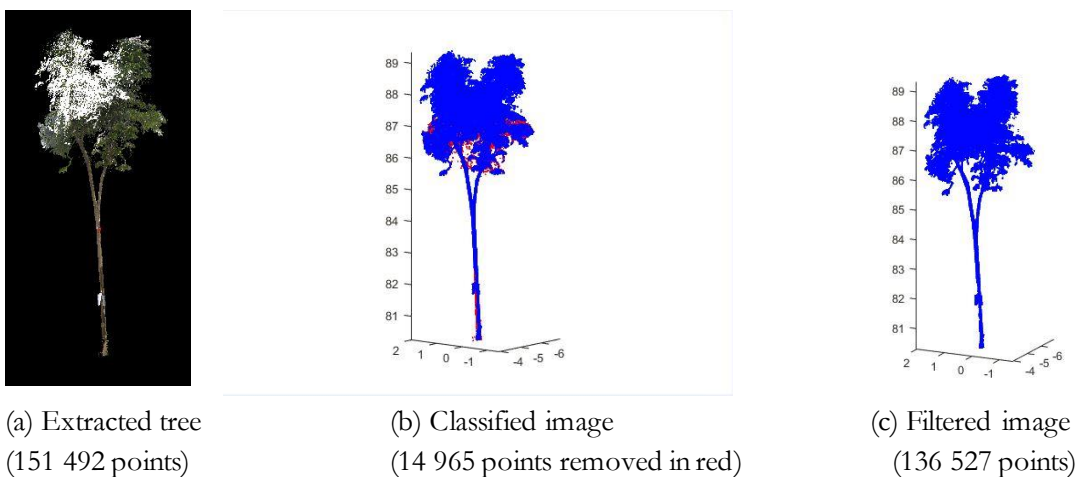
Figure 18: Filtering Process

3.12.3   Optimum parameters for QSM modelling

After initial filtering the filtered point cloud is used as an input into the QSM. The QSM is constructed by the code:

qsm_tree(P,PatchDiam1,BallRad1,nmin1,PatchDiam2Min,PatchDiam2Max,BallRad2,nmin2,lcyl,OnlyTree ,Tria,string,FilRad); where:

P	(Filtered) point cloud, (m_points x 3)-matrix, the rows give the coordinates of the points.
PatchDiam1	Cover set size of the first uniform-size cover.
BallRad1	Ball size used for the first cover generation.
Nmin1	Minimum number of points in BallRad1-balls.
PatchDiam2Min	Minimum patch size of the cover sets in the second cover.
PatchDiam2Max	Maximum cover set size in the base of the stem in the second cover.
BallRad2	Maximum ball size used for the second cover generation.
Nmin2	Minimum number of points in BallRad2-balls.
Lcyl	Cylinder length/radius ratio. Can have multiple values, in which case makes as many models with the same segmentations.
OnlyTree	Logical value, true if only points from the tree to be modelled, in which case defines the base of the trunk as the lowest part of the point cloud.
Tria	Logical value, if true, then make triangulation for the stem up to first branch.
String	Name string for saving output files.
FilRad	Optional input, relative radius for outlier point filtering. Can have multiple values in which case makes as many models with the same segmentations.

When the parameters for reconstructing the tree are being set the following rules of thumb are kept:

➢ The BallRad1 and BallRad2 should always have a value larger than for PatchDiam1 and PatchDiam2 Max, for example, BallRad2 = Patch Diam2Max + 0.01 (Raumonen et al., 2013). The BallRad should be bigger to ensure that cover sets next to each other intersect and are neighbours (Raumonen et al., 2013). In this study values of 0.14 and 0.13 metres were used respectively for the values of BallRad1 and BallRad 2.

➢ Values for PatchDiam1 and BallRad1 are not very important but they should be large as compared to PatchDiam2Min. Values of 8-16 cm work for PatchDiam1 (Raumonen et al., 2013). The values for PatchDiam1 and BallRad1 are used in the first segmentation and remove points that do not belong to the tree such as ground or understory points (Raumonen et al., 2013). The value used for PatchDiam1 used in this study was 0.12 metres.

➢ The values for PatchDiam2Min need to be smaller and should be close to the values of the smallest branch to be modelled (Åkerblom, 2012). PatchDiam2Min parameter governs the size of the cover set and this affects the result of the QSM (Raumonen et al., 2013). This value decreases quadratically from the base to the tip along the branches (Åkerblom, 2012; Raumonen et al., 2013). Values for PatchDiam2Min used in this study ranged from 0.01 to 0.05 metres depending on the tree to be modelled.

➢ Lycl controls the average relative length of the cylinders and the bigger the lcyl is the longer the fitted cylinders on average (Raumonen et al., 2013). Shorter cylinders can better model the local diameter of the branch, but on the other hand, their direction can be more varying and noisy and

can make the diameter too large or too small (Raumonen et al., 2013). Lcyl can have multiple values e.g. (1 3 5). In this study lcyl values used were 3, 5 and 8 depending also on the tree modelled.

➢ FilRad defines the relative radius for outliner point filtering before least square fitting (Raumonen et al., 2013). The default value for FilRad is 3.5 and this implies that points that are farther than 3.5 times the estimated radius from the axis are filtered from the region (Raumonen et al., 2013). The default value is large and has little effect but, depending on the noise and co-registration accuracy smaller values such as 1.5 and 2.5 are used to ensure that the fitted cylinders are not too big (Raumonen et al., 2013). FilRad like lcyl has multiple values. FilRad values used in this study were 1.5, 2.5 and 3.5 also depending on the tree to be modelled.

➢ Nmin is the minimum points in a single cover set. This value sets the threshold if a cover set is kept or is discarded in the reconstruction process and it is robust to a certain threshold (Calders et al., 2015). Large values lead to an underestimation of volume in the crown, but small values lead to overestimation of volume in the crown (Calders et al., 2013).

In running the QSM algorithm, the human interface is on the selection/input of optimum modelling parameters. Careful selection is required as the parameters affect the quality of the reconstruction. Optimum modelling parameters were selected by varying three inputs that is the Patch Diam 2Min, lycl and the FilRad with PatchDiam2Min being the most important parameter in the reconstruction process. All possible combinations of the three parameters were used for modelling. The combination of parameters that had the smallest mean point to model distance were selected as the optimum parameters for modelling. The optimum modelling parameters for some of the 100 trees are in Appendix 4. The resulting QSM was compared visually with the point cloud to assess the quality of the reconstruction as recommended by Calders et al. (2013). Figure 19 shows an example of a visual comparison of a reconstruction, in this case, an incorrect reconstruction.

(a) Filtered image   (b) Final QSM
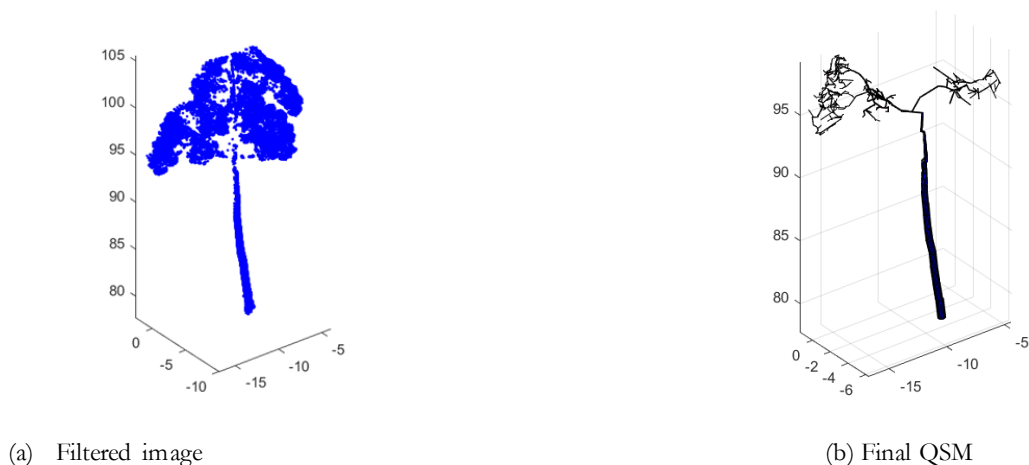
Figure 19: Example of incorrect reconstruction

3.12.4   Main steps in the reconstruction process

Figure 20 shows the main stages in the reconstruction of a QSM model. The flow chart in Figure 20 and subsections describe the stages of the reconstruction in detail.
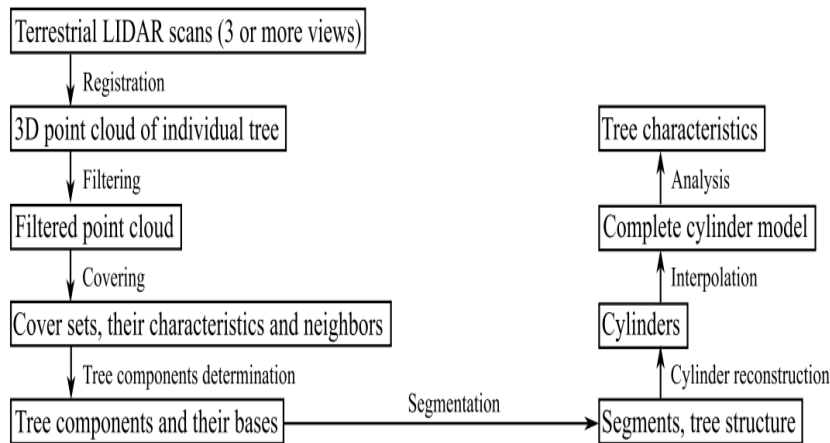
Figure 20: Main steps in the reconstruction process (Raumonen et al., 2013)

3.12.5 Covering

A cover set is defined as a spherical environment of the centre point with a radius r (Åkerblom, 2012). The algorithm uses the principle of the set theory and if the point cloud is P then the cover set is a subset of P and the union of all the cover sets is a complete point cloud (Åkerblom, 2012). The collection of all the cover sets is the cover of the point cloud (Åkerblom, 2012). The cover sets are like building blocks that build the tree from the bottom to the top (Calders et al., 2015). The cover sets are generated by spherical neighbourhoods of randomly selected points from the point cloud (Åkerblom, 2012). The cover sets are governed by two parameters that is the diameter (d) which defines the minimum distance between the centres of two balls and radius (r) which is the radius of the spherical balls (Raumonen et al., 2013; Åkerblom, 2012). The radius (r) is either a constant or varies for all the cover sets. The size of the cover set radius should be chosen according to the size of the scanned object that means prior information about the object must be known (Åkerblom, 2012). If the size of the radius is too big it implies that finer details of the object will not be modelled and if it's too small the point cloud will be divided into too many disconnected components (Raumonen et al., 2013). For trees, the rule of thumb is that the radius of the cover sets should be equal to the size of the smallest branch to be modelled (Åkerblom, 2012). d and r should be as small so that the cover sets conform to the details of the surface to be modelled and they should be large enough so as to reduce the computational time of modelling and they can be reliably used to estimate different characteristics of the object (Raumonen et al., 2013). The parameter (d) diameter should be smaller or equal to (r) the radius (d ≤ r) (Raumonen et al., 2013). The diameter controls the amount of intersection between the cover sets by avoiding a chosen centre point to be in multiple cover sets (Raumonen et al., 2013). In the case of trees d is approximately 1 to 3 cm (Raumonen et al., 2013; Åkerblom, 2012). The cover sets should intersect and if two cover sets intersect there are called neighbours (Åkerblom, 2012). The neighbour relation determines the connectedness of the point cloud (Åkerblom, 2012). The characterization of the cover sets involves estimating the direction, size and dimension for each cover set and these are classified into three classes that is cover sets that belong to ground components of the tree, the main stem and the branches (Åkerblom, 2012). The cover sets that belong to the ground are filtered out because there are not important in the reconstruction process (Åkerblom, 2012).

3.12.6   Tree Components determination

The step that follows cover set generation is the extraction of cover sets that concern the tree, this is done by modelling the base of the trunk from the bottom of the point cloud (Calders et al., 2015; Raumonen, et al., 2013). The aim of this stage of reconstruction is to form one single component from the base upwards. Any point cloud that belongs to the ground is removed and the base of the trunk of the tree is defined (Åkerblom, 2012; Raumonen, et al., 2013). Åkerblom, (2012) defined a component as a maximum set of connected cover sets. The aim of forming as many components as possible is such that each cover set is part of a component which would imply that all the cover sets are connected to each other (Åkerblom, 2012). This is achieved by altering the neighbour relations of the cover sets such that at the end all the separate components are connected into one component which is the tree (Calders et al., 2015). Figure 21 (a) & (b) below show the concept of connected components. Figure 21 (a) "the points p and q are in the same component because there is a chain of overlapping balls connecting them but v and w are in different components because there are no balls connecting them" and Figure 21 (b) "an arbitrary ball (red) is chosen and it's expanded by an iterative process where overlapping balls are added to the existing ones."

(a) Definition of connected components   (b) Determination of connected components
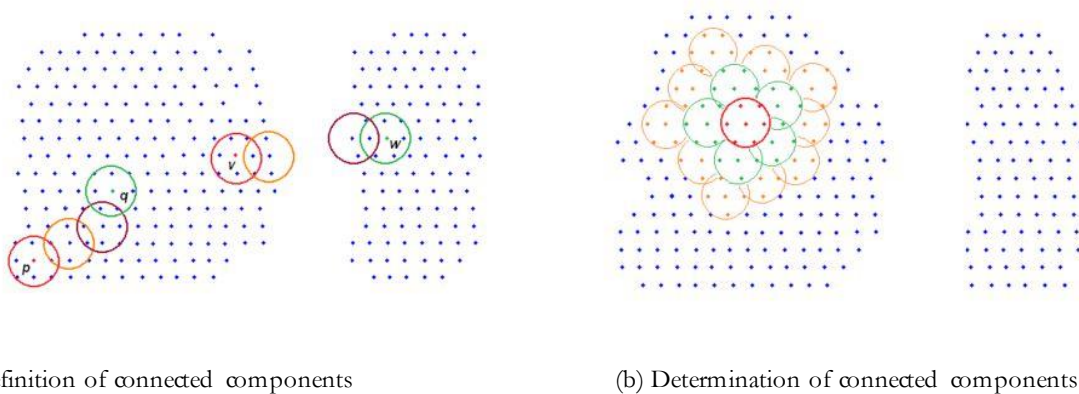
Figure 21: Tree component determination (Raumonen et al., 2012).

3.12.7   Segmentation

Segmentation is a process that takes place after defining tree components and the components are segmented into stem and branches (Calders et al., 2015). The components are partitioned into segments that resemble the whole part of a real branch or trunk (Raumonen et al., 2013). The process of segmentation is based on the topology of the tree (Åkerblom, 2012). The segmentation describes the tree structure that is the branching relations of the child and parent branches for each branch (Raumonen et al., 2013). Segmentation is controlled by the cover sets and their neighbour relations and starting from the base it is a step by step process along the formed components (Raumonen et al., 2013). The segmentation process occurs twice, with the first segmentation using the large cover sets to define the local size of the branches based on the branching order, branch position and height (Calders et al., 2015). This results of the first segmentation are used for the second segmentation where the cover set is much smaller and the size decreases linearly along the branch from the base to the tip and with increasing height and branching order the branch base will decrease (Calders et al., 2015).

3.12.8   Cylinder reconstruction

The segments are reconstructed with cylinders which approximate the radius and orientation of each branch (Raumonen et al., 2013). The cylinders are fitted in a least square sense and the length of each cylinder is defined by the parameter lcyl (Calders et al., 2015). To remove unrealistic cylinders the radius of the cylinders are checked by examining the radius of the parent and child segments, if the child segment has a radius

greater than the radius of the parent segment it is set to the radius of the parent and the diameter of the branch decrease as the distance from its base increases (Raumonen et al., 2013; Calders et al., 2015). Along the segment, the radius is controlled by a parabola shaped taper that makes the radius decrease towards the tip (Calders et al., 2015).

3.12.9   Complete cylinder model

The cylinder model is completed by refining the errors that could have risen and this is done by closing the gaps between the parent and child cylinders so as to reduce errors for the tree statistics (Raumonen et al., 2013). The gaps between the cylinders are closed using previously fitted cylinders (Raumonen et al., 2013). Figure 22 "the green cylinder has no extension and the blue one has no parent, the gap is filled by the red cylinder".
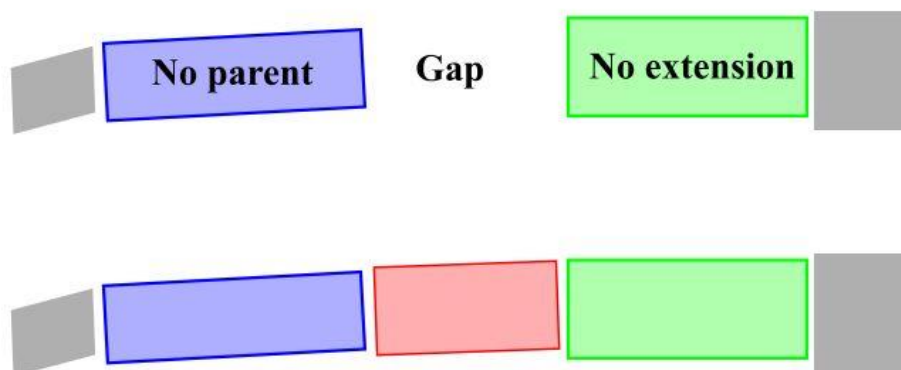
Figure 22: Filling gaps (Raumonen et al., 2013)

3.12.10   Tree characteristics

The final cylinder model gives characteristics of the tree such as volume and length of the trunk, branches and also the total tree volume. The model also gives the number of branches, the angles between the child and parent branches (Raumonen et al., 2013). An example of the output of the model is found in Appendix 6. The above ground biomass of a tree was determined by the volume and the density of the tree.

3.13 Statistical Analysis

The data was analysed statistically and the details of the analysis are described in the following sections below.

3.13.1   Descriptive statistics

Descriptives of the field and TLS measured parameters DBH and height were conducted to observe the distribution of the data. Shapiro wik tests of normality were conducted on the parameters.

3.13.2   Comparison of Field & TLS DBH and Height

To assess the relationship between the parameters measured in the field and from the TLS, a correlation analysis was carried out. To test the significance difference a t- test was used.

3.13.3   Comparison of allometric and QSM AGB

Above Ground biomass was deduced by using an allometric equation from Chave et al. (2014) (AGB= $[0.0673* (p*D^2H)$ ^0.976]. The AGB from the QSM was derived by multiplying the volume by the wood density. The relationship was assessed by the use of correlation and to test the significance difference between the above ground biomass a t- test was used.

3.13.4   Distribution of AGB on tree components

To assess the differences in the AGB from the different parts of a tree a t- test was used to investigate if there is a significant difference in the distribution of above ground biomass on different parts of the tree.

3.13.5   Comparison of specific and default wood density

AGB was calculated using either the default wood density value or species specific wood density values. $0.57 g/cm^3$ is the default value of tropical tree species in Asia (Hirata et al., 2012). Species specific wood density values were obtained from the World Agroforestry Centre Wood Density Database (World Agroforestry Centre, 2011). To test the significance in using either default or species specific wood density in determining AGB a t- test was used.

3.14 Sensitivity Analysis

There are parameters that can affect the volume reconstruction of the tree. In this study, the impact of the QSM input parameters on the volume was assessed. This was conducted on the number of runs, cover set diameter and the nmin values. Different values of these parameters were tested to deduce their effect of the volume derived from the reconstruction.

3.14.1   Different runs on volume derivation

The cover set generation is random in the reconstruction algorithm and thus, the final QSM is different for each run even if the same parameters are used (Calders et al., 2015; Raumonen et al., 2013; Åkerblom, 2012). A number of different runs were tested using a one-way analysis of variance.

3.14.2   Cover set diameter and volume derived

The cover set diameter is one of the most important parameters that is critical in modelling an accurate QSM reconstruction. An incorrect value of this parameter can lead to an underestimation or overestimation of the volume and thus the derived AGB (Calders et al., 2015). In this study, the cover set diameters to model the trees ranged from 0.01m to 0.05 metres. To test if there is a significance difference in the size of the cover set diameter and the volume derived a one-way analysis of variance and a post hoc test was carried out.

3.14.3   Nmin values and crown volume

Nmin which is a value that controls the minimum threshold of points to be included in a single cover set affects the reconstruction(Calders et al., 2015; Calders et al., 2013). Small values can lead to overestimation of volume in the canopy and too large values to an underestimation of the volume of the canopy (Calders et al., 2013). Nmin values in the reconstruction are two that is nmin 1 & 2 that are used in the first and second segmentation of the reconstruction process. A test was conducted to investigate the effect of varying the nmin values on the crown volume. A one-way ANOVA with a post hoc test was used to test the hypothesis.

4 RESULTS

4.1 Extraction of individual Trees

A total of 821 trees were measured in the field from 26 plots. Trees were manually extracted from each of the plots and a total of 657 trees were extracted successfully. A total of 164 trees were recorded missing. The extraction percentage for all the plots was 80.02%. Detailed extraction per plot is summarized in Table 6 and examples of extracted trees are shown in Figure 23.

Table 6: Trees extracted from TLS point clouds

Plot No	Field recorded	TLS derived	Extraction %	Missing trees	Plot No	Field recorded	TLS derived	Extraction %	Missing trees
1	17	16	94.12	1	14	35	16	45.7	19
2	25	23	92	2	15	38	20	52.6	18
3	30	27	90	3	16	30	17	57	13
4	25	24	96	1	17	36	22	61.11	14
5	23	21	91.3	2	18	37	36	97.3	1
6	26	26	100	0	19	29	23	79.3	6
7	29	26	89.7	3	20	25	22	88	3
8	26	25	96.15	1	21	43	41	95.3	2
9	31	28	90.3	3	22	39	37	94.87	2
10	25	12	48	13	23	31	17	54.8	14
11	29	19	65.5	10	24	26	26	100	0
12	36	18	50	18	25	23	21	91.3	2
13	25	13	52	12	26	27	26	96.3	1
No of plots	**Total trees**	**TLS derived**		**Missing trees**		**TLS derived %**		**Missing %**	
26	**821**	**657**		**164**		**80.02**		**19.98**	

Figure 23: Examples of extracted trees displayed in true colour

4.2 Descriptive Statistics of data

Using SPSS descriptive statistics was carried out on DBH and height measured from the field and from the TLS. Details of the descriptive are described in the following section.

4.2.1 DBH and Height

A total of 42 trees were removed because they had field measurements of height missing and thus the number of trees reduced to 615. Descriptive statistics was conducted on both the field parameters that is DBH and height and also on TLS derived parameters DBH and height. A mean DBH of 22.99cm and 22.85cm was recorded respectively from the measured field DBH and TLS DBH (Figure 24a & b) while Field and TLS Height showed a mean of 14.3 metres and 16.74 metres respectively (Figure 25 a & b).

(a) (b)
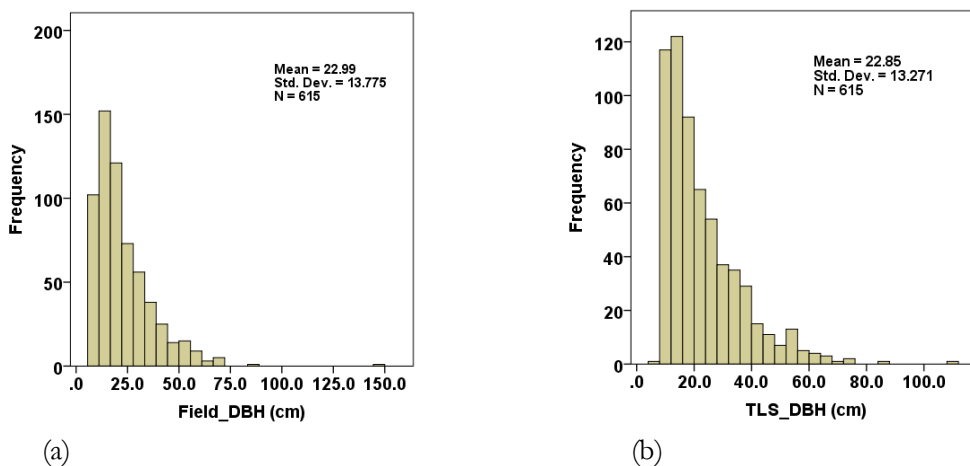
Figure 24: Distribution of DBH (a) Field DBH and (b) TLS DBH

(a) (b)
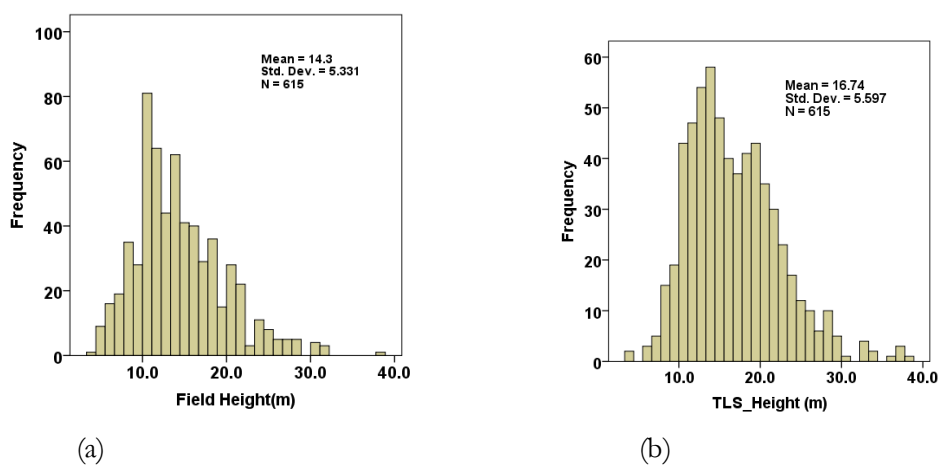
Figure 25: Distribution of Height (a) Field Height and (b) TLS Height

4.2.2 Normality tests of DBH

Normality Tests (Table 7) were conducted on the DBH and height derived from the field and from the TLS. A Shapiro _wik test (p <0.05) and a visual review of the histograms showed that both DBH and height were not normally disturbed. A visual inspection of the DBH histograms showed that there were both positively skewed. A visual examination of the height histograms revealed that they were less skewed. In this study parameters derived from TLS were used for analysis.

Table 7: DBH and Height normality Tests

	Shapiro_wik		
	Statistic	df	Sig
Field DBH	0.802	615	9.1E-27
TLS DBH	0.840	615	2.0E-24
Field Height	0.958	615	3.6E-12
TLS Height	0.962	615	1.4E-11

4.3 Relationship between TLS derived parameters (DBH & Height) with ground measurements

Out of the 615 observations, a total of 15 observations were removed as outliers. A total of 600 observations were used to assess the relationship between DBH and height derived from the field and that derived from TLS. The scatter plot of field and TLS DBH (Figure 26a) shows a high correlation between the DBH measured in the field and the one measured from TLS a correlation coefficient (r) of 0.996 and a coefficient of determination of (R^2) of 0.993. The residual mean squared error (RMSE) for DBH was 1.1cm. The scatter plot of field and TLS height (Figure 26b) shows a low correlation between height measured in the field and height measured from the TLS with a correlation coefficient (r) of 0.767 and a coefficient of determination of (R^2) of 0.589. The RMSE for height was 3.4metres. The regression statistics can be found in Appendix 5.

(a)   (b)
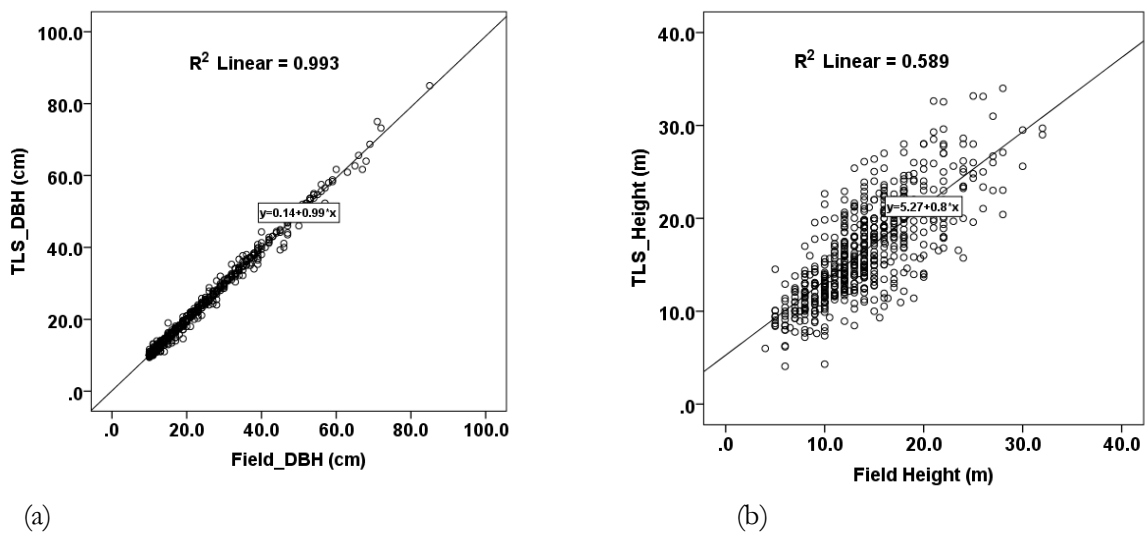
Figure 26: Scatter plot (a) Field and TLS DBH and (b) Field and TLS Height

F test two samples for variances

To determine which t-test to use an F test two sample for variances was used. The null hypothesis tested if the samples have equal variances. The null hypothesis was accepted in both cases (p>0.05) (Table 8) and the t-test used in both cases was a two sample t-test assuming equal variances.

Table 8: F test for variances

	Field Height (m)	TLS_Height (m)	Field_DBH (cm)	TLS_DBH (cm)
Mean	14.1	16.5	22.8	22.6
Variance	25.2	27.4	166.5	163.2
Observations	600	600	600	600
df	599	599	599	599
F	0.92		1.0	
P(F<=f) one-tail	0.14		0.40	
F Critical one-tail	0.87		1.14	

T-test assuming equal variances

To test whether the relationship between DBH and height measured in the field and that measured using TLS is significant a t- test assuming equal variances was used to test the hypothesis. Results showed (Table 9) that there is no significant difference ($p > 0.05$) between DBH measured in the field and DBH derived from TLS. In the case of height, the results show that there is a significance difference ($p < 0.05$) between height measured from the field and height derived from the TLS.

Table 9: t- tests for DBH & Height

	Field_DBH (cm)	TLS_DBH (cm)	Field Height (m)	TLS_Height (m)
Mean	22.8	22.6	14.1	16.5
Variance	166.5	163.2	25.2	27.4
Observations	600	600	600	600
Pooled Variance	164.8		26.3	
df	1198		1198	
t Stat	0.23		-8.35	
P(T<=t) two-tail	0.82		1.88E-16*	
t Critical two-tail	1.96		1.96	

*.Significant at 95% level of significance

4.3.1   Relationship between Field and TLS derived parameters per plot

The relationship between field and TLS derived parameters that is DBH and height was assessed for all the 26 plots measured in the field (Table 10 & Table 11) respectively. The R^2 was high for DBH and generally low for the height in all the plots with the lowest value being recorded in plot 8 of 0.3.

Table 10 : Plot wise comparison Field DBH & TLS DBH

Plot	1	2	3	4	5	6	7	8	9	10	11	12	13
R	0.99	0.99	0.98	0.99	0.99	0.99	0.99	0.99	0.99	0.99	0.99	0.99	0.99
R^2	0.99	0.98	0.97	0.99	0.99	0.99	0.99	0.99	0.99	0.98	0.99	0.98	0.98
RMSE(cm)	0.3	0.7	2.5	0.3	1.56	0.30	0.31	0.37	0.64	1.08	1.03	1.02	1.43
Plot	14	15	16	17	18	19	20	21	22	23	24	25	26
R	0.99	0.99	0.99	0.99	0.99	0.99	1	0.99	0.99	0.99	0.99	0.99	0.99
R^2	0.99	0.99	0.98	0.98	0.99	0.98	1	0.99	0.98	0.99	0.99	0.99	0.99
RMSE(cm)	1.13	0.9	1.72	0.65	0.96	2.05	4.32E-15	1.01	1.36	0.65	1.63	1.24	1.01

Table 11: Plot wise comparison Field Height and TLS Height

Plot	1	2	3	4	5	6	7	8	9	10	11	12	13
R	0.83	0.82	0.79	0.73	0.74	0.80	0.77	0.54	0.73	0.88	0.82	0.97	0.81
R^2	0.69	0.67	0.63	0.54	0.56	0.65	0.59	0.30	0.55	0.77	0.68	0.94	0.66
RMSE(m)	1.79	1.62	2.46	2.2	3.0	2.3	2.8	1.52	3.14	1.37	2.55	1.01	2.18
Plot	14	15	16	17	18	19	20	21	22	23	24	25	26
R	0.83	0.76	0.96	0.72	0.86	0.88	0.88	0.79	0.91	0.95	0.85	0.84	0.83
R^2	0.7	0.58	0.93	0.52	0.74	0.78	0.77	0.64	0.84	0.91	0.74	0.71	0.70
RMSE(m)	2.13	2.55	2.33	1.96	2.0	3.3	2.76	2.53	2.58	2.83	2.18	3.67	2.54

4.4 Quantitative Structure Modelling Above Ground Biomass

Out of all the 615 trees extracted, 100 trees were chosen for the reconstruction algorithm. The trees were chosen on the grounds of extraction quality. The trees were selected across all the 26 plots (Figure 27) and represented the distribution of the DBH observed in the study area. Using the optimum modelling parameters the QSM was run in MATLAB five times for each tree and the means and standard deviations were computed. The output of the MATLAB run is a Matlab file called "ModelData" which contains the cylinder data, the branch data, tree attributes, run data and point to model statistics. The output tree attributes gives the total volume of the tree, trunk, branches and branch order data. An example of the output is given in Appendix 6. The QSM also gives an output of four figures that is (Figure 28 a- d) (a) the filtered point cloud, (b) QSM and segmented point cloud, the colour indicates the branching order (c) QSM model the cylinder colour marks the branching order, and (d) triangulation model of the bottom part of the trunk . Using the volume derived from the QSM and the wood density the above ground biomass per tree was calculated. In this study a default wood density (DWD) value of 0.57g/cm³ (Hirata et al., 2012) and species specific wood density (SWD) values per species obtained from the World Agroforestry Centre Wood Density Database (World Agroforestry Centre, 2011) were used to calculate the above ground biomass. 71% of the observations had canopy biomass greater than trunk biomass whilst 29% of the observations had trunk biomass greater than canopy biomass. The analysis was conducted considering observations where the trunk biomass was greater than canopy biomass and observations where canopy biomass was greater than trunk biomass factoring in differences if either default wood density or species specific wood density was used for calculation.
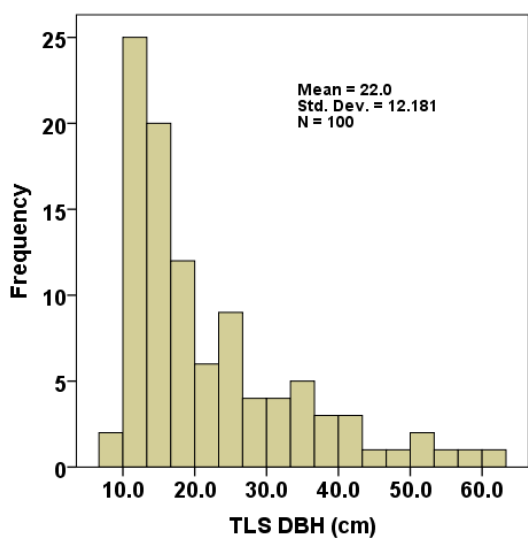
Figure 27: Distribution of DBH of trees used for reconstruction algorithm (QSM)
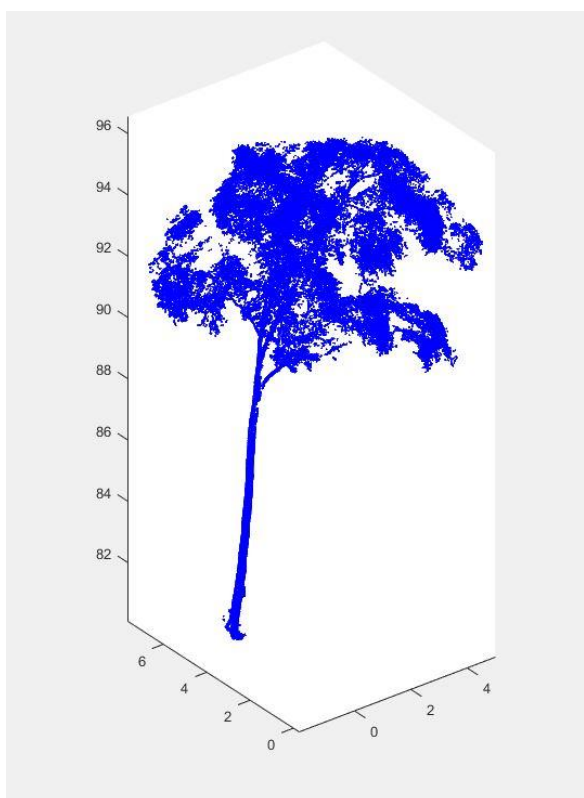
(a) Filtered Point Cloud
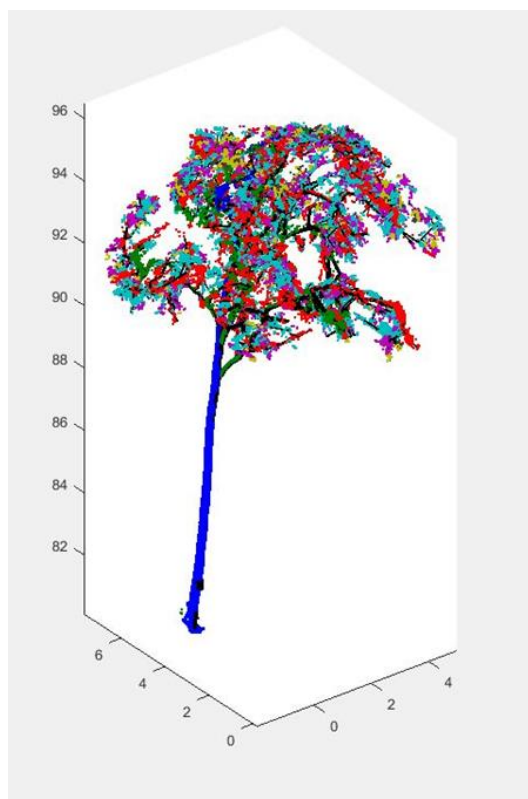
(b) QSM and segmented point doud
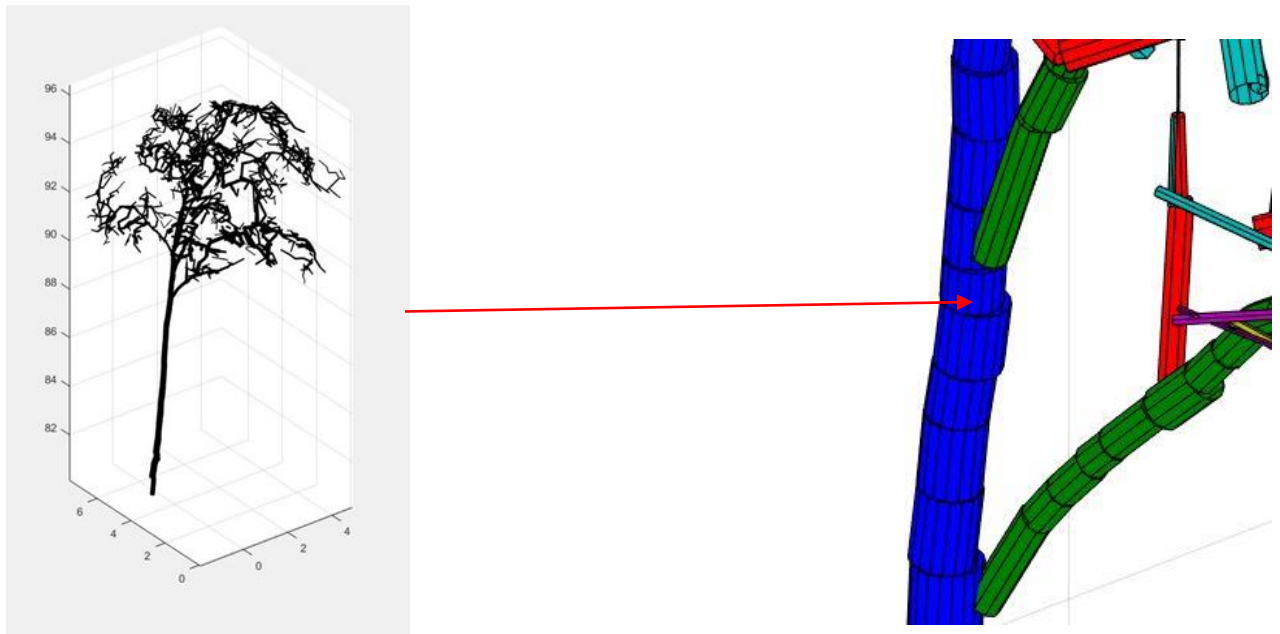
1484 cylinders

(c) QSM model the cylinder colour marks the branching order (1st order blue, second order green, third order red etc.)
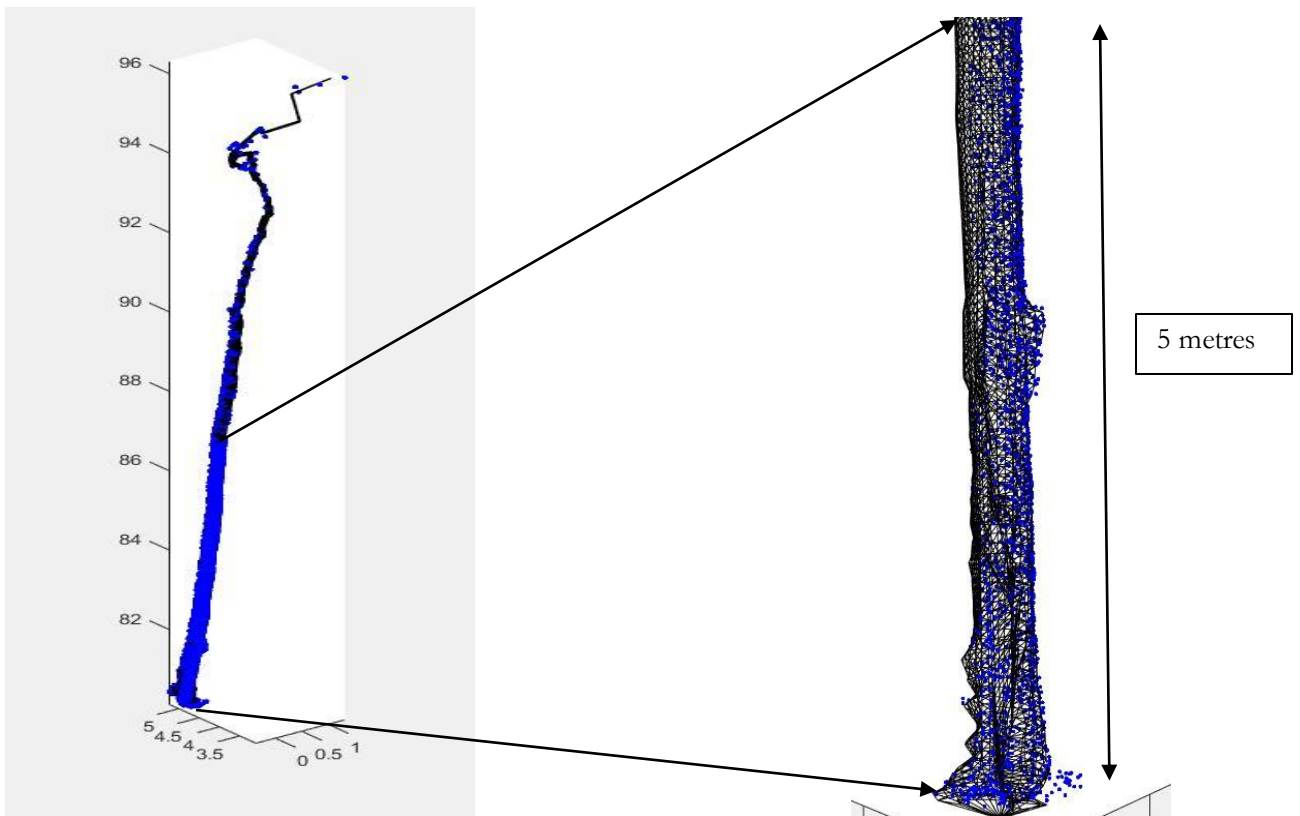
(d) Triangulation model of the bottom part of trunk

Figure 28: QSM outputs

4.5 Relationship between Above Ground Biomass from Allometric equation and QSM

Observations Trunk AGB > Canopy AGB

Out of the 100 observations used for the reconstruction, 29 observations had trunk biomass greater than canopy biomass. These 29 observations showed results that are normal to previous studies that reported a higher percentage of above ground biomass in the trunk than the branches. Of the 29 observations four (4) observations were removed as outliers because there were distance from other observations and thus 25 observations were used for analysis. AGB was derived using an allometric equation (AGB= [0.0673* (p*D²H) ^0.976] from (Chave et al., 2014). The AGB derived from the allometric equation was compared with AGB derived from QSM. The scatter plots (Figure 29a & b) show the relationship between AGB derived from the allometric equation and from QSM using either species specific wood density or default wood density for calculation. The default wood density is $0.57 g/cm^3$, which is the FAO default value for tropical tree species in Asia. Using the default value of wood density value for calculating the AGB the coefficient of determination (R^2) between allometric and QSM was 0.968 with an RMSE of 120.3Kg/tree. Using species specific wood density for calculating the AGB the coefficient of determination was 0.934 with an RMSE 131.6Kg/tree.

(a) Default wood density   (b) Species specific value wood density
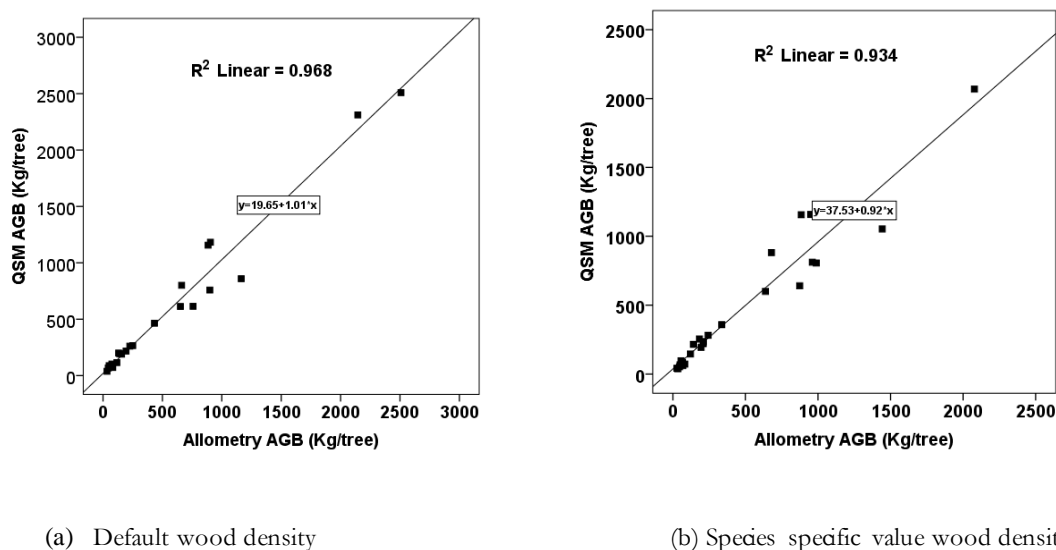
Figure 29: Scatter plots allometry & QSM AGB (a) Default wood density (b) Species specific wood density

4.5.1   Testing the relationship between Allometry and QSM AGB

F test two samples for variances

An F test two sample for variances was used to determine which t-test to use to test the hypothesis of difference between AGB derived from allometric equations or from QSM. The null hypothesis tested by the F test was the samples have equal variances. The null hypothesis was accepted in both cases ($p > 0.05$) that is AGB derived using either species specific or default wood density values (Table 12) and the t-test used in both cases was a two sample t-test assuming equal variances.

Table 12: F test for variances

	Allometry AGB (DWD)	QSM AGB (DWD)	Allometry AGB (SWD)	QSM AGB (SWD)
Mean	508.8	532.7	462.3	463.9
Variance	419375.4	440157.9	277522.4	252673.7
Observations	25	25	25	25
df	24	24	24	24
F	0.95		1.09	
P(F<=f) one-tail	0.45		0.41	
F Critical one-tail	1.98		1.98	

T-test assuming equal variances

To test if there is a significant difference in the AGB derived from allometric equations and QSM a t-test assuming equal variances was carried out. Results show (Table 13) that there is no significant difference ($p>0.05$) in either above ground biomass derived from allometric equations or from QSM in the 25 observations where the trunk biomass was greater than canopy biomass.

Table 13: t-test allometry and QSM AGB

	Allometry AGB (DWD)	QSM AGB (DWD)	Allometry AGB (SWD)	QSM AGB (SWD)
Mean	508.8	532.7	462.3	463.9
Variance	419375.4	440157.9	277522.4	252673.7
Observations	25	25	25	25
Pooled Variance	429766.6		265098.1	
df	48		48	
t Stat	-0.128		-0.011	
P(T<=t) two-tail	0.89		0.99	
t Critical two-tail	2.01		2.010	

4.5.2 Testing the difference between the use of default & species specific wood density values in estimating AGB

F test two samples for variances

To determine which t-test to use an F test two sample for variances was used. The null hypothesis tested by the F test was the samples have equal variances. The null hypothesis was accepted in both cases ($p>0.05$) (Table 14) and the t test used was a two sample t-test assuming equal variances.

Table 14: F test for variances

	Allometry AGB (DWD)	*Allometry AGB (SWD)*	*QSM AGB (DWD)*	*QSM AGB (SWD)*
Mean	508.8	462.3	532.7	463.9
Variance	419375.4	277522.4	440157.9	252673.7
Observations	25	25	25	25
df	24	24	24	24
F	1.5		1.7	
P(F<=f) one-tail	0.159		0.091	
F Critical one-tail	1.98		1.98	

T-test assuming equal variances

To test if there is a significant difference in using either species specific or default wood density values in estimating AGB a t-test assuming equal variances was carried out. Results show (Table 15) that there is no significant difference ($p > 0.05$) in either using a default value of density or species specific wood density value for the 25 observations where trunk AGB was greater than canopy AGB.

Table 15: t-test for default and species specific wood density

	Allometry AGB (DWD)	*Allometry AGB (SWD)*	*QSM AGB (DWD)*	*QSM AGB (SWD)*
Mean	508.8	462.3	532.7	463.9
Variance	419375.4	277522.4	440157.9	252673.7
Observations	25	25	25	25
Pooled Variance	348448.9		346415.8	
df	48		48	
t Stat	0.28		0.41	
P(T<=t) two-tail	0.78		0.68	
t Critical two-tail	2.01		2.01	

Observations Canopy AGB > Trunk AGB

Out of the 100 observations used for the reconstruction, 71 observations had canopy biomass greater than trunk biomass. These observations showed results that deviated from the normal as the canopy biomass was greater than the trunk. Of the 71 observations six (6) observations were removed as outliers. The scatter plots (Figure 30a & b) show the relationship between AGB derived from the allometric equation and from QSM using either species specific or default wood density. Using the default value of wood density the coefficient of determination (R^2) between allometric and QSM AGB was 0.817 with an RMSE of 163Kg/tree. Using species specific wood density the coefficient of determination was 0.797 with an RMSE 198Kg/tree.

(a) Default value wood density   (b) Species specific wood density
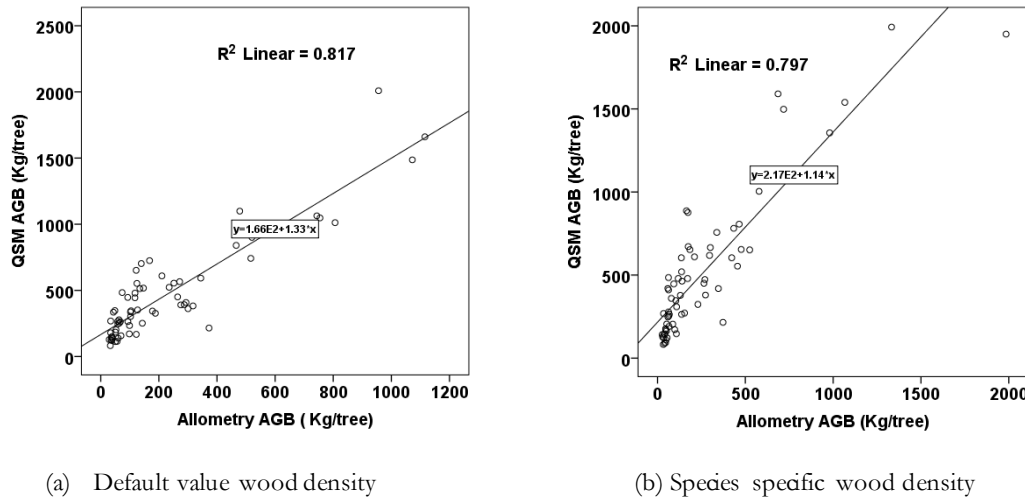
Figure 30: Scatter plots allometry & QSM AGB (a) Default wood density (b) Species specific wood density

4.5.3 Relationship between Allometry and QSM AGB

F test two samples for variances

An F test two sample for variances was used to determine which t- test to use. The null hypothesis tested by the F test was the samples have equal variances. The null hypothesis was rejected in both cases (p<0.05) (Table 16). The t-test used was a two sample t-test assuming unequal variances.

Table 16: F test for variances

	Allometry AGB (DWD)	QSM AGB (DWD)	Allometry AGB (SWD)	QSM AGB (SWD)
Mean	223.2	463.8	256.1	509.7
Variance	65874.2	143214.8	116171	191003.7
Observations	65	65	65	65
df	64	64	64	64
F	0.46		0.61	
P(F<=f) one-tail	0.0011*		0.0243*	
F Critical one-tail	0.66		0.66	

*.Significant at 95% level of significance

T-test assuming unequal variance

A t –test assuming unequal variance was used to test the hypothesis of a difference in AGB derived from the allometric equation or from QSM. Results show (Table 17) that there is a significant difference ($p < 0.05$) in above ground biomass derived from allometric equations and from QSM in the 65 observations where the canopy was greater than trunk AGB.

Table 17:   t-test allometry and QSM AGB

	Allometry AGB (DWD)	QSM AGB (DWD)	Allometry AGB (SWD)	QSM AGB (SWD)
Mean	223.2	460.1	256.1	509.7
Variance	65874.2	144567.4	116171	191003.7
Observations	65	64	65	65
df	110		121	
t Stat	-4.14		-3.69	
P(T<=t) two-tail	6.79E-05*		0.0003*	
t Critical two-tail	1.98		1.98	

*.Significant at 95% level of significance

4.5.4   Testing the difference between Default & Species-specific wood density values

F test two samples for variances

To determine which t-test to use an F test two sample for variances was used. The null hypothesis tested was the samples have equal variances. The null hypothesis was rejected in allometry AGB case ($p < 0.05$) (Table 18) and the t test using unequal variance was used. In the case of QSM the null hypothesis was accepted ($p > 0.05$) and a two sample t-test assuming equal variances was used.

Table 18: F-test for variance

	Allometry AGB (DWD)	Allometry AGB (SWD)	QSM AGB (DWD)	QSM AGB (SWD)
Mean	223.2	256.1	463.8	509.7
Variance	65874.2	116171	143214.8	191003.7
Observations	65	65	65	65
df	64	64	64	64
F	0.57		0.75	
P(F<=f) one-tail	0.012*		0.126	
F Critical one-tail	0.66		0.66	

*.Significant at 95% level of significance

T-test assuming unequal variance

To test if there is a significant difference in using species specific or default wood density values in estimating AGB a t-test assuming unequal variances was carried out for AGB derived using allometric equations. Results show (Table 19) that there is no significant difference (p> 0.05) in either using a default value or species specific wood density value.

Table 19: t-test for default & species specific wood density (Allometry AGB)

	Allometry AGB (DWD)	*Allometry AGB (SWD)*
Mean	223.1	256.1
Variance	65874.2	116171
Observations	65	65
df	119	
t Stat	-0.621	
P(T<=t) two-tail	0.536	
t Critical two-tail	1.98	

### T-test assuming equal variance

To test if there is a significant difference in using species specific or default wood density values in estimating AGB using QSM a t-test assuming equal variances was carried out. Results show (Table 20) that there is no significant difference (p> 0.05) in either using a default or species specific wood density value.

Table 20: t-test for default and species specific wood density (QSM AGB)

	QSM AGB (DWD)	*QSM AGB (SWD)*
Mean	463.8	509.7
Variance	143214.8	191003.7
Observations	65	65
Pooled Variance	167109.2	
df	128	
t Stat	-0.639	
P(T<=t) two-tail	0.524	
t Critical two-tail	1.98	

4.6 Distribution of Above Ground Biomass on tree components

Observations canopy > trunk AGB

Using an F test two sample for variances the null hypothesis was rejected in both cases (p<0.05) (Table 21). The null hypothesis tested by the F test was the samples have equal variances. A t -test assuming unequal variance was selected as the appropriate test. The t-test conducted showed that there is a significant difference (p<0.05) in branch and trunk biomass regardless of the value of the wood density used (Table 22).

Table 21: F test two samples for variances

	Default Wood Density		Species specific Wood Density	
	Branch AGB (Kg/tree)	Trunk AGB (Kg/tree)	Branch AGB (Kg/tree)	Trunk AGB (Kg/tree)
Mean	374.2	178.7	412.6	189.1
Variance	117723.7	33898.7	154365	36893.6
Observations	71	71	71	71
df	70	70	70	70
F	3.47		4.18	
P(F<=f) one-tail	2.3E-07*		4.8E-09*	
F Critical one-tail	1.48		1.48	

*.Significant at 95% level of significance

Table 22: t-test assuming unequal variance (observations canopy greater than trunk)

	Default Wood Density		Species specific Wood Density	
	Branch AGB (Kg/tree)	Trunk AGB (Kg/tree)	Branch AGB (Kg/tree)	Trunk AGB (Kg/tree)
Mean	374.2	178.7	412.6	189.1
Variance	117723.7	33898.7	154365	36893.6
Observations	71	71	71	71
df	107		102	
t Stat	4.23		4.31	
P(T<=t) two-tail	4.95E-05*		3.83E-05*	
t Critical two-tail	1.98		1.98	

*.Significant at 95% level of significance

Observations trunk > canopy AGB

To determine which t-test to use an F test two sample for variances was used. The null hypothesis tested was the samples have equal variances. The null hypothesis was rejected in both cases (p<0.05) (Table 23) and the t test using unequal variance was used as the appropriate test. The t-test conducted show that there is a significant difference (p<0.05) in branch and trunk biomass regardless of the value of the wood density used (Table 24).

Table 23: F test two samples for variances

| | Species specific Wood Density | | Default Wood Density | |
	Trunk AGB (Kg/tree)	Branch AGB (Kg/tree)	Trunk AGB (Kg/tree)	Branch AGB (Kg/tree)
Mean	468.3	215.5	487.6	220.8
Variance	278747.9	60555.2	301881.7	67038.2
Observations	29	29	29	29
df	28	28	28	28
F	4.60		4.50	
P(F<=f) one-tail	6.34E-05*		7.79E-05*	
F Critical one-tail	1.88		1.88	

*.Significant at 95% level of significance

Table 24: t-test assuming unequal variance (observations trunk greater than canopy)

| | Species Specific wood Density | | Default Wood Density | |
	Trunk AGB (Kg/tree)	Branch AGB (Kg/tree)	Trunk AGB (Kg/tree)	Branch AGB (Kg/tree)
Mean	468.3	215.5	487.6	220.8
Variance	278747.9	60555.3	301881.7	67038.2
Observations	29	29	29	29
df	40		40	
t Stat	2.34		2.37	
P(T<=t) two-tail	0.025*		0.023*	
t Critical two-tail	2.02		2.02	

*.Significant at 95% level of significance

4.7 Sensitivity Analysis

A sensitivity analysis was conducted on the number of runs, cover set diameter and the nmin values. Keeping all other parameters constant, different values of these parameters were tested to assess their effect on the volume derived from the reconstruction.

4.7.1 Effect of Different runs on QSM derived volume

In running the QSM, it is recommended that when deriving volume, the model is run at least 5 times per tree because the cover sets are generated at random and even when using the same parameters the QSM output is different each time (Raumonen et al., 2013; Calders et al., 2015). To assess the robustness of the reconstruction different runs were implemented to test the effect of the number of runs on the volume derived. Different runs were conducted from as little as 5 runs to 100 runs. Means and standard deviations were computed for each of the runs. A one-way analysis of variance was carried out to determine if there is a significance difference in the volume derived from the different runs. An F test (Table 25) revealed a non-significant relationship (p>005). The null hypothesis was accepted and it was concluded that different runs do not have a significant difference on the volume derived from the QSM reconstruction.

Table 25: One-way ANOVA- Effect of different runs on volume

Groups	Count	Sum	Average	Variance
Five runs	5	4867	973.4	10515.8
Ten runs	10	9533	953.3	9392.7
twenty _runs	20	19259	962.95	8051.2
thirty runs	30	29049	968.3	8413.8
fifty runs	50	47977	959.54	9068.5
seventy five runs	75	71477	953.03	8586.7
hundred runs	100	95511	955.11	8813.2

ANOVA

Source of Variation	SS	df	MS	F	P-value	F crit
Between Groups	7813.8	6	1302.3	0.149	0.98	2.13
Within Groups	2475846.7	283	8748.6			
Total	2483660.5	289				

4.7.2   Effect of cover set diameter on volume

The cover set diameter is one of the most important parameters that is critical in modelling an accurate QSM reconstruction. This value is determined by the value of PatchDiam2Min that is set before running the model. An incorrect value of this parameter can lead to an underestimation or overestimation of the volume and thus the AGB derived (Calders et al., 2015). In this study, the cover set diameters to model the trees ranged from 0.01m to 0.05 metres. To test if there is a significance difference in the size of the cover set diameter and the volume derived a one-way analysis of variance was carried out (Table 26). An F test showed a ($p < 0.05$) and thus it was concluded that there is a significance difference in the cover set diameter and the volume derived. The results (Table 26) also show that the volume derived increases with an increase in the cover set diameter A post hoc test was conducted to determine which cover sets have a significance difference in the volume derived (Table 27). Table 27 shows the cover set diameters that have a significance difference in the volume derived were 0.01 metres & 0.04 metres and 0.01 & 0.05 metres. The full results of the post hoc test are found Appendix 7.

Table 26: One-way ANOVA – Effect of cover set diameter on volume

Groups	Count	Sum	Average	Variance
CS=0.01	5	3445	689	477
CS=0.02	5	4026	805.2	3500.2
CS=0.03	5	4120	824	11574
CS=0.04	5	4401	880.2	5163.7
CS=0.05	5	4666	933.2	9607.7

ANOVA

Source of Variation	SS	df	MS	F	P-value	F crit
Between Groups	168173	4	42043.26	6.93	0.0011*	2.866081
Within Groups	121290.4	20	6064.52			
Total	289463.4	24				

*.Significant at 95% level of significance

Table 27: PostHoc test Cover Set diameter

Cover Set Diameter (I)	Cover set Diameter (J)	Mean Difference (I-J)	Std.Error	Sig	95% Confidence Interval	
					Lower Bound	Upper Bound
0.01	0.04	-191.200*	49.252	0.007	-338.58	-43.82
	0.05	-244.200*	49.252	0.001	-391.58	-96.82
0.04	0.01	191.200*	49.252	0.007	43.82	338.58
0.05	0.01	244.200*	49.252	0.001	96.82	391.58

* The mean difference is significant at the 0.05 level.

4.7.3   Effect of nmin values on crown volume

Nmin which is a value that controls the minimum threshold of points to be included in a single cover set for reconstruction affects the final QSM model (Calders et al., 2013). Small values can lead to overestimation of volume in the canopy and too large values to an underestimation of the volume of the canopy (Calders et al., 2013). Nmin values in the reconstruction are two that is nmin 1 & 2 that are used in the first and second segmentation of the reconstruction process. A test was conducted to investigate the effect of varying the nmin values on the crown volume. A one-way ANOVA was conducted (Table 28) to see if there are any significant differences in the crown volume with varying nmin values. The test revealed a significant difference ($p < 0.05$) in the nmin values and the volume derived in the crown. A post hoc test was carried out to see which values have a significant difference (Table 29). Results revealed significance differences in all the nmin values used except for nmin values 5 & 3 and nmin values 7 & 5.

Table 28: One-way ANOVA nmin values on canopy volume

	Sum of Squares	df	Mean Square	F	Sig.
Between Groups	100775.4	3	33591.8	23.9	0.000004*
Within Groups	22477.2	16	1404.8		
Total	123252.6	19			

*.Significant at 95% level of significance

Table 29: Post Hoc test nmin values on canopy volume

(I) nmin	(J) nmin	Mean Difference (I-J)	Std. Error	Sig.	95% Confidence Interval	
					Lower Bound	Upper Bound
nmin 3 & 1	nmin 5 & 3	88.600*	23.705	.009	20.78	156.42
	nmin 7 & 5	113.600*	23.705	.001	45.78	181.42
	nmin 10 & 7	199.200*	23.705	.000002	131.38	267.02
nmin 5 & 3	nmin 3 & 1	-88.600*	23.705	.009	-156.42	-20.78
	nmin 7 & 5	25.000	23.705	.721	-42.82	92.82
	nmin 10 & 7	110.600*	23.705	.001	42.78	178.42
nmin 7 & 5	nmin 3 & 1	-113.600*	23.705	.001	-181.42	-45.78
	nmin 5 & 3	-25.000	23.705	.721	-92.82	42.82
	nmin 10 & 7	85.600*	23.705	.011	17.78	153.42
nmin 10 & 7	nmin 3 & 1	-199.200*	23.705	.000002	-267.02	-131.38
	nmin 5 & 3	-110.600*	23.705	.001	-178.42	-42.78
	nmin 7 & 5	-85.600*	23.705	.011	-153.42	-17.78

*. The mean difference is significant at the 0.05 level.

It was observed (Table 30) that an increase in the values of nmin 1 & nmin2 result in a decrease in the canopy volume.

Table 30: nmin values and canopy volume

Runs	Nmin 3 & 1	Nmin 5 & 3	Nmin 7 & 5	Nmin 10& 7
1	0.439	0.25	0.218	0.17
2	0.269	0.241	0.247	0.12
3	0.385	0.299	0.264	0.148
4	0.36	0.253	0.236	0.139
5	0.308	0.275	0.228	0.179
Mean canopy Volume (m³)	**0.3522**	**0.2636**	**0.2386**	**0.153**

4.8 Carbon Stock of individual Trees

Carbon was calculated by multiplying the above ground biomass by 0.47 (IPCC, 2006). The distribution of the selected trees used for modelling is displayed in Figure 31. The mean carbon is 294.09Kg/tree for the above ground biomass calculated using species specific wood density values whilst it is 281.13Kg/tree for AGB calculated using the default wood density value of 0.57g/cm^3.
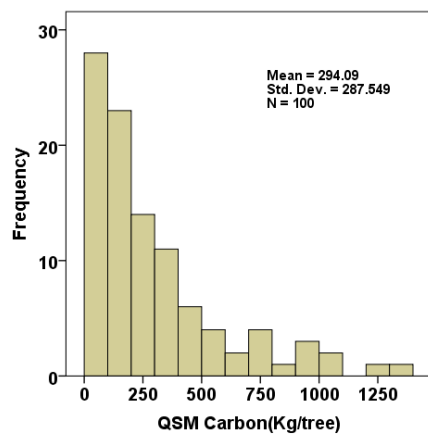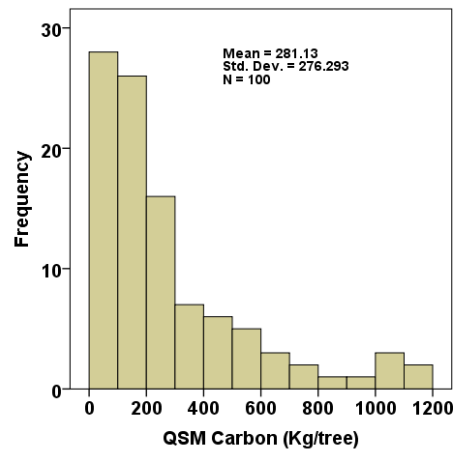
(a)   Species specific Wood density   (b) Default Wood Density

Figure 31: Carbon distribution (a) Species specific wood density (b) Default wood density

5 DISCUSSION

5.1 Point Cloud Acquisition and Registration

The point cloud data in this study was acquired using a RIEGL VZ 400 Terrestrial Laser Scanner. The point clouds were collected using a multiscan instrument position setup with one centre scan and three outside scans. Registration of the point clouds was done by the use of tie points and the registration accuracies for all the 26 plots ranged from 0.0127m to 0.0224m. It was observed that trees that were further away from the scanner had low point density. This was also mentioned in Pfeifer et al. (2004). They stated that point density decreases with the distance from the scanner and low point density is observed in trees that are further from the scanner and in higher parts of the tree. In this study, a total of 15 tie points were used to register the point cloud 12 cylindrical retro reflectors and 3 circular retro reflectors. The cylindrical reflectors were placed on top of approximately 1 metre high sticks and the circular reflectors were placed on the stem of trees. A high number of tie points could explain the high accuracy in registration of the scans. This was reported in Bienert et al. (2006), were they used a total of 19 targets for registration and they achieved a high accuracy. They used a lot of targets because of high occlusions and the targets were distributed inside and outside the plot. Plots such as the study plots 3, 15, 17 and 21 have a registration accuracy of 0.02m and above which was slightly higher as compared to the rest of the plots. Hopkinson et al. (2004) explained that this could be due to the fact that some multi scans do not align correctly. Some scans intersect and do not merge uniformly on the stem. Placing of reflectors higher than 3 metres from the ground was indicated as a possibility to increase the registration accuracy of point clouds from multi scans (Pfeifer et al., 2004). Some of the errors and uncertainties involved in collecting point cloud data include instruments accuracies, beam divergence, interception of pulses by other surfaces, uneven surfaces such as tree bark, the reflectivity of the target and the incidence angles of pulse inception (Okatani & Deguchi, 2002; Lovell et al., 2003).

5.2 Extraction of trees

A total of 821 trees were measured in the field and 657 trees were extracted manually. A total of 164 trees were recorded missing and this can be attributed to occlusions (Figure 32) a tree being in the shadow of another tree or a tree falling in the scan shadow. Trees that are standing close to the scanner fall in the scan shadow and thus will not be scanned (Bienert et al., 2006; Jung et al.,2011). In the case of this study the minimum range was set at 1.5m and thus, any tree that was in this range was not scanned because it fell in the scan shadow. Some of the trees were recorded missing because they were further away from the scan and could not be identified, the tree number/tag could not be read because of the low point density.

Figure 32: Dense undergrowth causing occlusions

The 615 trees were extracted manually. Manual extraction involves removing of unrelated vegetation points from each individual tree. This is a time consuming process and it is even more challenging in closed canopy forests with high stem densities like Ayer Hitam. Raumonen et al. (2015) reported that extracting individual trees manually from point clouds is a time consuming, they reported a couple of hours to extract an oak tree and observed that the extraction is not reliable if branches of nearby trees overlap. Occlusions were mentioned as a problem by Van der Zande et al. (2006). They stated that the major problem with Terrestrial Lidar in the forest is occlusion, which is caused by lower branches, adjacent trees and the understory that lead to low point density and poor descriptions of the crown and partially or totally hidden trees. Jung et al. (2011) illustrated the error in extraction that arises from overlapping canopies (Figure 33). They reported that overlapping crowns increase with stem density and the resulting errors of extraction lead to errors also in tree growth parameters such as height and crown projection area.
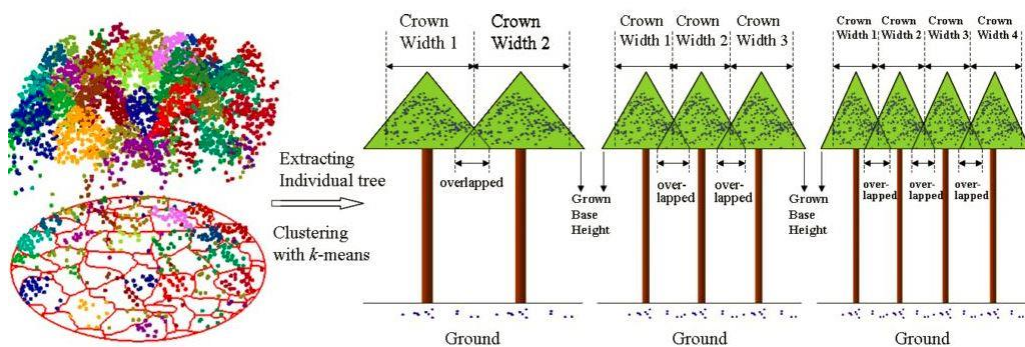
Figure 33: Overlapping crowns (Jung et al., 2011)

This was also observed in this study where occlusions and overlapping canopies resulted in badly extracted trees (Figure 34) which also compromise the derivation of tree height. Extraction of trees in heterogeneous forests was recorded by Pitkänen & Maltamo, (2004) and Yu et al. (2011), of 70% and 69% respectively which is slightly lower than 80.02% which was recorded in this study.

Figure 34: Bad extraction displayed in true colour

5.3 DBH measurement

DBH was measured in the field at 1.3metres above the ground with a diameter tape. Van Laar & Akça, (2007) stated that the diameter tape produces biassed estimates if the stem is not perfectly circular and errors are observed especially in large trees where it is difficult to verify the position of the diameter tape at the back of the tree or the tape is slanted or sags. This challenge was observed in the field on large diameter trees and large buttress trees (Figure 35).

Figure 35: Large buttress tree

TLS DBH is measured as the horizontal distance at 1.3 metres (above the ground) assuming a circular stem. Occlusions lead to low point cloud density and thus, errors in the measurement can occur because a perfect semi-circle is not formed for correct measurement of DBH from the point clouds. Cushman et al. (2014) alluded to the fact that the assumption of being circular at breast height is not always true, especially for a tree with buttress. Calders et al. (2015) also mentioned that the errors which occur when measuring DBH from TLS data assuming a circle at 1.3metres. They observed that because of occlusions a circle is not the most optimal fit for estimating DBH (Figure 36). The linear regression of the relationship between DBH measured in the field and TLS showed an RMSE of 1.1cm and coefficient of determination of 0.993. Calders et al. (2015) reported an RMSE of 2cm and slope of 0.98 when comparing field measured DBH against TLS on a native *Eucalyptus* open forest in Victoria Australia.

(a) No occlusions   (b) Partial Occlusions   (c) Occlusion
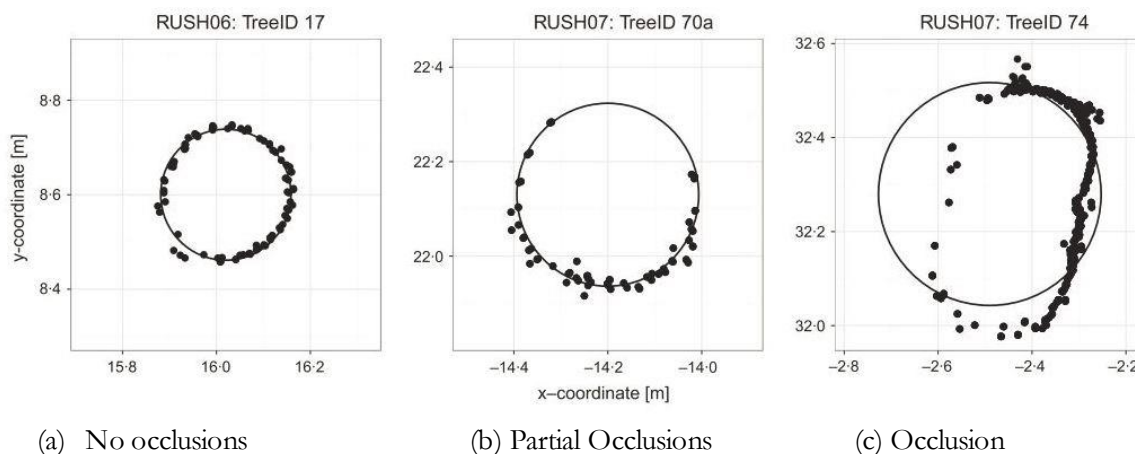
Figure 36: DBH derived through circle fitting (Calders et al., 2015)

5.4 Height Measurements

Height was measured in the field using a Leica DISTO D510 which has an accuracy of ±1mm ("DISTO D510 | Laser Distance Measurer | Leica Geosystems," 2016). It was however very difficult to accurately measure tree height due to the dense canopy which made it challenging to distinguish the top of trees. This fact was mentioned in Dassot et al. (2011); Hopkinson et al. (2004); Clark et al. (2004) & Williams et al. (1994), where they also observed inaccuracies in height measurement in high canopy cover conditions because of failure to identify the exact tree top which leads to approximation of the tree top. This leads to an underestimation or overestimation of the tree height (Figure 37). Williams et al. (1994) stated that the bias in height measurement is larger for tall trees in dense forests because the tops are not well defined. Calders et al. (2015) observed an underestimation of tree height for trees of up to 16 metres and an overestimation in trees taller than 16 metres.
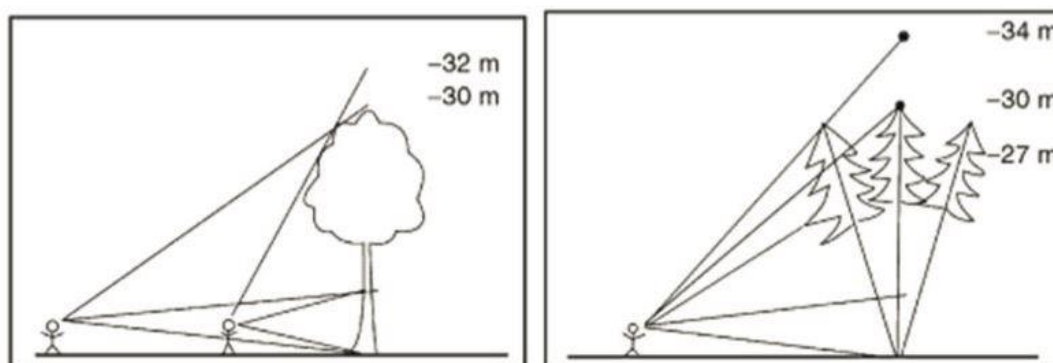
Figure 37: Errors in height measurement (Köhl et al., 2006).

The linear regression of field measured height and TLS derived height had an RMSE of 3.4 metres and a coefficient of determination (R^2) of 0.59. This can be attributed to the under sampling nature of Terrestrial LiDAR in closed canopy forests coupled with the errors of height measurements from the field. The under sampling nature of Terrestrial LiDAR was reported in Falkowski et al. (2008); Clark et al. (2004) & Hopkinson et al. (2004). They attributed the underestimation to the laser pulse canopy penetration. The

pulse actually hitting the apex of the tree and the influence of shadowing in the lower canopy produce the error. Krooks et al. (2014) concluded that TLS leads to an underestimation of 1-3 metres which is caused by geometry that causes occlusions in the highest part of the canopy. Williams et al. (1994) concluded that height measurements are less accurate in deciduous stands as compared to conifers. This was also supported by Dassot et al. (2011) & Clark et al. (2004), who attributed the errors to the multi-tiered and overlapping nature of the vegetation and laser pulses penetrating below crown surfaces until the inner crown reflect a detectable first return. Hopkinson et al. (2004) mentioned that this conclusion is more site specific because in some plots they recorded R^2 of 0.86 but in some 0.13. This was also true in this study. Looking at the plot wise relationship between the field and TLS height, plot 8 had an R^2 of 0.30 while plot 23 had an R^2 of 0.91. This can be attributed to the differences in canopy structure whether it is open or closed in the selected plot (Figure 38).

Figure 38: Closed canopy in Ayer Hitam

5.5 Distribution of TLS DBH and Height

 In this study, the distribution of both DBH and height measured in the field and derived from TLS were analysed. DBH was not normally distributed and was skewed. Skewness is the lack of symmetry in data (Field et al., 2012). A skewed distribution can be either positively skewed where most frequencies are towards the more positive scores or can be negatively skewed where most frequencies are towards the lower or more negative scores (Field et al., 2012) (Figure 39). In this study DBH was positively skewed (Figure 24) because only trees with a DBH equal to or greater than 10cm were measured. Brown, (2002) observed that trees with a DBH less than 10cm are insignificant in contributing towards total above ground biomass.
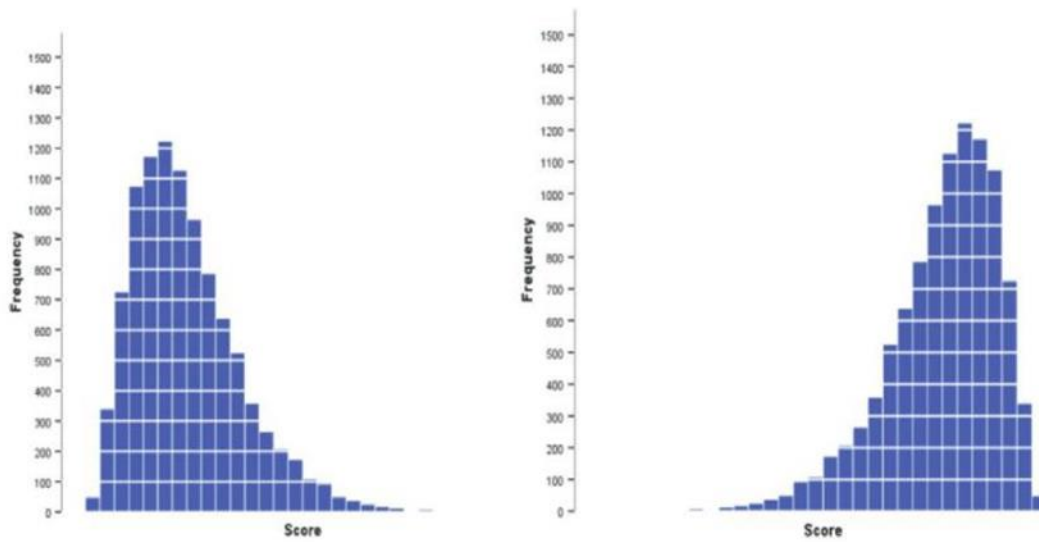
(a)   Positive skewed   (b) Negative skewed

Figure 39: Positive & negative skewness (Field et al., 2012).

Height distribution showed a mean height of 16.74 m. The graph appeared to follow a normal distribution (Figure 25) with the majority of the trees falling in the height class 10-25 metres. Few trees were observed in the height class 5-10 metres and > 30metres. This can be attributed to the structure of the tropical rain forest where trees in the height class 5 -10 metres belong to the understory layer, 10 – 25 metres in the canopy layer which contains the majority of the trees and trees > 30metres belonging to the emergent layer usually characterised by species with large buttresses (Figure 40). These results are almost similar to Nurul-Shida et al. (2014). They observed the majority of trees in the height class of 10-24.9metres and very few trees in the height class >35metres. The tallest tree for Dipterocarp was 38 m and for Non_dipterocarp was 35m in Ayer Hitam Forest Reserve.
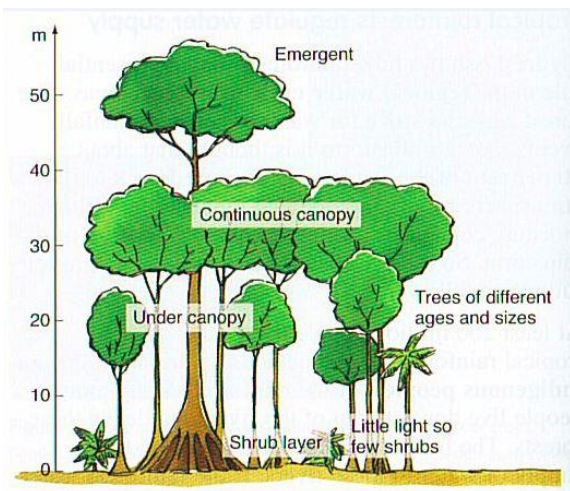
Figure 40: Tropical rainforest structure

 (Source: "Eco - Key services - Ace Geography," 2016)
http://www.acegeography.com/eco---key-services.html

5.6 Wood density (species specific or default)

In this study above ground biomass was derived using allometric equation AGB= $[0.0673*(p*D^2H)$^0.976] (Chave et al., 2014). With the resulted QSM volume, above ground biomass was derived by multiplying the volume with the wood density. In both cases, wood density was used to estimate the amount of above ground biomass in each tree. A value of $0.57g/cm^3$ which is the FAO default value for tropical tree species in Asia (Hirata et al., 2012) was used to calculate the above ground biomass. Also using species specific wood density values derived from the World Agroforestry Centre Wood Density Database (World Agroforestry Centre, 2011) above ground biomass was calculated. Results showed that there is no significant difference in using either the FAO default wood density value or the species specific wood density value in calculating above ground biomass. Nogueira et al. (2005) carried out a wood density study in the Amazon and found that wood density differs among tree sections, being higher at breast height, at the base of the tree stem and lower at the top of the bole. In this study one wood density value was applied to the whole tree and this could explain the non-significance observations. Calders et al. (2015) also noticed the error in estimating above ground biomass from using basic densities that are derived from samples across a range of DBH, they stated that this may introduce uncertainty in the conversion of volume to above ground biomass of an individual tree because basic density is lower for small DBH trees and higher for large DBH trees. Basuki et al. (2009) compared the wood density of *Dipterocarpus grandiflorus* and concluded that at a DBH of 18.8cm the wood density was $0.56g/cm^3$ and at a DBH of 44cm it was $0.75g/cm^3$ while the wood density for the species is just given as $0.62g/cm^3$ without any indication of the diameter.

5.7 Allometric equations

The allometric equation from Chave et al. (2014) AGB= $[0.0673*(p*D^2H)$^0.976], where ABG= above ground biomass (Kg/tree), p= Wood specific gravity (gcm^{-3}), D =diameter at breast height (DBH cm) and H= tree height (m) was used in this study. Chave et al. (2014) observed that this allometric equation underestimates the above ground biomass by 20%, especially for large trees. This is because large trees contribute a greater percentage of the above ground biomass in a tropical forest stand. Sampling bias was also mentioned in deriving the allometric equation, especially when the research is done concurrently with logging activities because trees with better form are selected over trees which are damaged or have deformities (Chave et al., 2014; Clark & Kellner, 2012). Kearsley et al. (2013) mentioned the fact that the error in tree height measurement is propagated into AGB estimates this leads to the inaccuracies in the estimation of AGB. Errors in height estimation were also observed in this study and contributed to inaccuracies in the above ground biomass derived. Some of the errors associated with using allometric equations to estimate above ground biomass include overestimation or underestimation of tree biomass when an allometric equation is applied without considering stand age (Peichl & Arain, 2007). Multispecies allometric equations are a source of uncertainty in the estimation of above ground biomass (van Breugel et al., 2011). In this study, a multi species allometric equation was used and this also brings uncertainty in the derived above ground biomass. van Breugel et al. (2011) argued that in a highly diverse forest like the forest in this study, even large samples represent much less than 43% of the local species pool and uncertainties in the above ground biomass estimates will remain and thus it is important to find a representative sample.

5.8 Estimation of Above Ground Biomass using QSM

Above ground biomass was estimated from the QSM volume derived and the wood density. A total of 100 trees were used for the reconstruction algorithm. In this study, 71% of the trees sampled had a bigger proportion of the above ground biomass in the canopy as compared to the stem. This deviated from what has been observed in previous studies on the distribution of above ground biomass on trees. Calders et al. (2015) gathered that QSM overestimates the AGB by 9.68% compared to an underestimation of 36.57% - 29.85% for allometric equations in a *Eucalyptus* open forest. The errors in allometric equations increase

exponentially with increasing DBH, whereas QSM derived AGB is independent of DBH. They also found out that 80% of the AGB at plot level is located in the lower 60% of the trees for a eucalyptus forest. Magalhães et al. (2015) also reported biomass distribution of 51% stem, 24% crown, 19% belowground biomass and 6% stem bark in a Mecrusse woodland in Mozambique. Peichl & Arain, (2007) carried out a research on the portioning of above and below ground biomass of white pine forests in Canada and found out that stem wood was the major above ground biomass pool in each stand with canopy biomass contributing 33% of the aboveground biomass. The errors that lead to this overestimation of the volume and thus aboveground biomass in the branches/canopy can be attributed to the following factors:

Presence of non –wooden material

The presence of leaves was reported by Krooks et al. (2014) & Raumonen et al. (2012). The reconstruction QSM algorithm assumes that all parts are woody and thus the presence of leaves cause an overestimation of volume in the crown of the trees. It was mentioned that the accuracy of the reconstruction is poor and produces large relative errors when there is the presence of needles or leaves (Raumonen et al., 2012) (Figure 41). This is because leaves cause an inaccuracy in the branch size measurement and thus make the cylinders too large leading to increased volumes and errors (Burt et al., 2013). In this study scanning of the trees was conducted with leaf on conditions. Filtering is recommended as a way of removing unwanted non-woody material from the point clouds, but there are trade-offs to the filtering. Intensifying the filtering removes most of the noise but there is a risk of removing points that belong to the tree and in the end, underestimate the volume from the crown. Intensifying the filtering also leads to poor/bad cylinder models because gaps and hanging cylinders are observed in the final cylinder model. Reducing the intensity of the filtering also leaves a lot of noise in the crowns from the leaves and thus leads to an overestimation of the volume derived from the canopy of the trees. Calders et al. (2013) reported that AGB estimated from the filtered point cloud was lower but if filtering is also not conducted the isolated points lead to wrong modelled cylinders, which increase the AGB estimates.
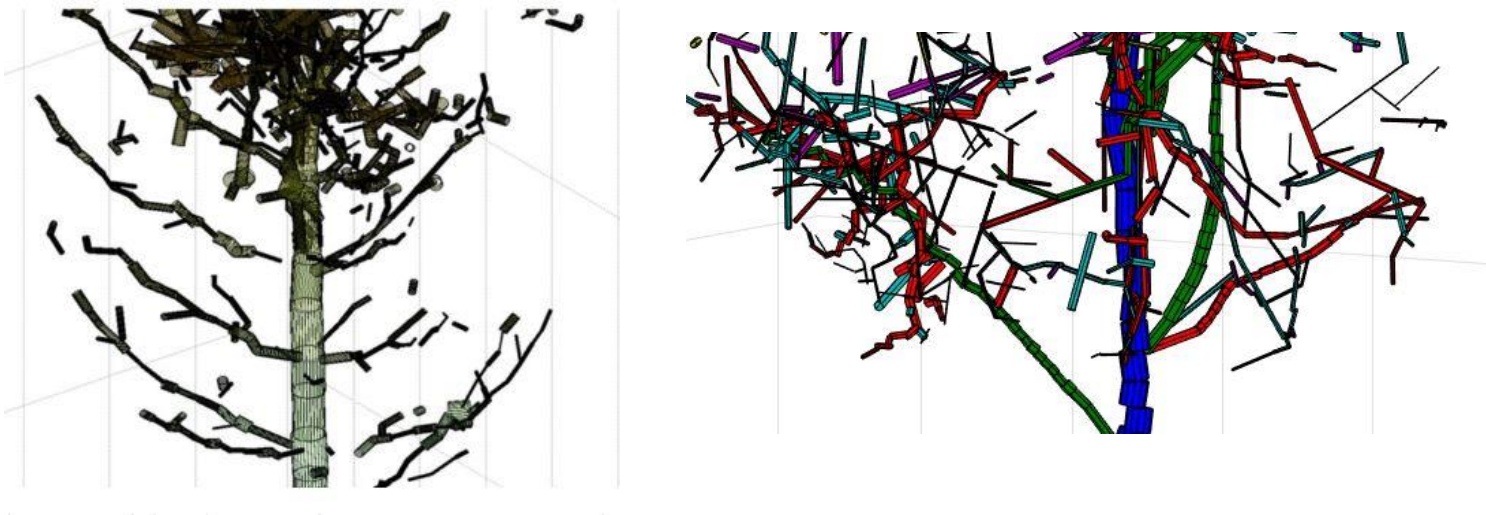
(a) (Krooks et al., 2014)   (b) From study

Figure 41: Bad reconstruction false cylinders and gaps

Point Cloud Registration

Registration errors also contribute to an overestimation of the volume derived from QSM reconstruction. The accuracy to which scans are registered affects the accuracy of the reconstruction (Calders et al., 2015; Krooks et al., 2014). Burt et al. (2013) deduced that a 1cm registration error can lead to an 8.8% total volumetric overestimation on a dataset. In this study plot registration errors ranged from 1.27 cm to 2.24cm. Registration errors lead to an increase in the apparent branch radius or replication of the branches (Burt et al., 2013). This error is substantial, in biomass estimation because the volume derived is proportional to the square of the radius (Burt et al., 2013). Registration error affects the structure of the tree to be reconstructed and it is independent of the algorithm (Burt et al., 2013). This error causes an increase in the cylinder radius and subsequently the derived volume (Burt et al., 2013). The distance to the target from the scanner and other factors such as wind add on to the error (Burt et al., 2013).

Wind

If a scan is taken during windy conditions, it affects the quality of the scans and thus produce an overestimation of the volume derived from branches. Scanning in the field is susceptible to target movements during and between scans (Krooks et al., 2014). Conducting a multi-scan as was the case in this study can lead to modelling the same branch section more than three times if the canopy has moved even by a few centimetres (Krooks et al., 2014). Hackenberg et al. (2015) also observed that points located at the tips of the branches scatter as a result of windy conditions. They reported overestimation and big cylinders for twigs which lead to a big overestimation of the volume in the crowns.

QSM Modelling parameters

The QSM has input parameters that govern the quality of the cylinder model derived. Calders et al. (2015) emphasized the need to get the value of the cover set to a correct value before reconstruction. The cover set size is critical because the use of an incorrect value can lead to volume estimation increases of 5000% (Calders et al., 2015). The value of the cover set reported in Calders et al. (2015), ranged from 0.02 to 0.09 metres. In this study cover set diameters values ranged from 0.01 to 0.05 metres. Disney et al. (2012) & Raumonen et al. (2013), mentioned that the error on the final cylinder model depends on the cover set size. Smaller cover sets maintain the fine details but are also vulnerable to errors due to noise in the data. If a large cover set is used, branches that are much smaller than the cover set are not recognised and thus are included in their parent branches (Disney et al., 2012). This causes the parent branches to be much larger and overestimate the branch volume (Disney et al., 2012). In this study in cases where large cover sets were found to be an optimal modelling parameter were vulnerable to error and thus had an influence on the final volume.

Size of the tree component and density of point clouds

The accuracy of the reconstruction is reported to be good for thick branches that have many points (Raumonen et al., 2012). Hackenberg et al. (2015) found out that tree components with a diameter greater than 10cm can be modelled accurately but smaller diameters such as 4cm are overestimated. In this study, it was observed that this was true also for small diameter components whereby the cylinders appeared larger and thus the volume for the small components on the tree were overestimated.

Non-circular branches and stems

One of the assumptions of the QSM is that the point cloud is a sample of a surface in 3D space and the surface is like a cylinder Raumonen et al. (2012); Raumonen et al. (2013), but in reality, this is not entirely true. Thus, errors arise in segmentation and geometric structure that is a real branch or leaf structure against the cylinder model (Calders et al., 2015; Krooks et al., 2014). The study was carried out in a tropical forest where the deciduous broadleaved trees do not usually follow a cylindrical shape. Pfeifer et al. (2004) stated that the cross section of branches is usually not circular and branches that grow sideways tend to have a more elliptical cross section due to gravity, also the axis of a branch is not a straight line but curved which makes the modelling of trees a challenging task.

Manual extraction of the individual trees

This process involves removing of unrelated vegetation points from each individual tree. In the case of this study in most of the plots, the crowns of the trees were touching each other and this presented difficulty to clearly seclude point clouds of neighbouring trees or the understory. An incorrect extraction has noise and this will be modelled as cylinders in the reconstruction leading to an overestimation of the volume of the branches (Figure 42).
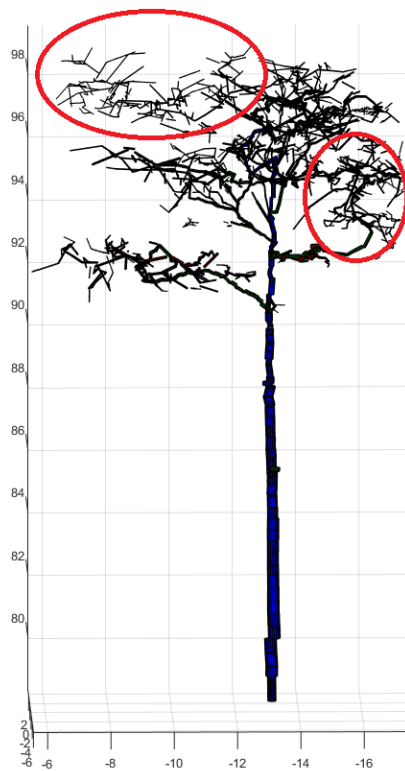
Figure 42: Crown from neighbouring trees highlighted in red

5.8.1   Number of QSM runs and derived volume

The cover set generation is random in the reconstruction algorithm and thus, the final QSM is different for each run even if the same parameters are used (Calders et al., 2015; Raumonen et al., 2013; Åkerblom, 2012). Raumonen et al. (2015) made five models per tree and Calders et al. (2015) made ten models per tree due to the randomness in cover set generation. Similarly, in this study, five models were made per tree. To test

if different runs have an effect on the volume derived a number of runs (5, 10, 20, 30, 50, 75 & 100) were tested on selected trees. Results showed that number of runs do not have a significant effect on the volume derived. These results are similar to Calders et al. (2015) who tested 20, 50 and 100 runs on a selected number of trees and found that there is no significant differences between the number of runs and the volume derived.

5.8.2   Cover set diameter and derived volume

Different cover set diameters were tested to determine the effect on volume derived. The cover set diameters tested were: 0.01, 0.02, 0.03, 0.04 and 0.05 metres. Results showed that there is a significance difference in cover set diameter and volume derived and post hoc tests showed significance differences between a cover set diameter of 0.01 & 0.04 metres and 0.01 & 0.05 metres. Results also showed that the volume derived increases with an increase in the cover set diameter. These results are similar to the ones in Raumonen et al. (2013) who observed an increase in the total volume with an increase in the cover set diameter. This is because when the trunk is correctly defined, all first order branches are found and with a larger diameter few second-order branches close to trunk are classified as first-order branches (Raumonen et al., 2013).

5.8.3   Nmin values and crown volume

Different nmin values were tested to see their effect on crown volume. Nmin values of (3&1, 5&3, 7&5 and 10&7) were tested. Results showed that there is a significant difference in nmin values and the crown volume. Post hoc tests revealed that there is significant differences in all the nmin values except for nmin values of 5&3 and 7 & 5. Results revealed that the smaller the nmin values the greater the volume modelled in the crown and the larger the nmin value the less the crown volume. These results are similar to Calders et al. (2013) who observed that large values of nmin lead to smaller estimates of volume while small values lead to many cylinders being modelled in the crown (Figure 43). This is because the nmin value is a threshold for which cover sets are kept and others are discarded in the reconstruction (Calders et al., 2015; Calders et al., 2013).
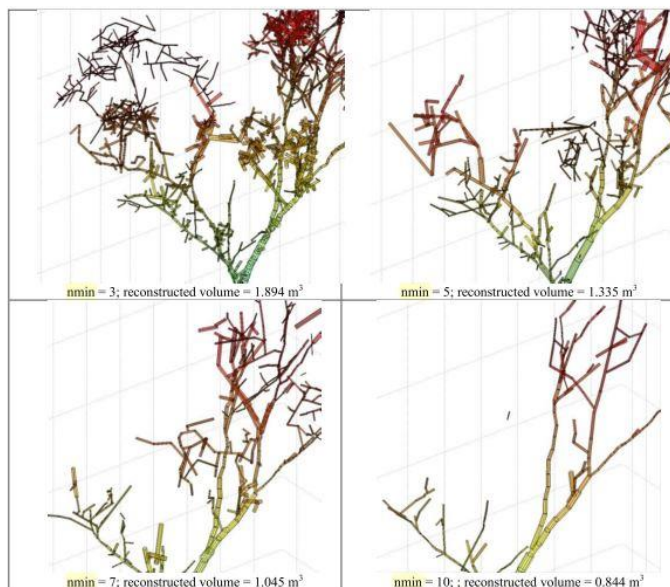
Figure 43: Effect of nmin on crown volume (Calders et al., 2013).

5.9 Limitations to the study

➢ Validation of QSM above ground biomass requires destructive sampling to be accurately validated and this was not possible in this study.

➢ Modelling different species using QSM required selection of optimum modelling parameters for each tree which was a time consuming process.

➢ Point cloud data pre-processing is time consuming, from acquisition to registration and extraction of individual trees.

➢ Acquisition of point cloud data with leaf on conditions posed a problem in the reconstruction of the trees and created a bias in the above ground biomass derived.

➢ Challenges in the manual extraction of individual trees and under sampling of the TLS in closed canopy forest leading to bias in tree parameters derived especially tree height.

➢ Terrestrial LiDAR equipment was heavy and it proved challenging to carry it on the terrain of the forest and thus purposive sampling was applied.

6 CONCLUSION AND RECOMMENDATIONS

6.1 Conclusion

 This study explored the feasibility of using Quantitative Structure Modelling (QSM) to estimate above ground biomass in a tropical rain forest of Ayer Hitam Malaysia. 100 trees were selected for the reconstruction algorithm selected on extraction quality and DBH distribution from all the 26 plots selected for this study. Above ground biomass was calculated by multiplying the QSM derived volume by the wood density and also using allometric equations. 71 of the trees showed greater biomass in the canopy as compared to the trunk, whilst 29 trees showed greater biomass in the trunk as compared to the canopy. The high biomass in the canopy was attributed to a lot of factors including the presence of leaves, wind, modelling parameters, size of the tree component, extraction of trees, non-circular branches and stem and point cloud registration. Different runs were tested to see their effect on the volume derived. No significant differences were observed in the number of runs and the resulting volume. Different cover set diameters were tested to observe their effect on the volume derived. There were significant differences in the cover set diameter and the volume derived and post hoc tests showed significant differences in cover set diameters of 0.01m & 0.04 m and 0.01 & 0.05m. An increase in the cover set diameter results in an increase in the volume. Different nmin values were tested to see the effect on canopy volume. Significant differences were observed between the nmin values and the canopy volume. Post hoc tests revealed differences in nmin values except nmin values of 5 & 3 and 7 & 5. An increase in the nmin value results in a decrease in the canopy volume. The carbon per tree was calculated by using a conversion factor of 0.47. Out of the 100 trees, the majority of the trees had a carbon content of 250Kg/tree with a few large trees having a carbon content of 1200Kg/tree and above with an average of 294Kg/tree when using species specific wood density and 281Kg/tree when using the FAO default wood density value. This approach is very promising in estimating above ground biomass. The following are the answers to research questions of this study:

Is there a significant difference between DBH derived from TLS and measured in the field?

Field measured DBH and TLS derived DBH had a high correlation. A correlation coefficient (r) of 0.996 and a coefficient of determination (R^2) of 0.993 was observed from the regression statistics. The RMSE was 1.1cm. An F-test and t-test revealed a non-significance relationship between DBH measured in the field and DBH derived from TLS. The null hypothesis was accepted ($p > 0.05$).

Is there a significant difference between height derived from TLS and measured in the field?

A low correlation was observation between field measured height and TLS derived height (r) of 0.767 and (R^2) of 0.589. An RMSE error of 3.4 metres was recorded. An F-test and a t –test revealed a significant difference between height measured in the field and height measured from TLS. The null hypothesis was rejected ($p < 0.05$).

Is there a significant difference in the above ground biomass derived from QSM and from allometric equations?

The 29 observations that had trunk biomass greater than canopy biomass showed no significant differences in the above ground biomass derived from QSM or from allometric equations. A strong relationship was observed with an R^2 of 0.968 and an RMSE of 120.3Kg/tree when using 0.57g/cm^3 wood density to calculate the above ground biomass. An R^2 of 0.934 and an RMSE of 131.61kg/tree when species specific

wood density was used for calculating the above ground biomass. The null hypothesis was not rejected ($p > 0.05$)

Completely different results were found for the 71 trees that had canopy biomass greater than trunk biomass. There was a significant difference in the above ground biomass derived from QSM and from allometric equations. An R^2 of 0.817 and an RMSE of 163Kg/tree was observed when 0.57g/cm^3 wood density was used to calculate the above ground biomass. When using the species specific wood density an R^2 of 0.797 with an RMSE of 198Kg/tree was observed. The null hypothesis was rejected ($p < 0.05$).

Is there a difference in the distribution of above ground biomass along the different parts of the tree?

The study revealed a significant difference in the distribution of above ground biomass in different tree components. The null hypothesis was rejected ($p < 0.05$) after conduction an F-test and a t-test.

Is there a difference in using either default or species specific wood density in estimating above ground biomass?

The study showed that there is no significant difference in using either a default value of wood density for tropical trees in Asia (0.57g/cm3) or species specific wood density value in calculating above ground biomass. The null hypothesis was not rejected ($p > 0.05$).

General conclusion
QSM derived above ground biomass overestimates the above ground biomass as compared to the allometry reference. In this study, the AGB was overestimated by 47% as compared to the allometry reference for the 100 trees used in the reconstruction. Bias in estimating AGB was mainly derived from height measurements, using multi species allometric equations and leaf on conditions of the trees. There is need to conduct the research with leaf off conditions and to validate the method with destructive samples.

6.2 Recommendations

➢ Separation of leaf and branch to reduce errors and improve the reconstruction of the trees.

➢ Automatization of finding optimum modelling parameters per tree to reduce the time especially when modelling heterogeneous forests.

➢ Conduct crown classification separately to enhance accurate tree extraction.

➢ Validation of above ground biomass derived from QSM through destructive sampling.

➢ Increase of registration accuracy by increasing number of reflectors and their height especially in dense tropical forests.

LIST OF REFERENCES

Abdullah, M., Yaman, A., & Jamaludin, M. (1999). Recreational opportunities for public use in Ayer Hitam Forest: Setting the stage and park management approach. *Pertanika Journal of Tropical Agricultural Science*, *22*(2), 161–166.

Åkerblom, M. (2012). *Quantitative tree modeling from laser scanning data. MSc Thesis.* Tampere University of Technology. Retrieved from http://dspace.cc.tut.fi/dpub/handle/123456789/21012.

Angelsen, A., & Wertz-Kanounnikoff, S. (2008). *Moving ahead with REDD. Issues, options and implications.* (Vol. 6). Centre for International Forestry Research,Bogor Barat,Indonesia,156p.ISBN 9789791412766. doi:10.1002/tqem.3310060102.

Asner, G. P., Mascaro, J., Muller-Landau, H. C., Vieilledent, G., Vaudry, R., Rasamoelina, M., van Breugel, M. (2012). A universal airborne LiDAR approach for tropical forest carbon mapping. *Oecologia*, *168*(4), 1147–1160. doi:10.1007/s00442-011-2165-z.

Basuki, T. M., van Laake, P. E., Skidmore, A. K., & Hussin, Y. A. (2009). Allometric equations for estimating the above-ground biomass in tropical lowland Dipterocarp forests. *Forest Ecology and Management*, *257*(8), 1684–1694. doi:10.1016/j.foreco.2009.01.027.

Bawon, P., & Yaman, A. R. (2007). *Multimedia Super Corridor Community Heritage.* Universiti Putra Malaysia,Faculty of Forestry,Serdang.ISBN 9789833455911.

Bhattarai, T., Skutsch, M., Midmore, D. &, & Shrestha, L. H. (2015). Carbon Measurement : An Overview of Forest Carbon Estimation Methods and the Role of Geographical Information System and Remote Sensing Techniques for REDD + Implementation. *Journal of Forest and ILvelihood*, (August).

Bienert, A., & Maas, H. (2009). Methods for the Automatic Geometric Registration of Terrestrial Laser Scanner Point Clouds in Forest Stands. *Iaprs, XXXVIII*, 93–98.

Bienert, A., Scheller, S., Keane, E., Mullooly, G., & Mohan, F. (2006). Application of Terrestrial Laser Scanners for the Determination of Forest Inventory Parameters. *ISPRS Commission V Symposium Image Engineering and Vision Metrology Volume XXXVI PART 5*, *36*(5), 2005–2008. Retrieved from http://www.isprs.org/proceedings/XXXVI/part5/paper/1270_Dresden06.pdf.

Boon, D. A. (1966). *Forest inventory. Photogrammetria* (Vol. 21). Springer,the Netherlands ISBN 9781402043796. doi:10.1016/0031-8663(66)90016-0.

Brown, S. (2002). Measuring carbon in forests: Current status and future challenges. *Environmental Pollution*, *116*(3), 363–372. doi:10.1016/S0269-7491(01)00212-3.

Burt, A., Disney, M. I., Raumonen, P., Armston, J., & Calders, K. (2013). Rapid characterisation of forest structure from TLS and 3D modelling. *International Geoscience and Remote Sensing Symposium (IGARSS 2013)*, 3387–3390. doi:10.1109/IGARSS.2013.6723555.

Calders, K., Armston, J., Newnham, G., Herold, M., & Goodwin, N. (2014). Implications of sensor configuration and topography on vertical plant profiles derived from terrestrial LiDAR. *Agricultural and Forest Meteorology*, *194*, 104–117. doi:10.1016/j.agrformet.2014.03.022.

Calders, K., Disney, M., Burt, A., Newnham, G., Murphy, S., Raumonen, P., Armston, J. (2015). Reducing uncertainties in above-ground biomass estimates using terrestrial laser scanning. In *SilviLaser SEPTEMBER 2015*.

Calders, K., Newnham, G., Burt, A., Murphy, S., Raumonen, P., Herold, M.,Kaasalainen, M. (2015). Nondestructive estimates of above-ground biomass using terrestrial laser scanning. *Methods in Ecology and Evolution*, *6*(2), 198–208. doi:10.1111/2041-210X.12301.

Calders, K., Newnham, G., Herold, M., Murphy, S., Culvenor, D., Raumonen, P., Disney, M. (2013). Estimating above ground biomass from terrestrial laser scanning in Australian Eucalypt Open Forest. *Silvilaser 2013, October 9-11, Beijing, China, di*(July 2015), 90–97.

Campbell, B. M. (2009). Beyond Copenhagen: REDD+, agriculture, adaptation strategies and poverty. *Global Environmental Change*, *19*(4), 397–399. doi:10.1016/j.gloenvcha.2009.07.010.

Castedo-Dorado, F., Gómez-García, E., Diéguez-Aranda, U., Barrio-Anta, M., & Crecente-Campo, F. (2012). Aboveground stand-level biomass estimation: A comparison of two methods for major forest species in northwest Spain. *Annals of Forest Science*, *69*(6), 735–746. doi:10.1007/s13595-012-0191-6.

Chave, J., Réjou-Méchain, M., Búrquez, A., Chidumayo, E., Colgan, M. S., Delitti, W. B. C., Vieilledent, G. (2014). Improved allometric models to estimate the aboveground biomass of tropical trees. *Global Change Biology*, 3177–3190. doi:10.1111/gcb.12629.

Clark, D. B., & Kellner, J. R. (2012). Tropical forest biomass estimation and the fallacy of misplaced concreteness. *Journal of Vegetation Science*, *23*(6), 1191–1196. doi:10.1111/j.1654-1103.2012.01471.x.

Clark, M. L., Clark, D. B., & Roberts, D. A. (2004). Small-footprint lidar estimation of sub-canopy elevation and tree height in a tropical rain forest landscape. *Remote Sensing of Environment*, *91*(1), 68–89. doi:10.1016/j.rse.2004.02.008.

Cushman, K. C., Muller-Landau, H. C., Condit, R. S., & Hubbell, S. P. (2014). Improving estimates of biomass change in buttressed trees using tree taper models. *Methods in Ecology and Evolution*, *5*(6), 573–582. doi:10.1111/2041-210X.12187.

Dassot, M., Constant, T., & Fournier, M. (2011). The use of terrestrial LiDAR technology in forest science: Application fields, benefits and challenges. *Annals of Forest Science*, *68*(5), 959–974. doi:10.1007/s13595-011-0102-2.

DiRocco, T. L., Ramage, B. S., Evans, S. G., & Potts, M. D. (2014). Accountable accounting: Carbon-based management on marginal lands. *Forests*, *5*(4), 847–861. doi:10.3390/f5040847.

Disney, M., Philip, L., & Raumonen, P. (2012). Testing a new vegetation structure retrieval algorithm from terrestrial lidar scanner data using 3D models. In *SilviLaser 2012* (pp. 177–183).

DISTO D510 | Laser Distance Measurer | Leica Geosystems. (2016). Retrieved February 10, 2016, from http://lasers.leica-geosystems.com/disto/d510.

Drake, J. B., Knox, R. G., Dubayah, R. O., Clark, D. B., Condit, R., Blair, J. B., & Hofton, M. (2003). Above-ground biomass estimation in closed canopy Neotropical forests using lidar remote sensing : factors, 147–159.

Eco - Key services - Ace Geography. (2016). Retrieved January 26, 2016, from http://www.acegeography.com/eco---key-services.html.

Englhart, S., Jubanski, J., & Siegert, F. (2013). Quantifying Dynamics in Tropical Peat Swamp Forest Biomass with Multi-Temporal LiDAR Datasets. *Remote Sensing*, *5*(5), 2368–2388. doi:10.3390/rs5052368.

Falkowski, M. J., Smith, A. M. S., Gessler, P. E., Hudak, A. T., Vierling, L. A., & Evans, J. S. (2008). The influence of conifer forest canopy cover on the accuracy of two individual tree measurement algorithms using lidar data. *Canadian Journal of Remote Sensing*, *34*, S1–S13. doi:10.5589/m08-055.

FAO. (2009). *State of the world's forests 2009*. FAO,Rome,Italy ISBN 9789251060575. doi:10.1209/epl/i2005-10515-2.

FAO, UNDP, & UNEP. (2008). UN Collaborative Programme on Reducing Emissions from Deforestation and Forest Degradation in Developing Countries (UN-REDD). *http://www.undp.org/mdtf/UN-REDD/docs/Annex-A-Framework-Document.pdf*, (June), -. doi:http://www.un-redd.org/Portals/15/documents/publications/UN-REDD_FrameworkDocument.pdf.

Field, A., Miles, J., & Field, Z. (2012). *Discovering Statistics Using R* (Vol. 58). SAGE,London,United Kingdom ISBN 9781847879066. doi:10.1111/insr.12011_21.

Fixed area plots - AWF-Wiki. (2013). Retrieved August 10, 2015, from http://wiki.awf.forst.uni-goettingen.de/wiki/index.php/Fixed_area_plots.

Frazer, G. W., Magnussen, S., Wulder, M. a., & Niemann, K. O. (2011). Simulated impact of sample plot size and co-registration error on the accuracy and uncertainty of LiDAR-derived estimates of forest stand biomass. *Remote Sensing of Environment*, *115*(2), 636–649. doi:10.1016/j.rse.2010.10.008.

Gibbs, H. K., Brown, S., Niles, J. O., & Foley, J. A. (2007). Monitoring and estimating tropical forest carbon stocks: making REDD a reality. *Environmental Research Letters*, *2*(4), 045023. doi:10.1088/1748-9326/2/4/045023.

Goetz, S., & Dubayah, R. (2011). Advances in remote sensing technology and implications for measuring and monitoring forest carbon stocks and change. *Carbon Management*, *2*(3), 231–244. doi:10.4155/cmt.11.18.

Hackenberg, J., Wassenberg, M., Spiecker, H., & Sun, D. (2015). Non Destructive Method for Biomass Prediction Combining TLS Derived Tree Volume and Wood Density. *Forests*, *6*(4), 1274–1300. doi:10.3390/f6041274.

Hani, U., Aziz, H., & Ming, H. Y. (2005). The negative impacts of development activities toward sustainability of Ayer Hitam Forest Reserve. *Esc5988 Environmental Research Projects*, (Marshall), 1–15.

Hasmadi Mohd, I., Amirin Khairul, M., & Hidayah Siti Noor, A. . (2008). Estimated DEM uncertainty in creating a 3-D of the UPM's Ayer Hitam Forest reserve in Selangor, Malaysia. *Geografia - Malaysian Journal of Society and Space*, *4*(1), 45–53. Retrieved from http://www.ukm.my/geografia.

Heng, R. K., & Tsai, L. I. M. M. (1999). An Estimate of Forest Biomass in Ayer Hitam Forest Reserve. *Pertanika Journal Tropical Agriculture Science*, *22*(2), 117–123.

Herold, M., & Skutsch, M. (2011). Monitoring, reporting and verification for national REDD + programmes: two proposals. *Environmental Research Letters*, *6*(1), 014002. doi:10.1088/1748-9326/6/1/014002.

Hildebrandt, R., & Iost, A. (2012). From points to numbers: A database-driven approach to convert terrestrial LiDAR point clouds to tree volumes. *European Journal of Forest Research*, *131*(6), 1857–1867. doi:10.1007/s10342-012-0638-1.

Hirata, Y., Takao, G., Sato, T., & Toriyama, J. (eds). (2012). *REDD-plus Cookbook*. REDD Research and Development Centre,Forestry and Forest Products Research Institute Japan,156pp.ISBN 9784905304135.

Holopainen, M., Vastaranta, M., Kankare, V., Räty, M., Vaaja, M., Liang, X., Kaasalainen, S. (2012). Biomass Estimation of Individual Trees Using Stem and Crown Diameter Tls Measurements. *ISPRS - International Archives of the Photogrammetry, Remote Sensing and Spatial Information Sciences*, *XXXVIII-5/*(August), 91–95. doi:10.5194/isprsarchives-XXXVIII-5-W12-91-2011.

Hopkinson, C., Chasmer, L., Young-Pow, C., & Treitz, P. (2004). Assessing forest metrics with a ground-based scanning lidar. *Canadian Journal of Forest Research*, *34*(3), 573–583. doi:10.1139/x03-225.

Houghton, R. (2005). *Tropical deforestation as a source of greenhouse gas emissions*. Amazon Institute for Environmental Research ISBN:858782712X. doi:10.1017/S0376892900029775.

Houghton, R. A., & Goetz, S. J. (2008). New Satellites Help Quantify Carbon Sources and Sinks. *Eos, Transactions American Geophysical Union*, *89*(43), 43–46. doi:10.1029/2003GB002142.Bergen.

Ibrahim, F. (1999). Plant Diversity and Conservation Value of Ayer Hitam Forest, Selangor, Peninsular Malaysia. *Pertanika Journal of Tropical Agricultural Science*, *22*(2), 73–83. Retrieved from http://psasir.upm.edu.my/3795/.

IPCC. (2003). *Intergovernmental Panel on Climate Change Good Practice Guidance for Land Use , Land-Use Change and Forestry*. Retrieved from the Institute for Global Environmental Strategies (IGES) for the IPCC.

IPCC. (2006). Chapter 4 forest land. *Forestry*, *4*(2), 1–29. doi:10.1016/j.phrs.2011.03.002.

Jung, S.-E., Kwak, D.-A., Park, T., Lee, W.-K., & Yoo, S. (2011). Estimating Crown Variables of Individual Trees Using Airborne and Terrestrial Laser Scanners. *Remote Sensing*, *3*(12), 2346–2363. doi:10.3390/rs3112346.

Kaasalainen, S., Krooks, A., Liski, J., Raumonen, P., Kaartinen, H., Kaasalainen, M., Mäkipää, R. (2014). Change detection of tree biomass with terrestrial laser scanning and quantitative structure modelling. *Remote Sensing*, *6*(5), 3906–3922. doi:10.3390/rs6053906.

Kearsley, E., de Haulleville, T., Hufkens, K., Kidimbu, A., Toirambe, B., Baert, G., Verbeeck, H. (2013). Conventional tree height–diameter relationships significantly overestimate aboveground carbon stocks in the Central Congo Basin. *Nature Communications*, *4*. doi:10.1038/ncomms3269.

Köhl, M., Magnussen, S. S., & Marchetti, M. (2006). *Sampling Methods, Remote Sensing and GIS Multiresource Forest Inventory*. Springer Science & Business Media ISBN 3540325727. Retrieved from https://books.google.com/books?hl=en&lr=&id=uspzLjVWNgMC&pgis=1.

Krooks, A., Kaasalainen, S., Kankare, V., Joensuu, M., Raumonen, P., & Kaasalainen, M. (2014). Tree structure vs. height from terrestrial laser scanning and quantitative structure models. *Silva Fennica*, *48*(2), 1–11. doi:10.14214/sf.1125.

Lemmens, M. (2011). *Geo-information: Technologies, Applications and the Environment (Google eBook)*. Springer Science & Business Media,The Netherlands ISBN 9400716672. doi:10.1007/978-94-007-1667-4.

Lepun, P., Faridah, H. I., & Jusoff, K. (2007). Tree species distribution in Ayer Hitam Forest Reserve, Selangor, Malaysia. *EEESD 07 Proceedings of the 3rd IASMEWSEAS International Conference on Energy Environment Ecosystems and Sustainable Development*, 75–81.

Lim, K., Treitz, P., Wulder, M., St-Onge, B., & Flood, M. (2003). LiDAR remote sensing of forest structure. *Progress in Physical Geography*, *27*(1), 88–106. doi:10.1191/0309133303pp360ra.

Lovell, J. L., Jupp, D. L. B., Culvenor, D. S., & Coops, N. C. (2003). Using airborne and ground-based ranging lidar to measure canopy structure in Australian forests. *Canadian Journal of Remote Sensing*, *29*(5), 607–622. doi:10.5589/m03-026.

Maas, H. -G., Bienert, A., Scheller, S., & Keane, E. (2008). Automatic forest inventory parameter determination from terrestrial laser scanner data. *International Journal of Remote Sensing*, *29*(5), 1579–1593. doi:10.1080/01431160701736406.

Magalhães, T. M., Seifert, T., Florestal, D. D. E., & Mondlane, U. E. (2015). Estimation of Tree Biomass , Carbon Stocks , and Error Propagation in Mecrusse Woodlands. *Open Journal of Forestry*, (April), 471–488. doi:10.4236/ojf.2015.54041.

Malhi, Y., & Grace, J. (2000). Tropical forests and atmospheric carbon dioxide. *Trends in Ecology & Evolution*, *15*(8), 332–337. doi:10.1016/S0169-5347(00)01906-6.

Næsset, E., Bollandsås, O. M., Gobakken, T., Gregoire, T. G., & Ståhl, G. (2013). Model-assisted estimation of change in forest biomass over an 11year period in a sample survey supported by airborne LiDAR: A case study with post-stratification to provide "activity data." *Remote Sensing of Environment*, *128*, 299–314. doi:10.1016/j.rse.2012.10.008.

Nelson, B. W., Mesquita, R., Pereira, J. L. G., Garcia Aquino De Souza, S., Teixeira Batista, G., & Bovino Couto, L. (1999). Allometric regressions for improved estimate of secondary forest biomass in the central Amazon. *Forest Ecology and Management*, *117*(1-3), 149–167. doi:10.1016/S0378-1127(98)00475-7.

Nogueira, E. M., Nelson, B. W., & Fearnside, P. M. (2005). Wood density in dense forest in central Amazonia, Brazil. *Forest Ecology and Management*, *208*(1-3), 261–286. doi:10.1016/j.foreco.2004.12.007.

Nurul-Shida, S., , Faridah-Hanum, I., , Wan Razali, W. M., & Kamziah, K. (2014). Community Structure of Trees in Ayer Hitam Forest Reserve,Puchong,Selangor,Malaysia. *The Malaysian Forester*, *77(1)*(August 2015), 73–86.

Okatani, I. S., & Deguchi, K. (2002). A Method for Fine Registration of Multiple View Range Images Considering the Measurement Error Properties. *Cviu*, *87*(1-3), 66–77. doi:10.1006/cviu.2002.0983.

Panholzer, H., & Prokop, A. (2013). Wedge-Filtering of Geomorphologic Terrestrial Laser Scan Data. *Sensors*, *13*(2), 2579–2594. doi:10.3390/s130202579.

Patenaude, G., Milne, R., & Dawson, T. P. (2005). Synthesis of remote sensing approaches for forest carbon estimation: reporting to the Kyoto Protocol. *Environmental Science & Policy*, *8*(2), 161–178. doi:10.1016/j.envsci.2004.12.010.

Peichl, M., & Arain, M. A. (2007). Allometry and partitioning of above- and belowground tree biomass in an age-sequence of white pine forests. *Forest Ecology and Management*, *253*(1-3), 68–80. doi:10.1016/j.foreco.2007.07.003.

Pfeifer, N., Gorte, B., Winterhalder, D., Sensing, R., & Range, C. (2004). Automatic Reconstruction of Single Trees From Terrestrial Laser Scanner Data. In *20th ISPRS Congress 114-119* (Vol. 35, pp. 1–6). Retrieved from http://www.isprs.org/congresses/beijing2008/proceedings/5_pdf/81.pdf.

Pitkänen, J., & Maltamo, M. (2004). Adaptive Methods for Individual Tree Detection on Airborne Laser Based Canopy Height Model. *International Archives of Photogrammetry, Remote Sensing and Spatial Information Sciences, XXXVI, 8/W2*, *36*, 187–191. Retrieved from http://www.researchgate.net/publication/228876216_Adaptive_methods_for_individual_tree_detection_on_airborne_laser_based_canopy_height_model/file/5046351aed61adb800.pdf.

Raumonen, P., Casella, E., Calders, K., Murphy, S., Åkerbloma, M., & Kaasalainen, M. (2015). Massive-Scale Tree Modelling From Tls Data. *ISPRS Annals of Photogrammetry, Remote Sensing and Spatial Information Sciences*, *II-3/W4*(March), 189–196. doi:10.5194/isprsannals-II-3-W4-189-2015.

Raumonen, P., Casella, E., Disney, M., Akerblom, M., & Kaasalainen, M. (2013). Fast automatic method for constructing topologically and geometrically precise tree models from TLS Data. *International Conference on Function-Structural Plant Models*, (June), 89–91. doi:10.13140/2.1.4259.9206.

Raumonen, P., Kaasalainen, M., Åkerblom, M., Kaasalainen, S., Kaartinen, H., Vastaranta, M., Lewis, P. (2013). Fast Automatic Precision Tree Models from Terrestrial Laser Scanner Data. *Remote Sensing*, *5*(2), 491–520. doi:10.3390/rs5020491.

Raumonen, P., Kaasalainen, S., Kaasalainen, M., & Kaartinen, H. (2012). Approximation of Volume and Branch Size Distribution of Trees From Laser Scanner Data. *ISPRS - International Archives of the Photogrammetry, Remote Sensing and Spatial Information Sciences*, *XXXVIII-5/*(January 2016), 79–84. doi:10.5194/isprsarchives-XXXVIII-5-W12-79-2011.

Riegl. (2005). RISCAN PRO Manual Version 1.2.0sp1.

RIEGL. (2014). RIEGL VZ-400, 3–6.

Riveiro, B., Morer, P., Arias, P., & De Arteaga, I. (2011). Terrestrial laser scanning and limit analysis of masonry arch bridges. *Construction and Building Materials*, *25*(4), 1726–1735. doi:10.1016/j.conbuildmat.2010.11.094.

Ruiz, L. A., Hermosilla, T., Mauro, F., & Godino, M. (2014). Analysis of the influence of plot size and LiDAR density on forest structure attribute estimates. *Forests*, *5*(5), 936–951. doi:10.3390/f5050936.

Ryan, C. M., Williams, M., & Grace, J. (2011). Above- and belowground carbon stocks in a miombo woodland landscape of mozambique. *Biotropica*, *43*(4), 423–432. doi:10.1111/j.1744-7429.2010.00713.x.

Stephenson, N. L., Das, a J., Condit, R., Russo, S. E., Baker, P. J., Beckman, N. G., Zavala, M. A. (2014). Rate of tree carbon accumulation increases continuously with tree size. *Nature*, *507*(7490), 90–3. doi:10.1038/nature12914.

Talbot, J., Lewis, S. L., Lopez-Gonzalez, G., Brienen, R. J. W., Monteagudo, A., Baker, T. R., Phillips, O. L. (2014). Methods to estimate aboveground wood productivity from long-term forest inventory plots. *Forest Ecology and Management*, *320*, 30–38. doi:10.1016/j.foreco.2014.02.021.

van Breugel, M., Ransijn, J., Craven, D., Bongers, F., & Hall, J. S. (2011). Estimating carbon stock in secondary forests: Decisions and uncertainties associated with allometric biomass models. *Forest Ecology and Management*, *262*(8), 1648–1657. doi:10.1016/j.foreco.2011.07.018.

Van der Zande, D., Hoet, W., Jonckheere, I., van Aardt, J., & Coppin, P. (2006). Influence of measurement set-up of ground-based LiDAR for derivation of tree structure. *Agricultural and Forest Meteorology*, *141*(2-4), 147–160. doi:10.1016/j.agrformet.2006.09.007.

Van Laar, A., & Akça, A. (2007). *Forest Mensuration*. Springer Science & Business Media, The Netherlands ISBN 9781402059902. doi:10.1007/978-1-4020-5991-9.

Vashum.T.K & Jayakumar.S. (2012). Methods to Estimate Above-Ground Biomass and Carbon Stock in Natural Forests - A Review. *Journal of Ecosystem & Ecography*, *02*(04). doi:10.4172/2157-7625.1000116.

Williams, M. S., Techniques, M. I., Forest, R. M., Station, R. E., Service, U. F., St, W. P., Sciences, F. (1994). Five Instruments for Measuring Tree Height : An Evaluation. *Southern Journal of Applied Forestry*, *18*(2), pp. 76–82(7).

World Agroforestry Centre. (2011). ICRAF Database - Wood Density. Retrieved January 14, 2016, from http://db.worldagroforestry.org/wd.

Yu Abit, L., Kamaruddin, I. S., Mohd-Rozhan, Z., Ina-Salwany, M. Y., & Mustafa-Kamal, A. S. (2012). Fish biodiversity survey (2009) of streams in the Ayer Hitam forest reserve, Puchong, Selangor. *Pertanika Journal of Tropical Agricultural Science*, *35*(1), 15–19.

Yu, X., Hyyppä, J., Vastaranta, M., Holopainen, M., & Viitala, R. (2011). Predicting individual tree attributes from airborne laser point clouds based on the random forests technique. *ISPRS Journal of Photogrammetry and Remote Sensing*, *66*(1), 28–37. doi:10.1016/j.isprsjprs.2010.08.003.

LIST OF APPENDICES

Appendix 1: Field measurement form

DATA COLLECTION SHEET (AYER HITAM TROPICAL RAIN FOREST RESERVE, MALAYSIA

Name of recorder.. **Date**..

Sample Plot No.		GPS Coordinates	X:		Grid cell No.	Slope (%)	Plot Radius	Undergrowth		Crown Cover (%)
			Y:					Y	N	

Tree No.	Species	DBH (cm)	Hgt 1 (Leica)	Hgt 2 (Haga)	Hgt 3 (TruPulse)	Crown diam.(m)	Tree No.	Species	DBH (cm)	Hgt 1 (Leica)	Hgt 2 (Haga)	Hgt 3 (TruPulse)	Crown diam.(m)
1							36						
2							37						
3							38						
4							39						
5							40						
6							41						
7							42						
8							43						
9							44						
10							45						
11							46						
12							47						
13							48						
14							49						
15							50						
16							51						
17							52						
18							53						
19							54						
20							55						
21							56						
22							57						
23							58						
24							59						
25							60						
26							61						
27							62						
28							63						
29							64						
30							65						
31							66						
32							67						
33							68						
34							69						
35							70						

Appendix 2: Slope correction table

Slope correction table

Plot size   500m²

Slope%	Radius(m)	Slope%	Radius(m)	Slope%	Radius(m)
0	12.62				
1	12.62	36	13.01	71	13.97
2	12.62	37	13.03	72	14.00
3	12.62	38	13.05	73	14.04
4	12.62	39	13.07	74	14.07
5	12.62	40	13.09	75	14.10
6	12.63	41	13.12	76	14.14
7	12.63	42	13.14	77	14.17
8	12.64	43	13.16	78	14.21
9	12.64	44	13.19	79	14.24
10	12.65	45	13.21	80	14.28
11	12.65	46	13.24	81	14.31
12	12.66	47	13.26	82	14.35
13	12.67	48	13.29	83	14.38
14	12.68	49	13.31	84	14.42
15	12.69	50	13.34	85	14.45
16	12.70	51	13.37	86	14.49
17	12.71	52	13.39	87	14.52
18	12.72	53	13.42	88	14.56
19	12.73	54	13.45	89	14.60
20	12.74	55	13.48	90	14.63
21	12.75	56	13.51	91	14.67
22	12.77	57	13.53	92	14.71
23	12.78	58	13.56	93	14.74
24	12.79	59	13.59	94	14.78
25	12.81	60	13.62	95	14.82
26	12.82	61	13.65	96	14.85
27	12.84	62	13.68	97	14.89
28	12.86	63	13.72	98	14.93
29	12.87	64	13.75	99	14.97
30	12.89	65	13.78	100	15.00
31	12.91	66	13.81	101	15.04
32	12.93	67	13.84	102	15.08
33	12.95	68	13.87	103	15.12
34	12.97	69	13.91	104	15.15
35	12.99	70	13.94	105	15.19

Source: Y.A.Hussin (2001) from lecture notes

Appendix 3: Multi Station Adjustment
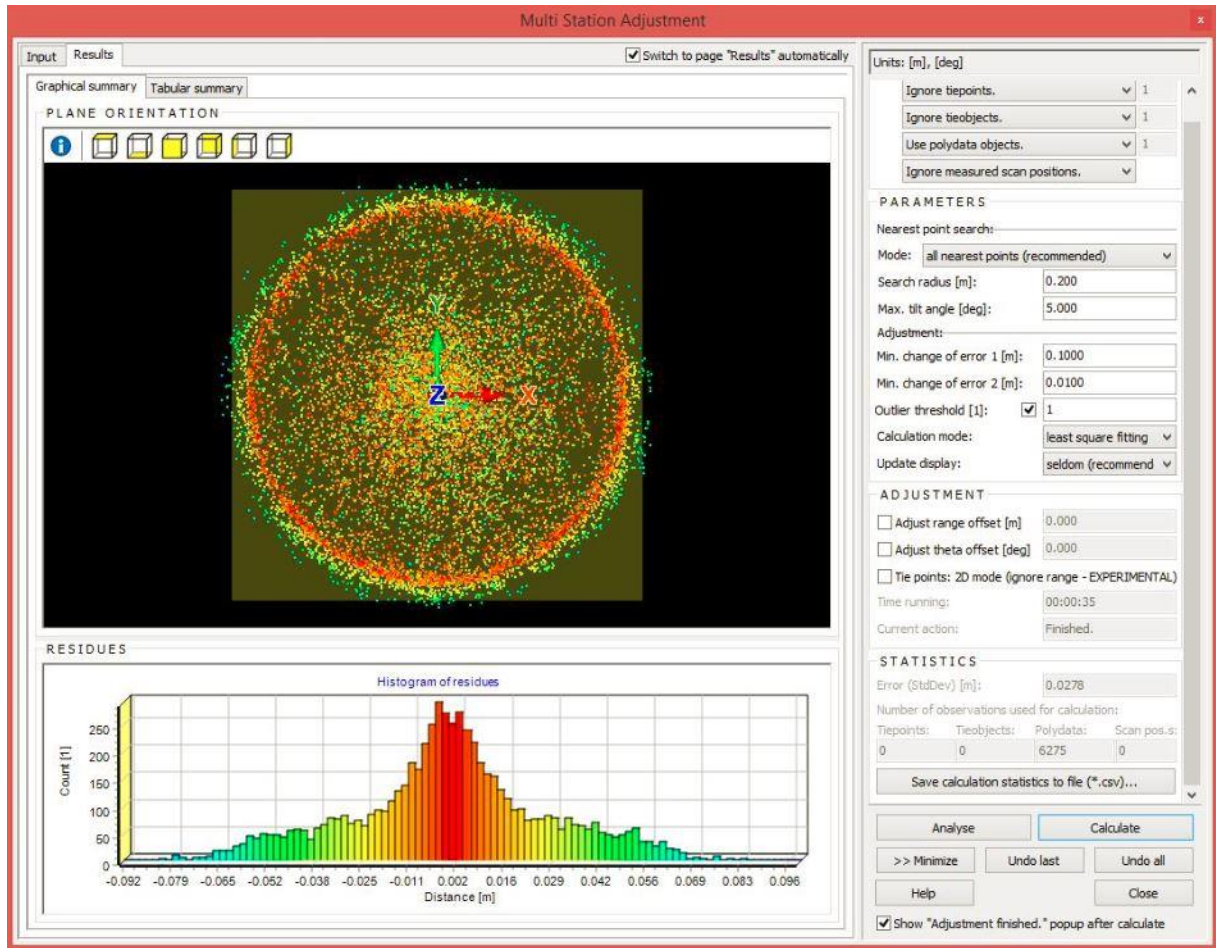
Appendix 4: Optimum modelling parameters for trees

Plot	Tree No	PD2MIN	PD2Max	lcy	FilRad	Median distance to QSM (mm)	Average distance to QSM(mm)
19	17	0.05	0.12	8	2.5	4.3	11.3
9	1	0.04	0.12	3	2.5	1.9	13.8
16	1	0.05	0.12	3	3.5	3.3	18.3
23	1	0.05	0.12	8	3.5	4	18.9
16	29	0.01	0.12	3	2.5	9	25.1
21	75	0.02	0.12	3	3.5	7.8	25.2
12	18	0.05	0.12	3	2.5	4.1	25.3
9	13	0.05	0.12	3	2.5	16.6	29
18	7	0.01	0.12	5	2.5	15.9	35.3
1	10	0.05	0.12	5	3.5	9.5	37.8
16	4	0.01	0.12	3	3.5	24.4	38.6
19	27	0.05	0.12	8	3.5	8.4	40.6
23	9	0.03	0.12	5	3.5	14.8	41
15	31	0.01	0.12	3	1.5	21.2	43.4
19	19	0.02	0.12	3	3.5	21.5	43.4
9	8	0.05	0.12	3	3.5	10	43.8
8	17	0.01	0.12	5	2.5	22.1	43.9
18	22	0.02	0.12	8	3.5	9.2	43.9
20	6	0.02	0.12	3	3.5	23.9	45.2
1	11	0.02	0.12	3	3.5	29.9	45.6
26	22	0.02	0.12	3	3.5	18.6	45.6
8	2	0.01	0.12	5	2.5	22.3	45.8
6	7	0.03	0.12	3	2.5	18.3	46.7
21	27	0.02	0.12	5	3.5	32.6	46.7
17	32	0.05	0.12	3	2.5	14.4	46.9
16	17	0.03	0.12	3	3.5	24	47.3
22	25	0.05	0.12	8	1.5	10.2	47.5

Appendix 5: Regression analysis Field and TLS parameters (DBH & Height)

DBH

Regression Statistics	
Multiple R	0.996454
R Square	0.99292
Adjusted R Square	0.992908
Standard Error	1.075718
Observations	600

ANOVA

	df	SS	MS	F	Significance F
Regression	1	97049.68	97049.68	83868.22	0
Residual	598	691.9868	1.157169		
Total	599	97741.66			

	Coefficients	Standard Error	t Stat	P-value
Intercept	0.139154	0.089271	1.558771	0.11958
Field_DBH	0.986482	0.003406	289.6001	0

Height

Regression Statistics	
Multiple R	0.76719
R Square	0.58858
Adjusted R Square	0.587892
Standard Error	3.363253
Observations	600

ANOVA

	df	SS	MS	F	Significance F
Regression	1	9676.995	9676.995	855.503	2E-117
Residual	598	6764.258	11.31147		
Total	599	16441.25			

	Coefficients	Standard Error	t Stat	P-value
Intercept	5.265382	0.408741	12.88196	1.1E-33
Field Height	0.801256	0.027394	29.24898	2E-117

Appendix 6: QSM Output

All points: 57888, First filtering: 895, Points left: 56993
   All points: 56993, Second filtering: 0, Points left: 56993
   All points: 57888, all filtered points: 895, Points left: 56993

Tree 7
PatchDiam1 = 0.12, BallRad1 = 0.14, nmin1 = 3
PatchDiam2Min = 0.03, PatchDiam2Max = 0.12, BallRad2 = 0.13
nmin2 = 1, lcyl = 3, Tria = 1, OnlyTree = 1, FilRad = 2.5
Progress:
Cover sets   0 min 0.2 sec, total: 0 min 0.2 sec
Tree sets   0 min 0.2 sec, total: 0 min 0.4 sec
   Maximum branch order: 13
   Maximum branch order: 4
Segments   0 min 1.4 sec, total: 0 min 1.8 sec
Cover sets   0 min 24.7 sec, total: 0 min 26.5 sec
Tree sets   0 min 20.9 sec, total: 0 min 47.4 sec
   Maximum branch order: 67
   Maximum branch order: 7
Segments   0 min 7.9 sec, total: 0 min 55.3 sec
CONSTRUCTING CYLINDER MODEL...
lcyl = 3, FilRad = 2.5
Cylinders   0 min 6.6 sec, total: 1 min 1.8 sec
Shortening the triangulated surface

Tree attributes:
Total volume = 174 L
Trunk volume = 107 L
Branch volume = 67.5 L
Total height = 14.5 m
Trunk length = 23.6 m
Branch length = 168 m
Number of branches = 242
Maximum branch order = 6
Total cylinder area = 14.3 m^2
Dbh (QSM) = 13.9 cm
Dbh (cylinder) = 13.9 cm
Dbh (triangulation) = 11.3 cm
Triangulated trunk volume = 1.86 L
Triangulated trunk length = 7.39 m
Mixed trunk volume = 27.5 L
Mixed total volume = 95 L

Branch order data:
Number of 1st-order branches = 45
Number of 2nd-order branches = 92
Number of 3rd-order branches = 67
Number of 4th-order branches = 30
Number of 5th-order branches = 7
Number of 6th-order branches = 1
Volume of 1st-order branches = 34.6 L
Volume of 2nd-order branches = 24.6 L
Volume of 3rd-order branches = 7 L
Volume of 4th-order branches = 1.2 L
Volume of 5th-order branches = 0.044 L
Volume of 6th-order branches = 0.001 L
Length of 1st-order branches = 4888 m
Length of 2nd-order branches = 7201 m
Length of 3rd-order branches = 3259 m
Length of 4th-order branches = 1109 m
Length of 5th-order branches = 320 m
Length of 6th-order branches = 18.1 m

   Median and average point distances to QSM: 18.6   48.4 mm
Distances   0 min 1.8 sec, total: 1 min 4.1 sec

Appendix 7: Post Hoc tests Cover Set Diameter

Dependent Variable: Total Volume
Tukey HSD

(I) Coverset Diameter	(J) Coverset Diameter	Mean Difference (I-J)	Std. Error	Sig.	95% Confidence Interval	
					Lower Bound	Upper Bound
Coverset Diameter =0.01metres	CoversetDiameter = 0.02 metres	-116.200	49.252	.168	-263.58	31.18
	CoversetDiameter =0.03metres	-135.000	49.252	.083	-282.38	12.38
	CoversetDiameter =0.04metres	-191.200*	49.252	.007	-338.58	-43.82
	CoversetDiameter = 0.05 metres	-244.200*	49.252	.001	-391.58	-96.82
CoversetDiameter = 0.02 metres	Coverset Diameter =0.01metres	116.200	49.252	.168	-31.18	263.58
	CoversetDiameter =0.03metres	-18.800	49.252	.995	-166.18	128.58
	CoversetDiameter =0.04metres	-75.000	49.252	.560	-222.38	72.38
	CoversetDiameter = 0.05 metres	-128.000	49.252	.109	-275.38	19.38
CoversetDiameter =0.03metres	Coverset Diameter =0.01metres	135.000	49.252	.083	-12.38	282.38
	CoversetDiameter = 0.02 metres	18.800	49.252	.995	-128.58	166.18
	CoversetDiameter =0.04metres	-56.200	49.252	.783	-203.58	91.18
	CoversetDiameter = 0.05 metres	-109.200	49.252	.214	-256.58	38.18
CoversetDiameter =0.04metres	Coverset Diameter =0.01metres	191.200*	49.252	.007	43.82	338.58
	CoversetDiameter = 0.02 metres	75.000	49.252	.560	-72.38	222.38
	CoversetDiameter =0.03metres	56.200	49.252	.783	-91.18	203.58
	CoversetDiameter = 0.05 metres	-53.000	49.252	.816	-200.38	94.38
CoversetDiameter = 0.05 metres	Coverset Diameter =0.01metres	244.200*	49.252	.001	96.82	391.58
	CoversetDiameter = 0.02 metres	128.000	49.252	.109	-19.38	275.38
	CoversetDiameter =0.03metres	109.200	49.252	.214	-38.18	256.58
	CoversetDiameter =0.04metres	53.000	49.252	.816	-94.38	200.38

*. The mean difference is significant at the 0.05 level.

Appendix 8: Pictures from the field